



HAL
open science

Joint radio and power resource optimal management for wireless cellular networks interconnected through smart grids

Mouhcine Mendil

► **To cite this version:**

Mouhcine Mendil. Joint radio and power resource optimal management for wireless cellular networks interconnected through smart grids. Signal and Image processing. Université Grenoble Alpes, 2018. English. NNT : 2018GREAT087 . tel-02102201

HAL Id: tel-02102201

<https://theses.hal.science/tel-02102201>

Submitted on 17 Apr 2019

HAL is a multi-disciplinary open access archive for the deposit and dissemination of scientific research documents, whether they are published or not. The documents may come from teaching and research institutions in France or abroad, or from public or private research centers.

L'archive ouverte pluridisciplinaire **HAL**, est destinée au dépôt et à la diffusion de documents scientifiques de niveau recherche, publiés ou non, émanant des établissements d'enseignement et de recherche français ou étrangers, des laboratoires publics ou privés.

THÈSE

Pour obtenir le grade de

DOCTEUR DE LA COMMUNAUTÉ UNIVERSITÉ GRENOBLE ALPES

Spécialité : **Signal, Image, Parole, Télécoms**

Arrêté ministériel : 25 mai 2016

Présentée par

Mouhcine MENDIL

Thèse dirigée par **Nouredine Hadjsaid** et codirigée par **Raphael Caire**

Préparée au sein du **CEA-LETI** et du **G2Elab**

dans l'École Doctorale **d'Électronique, Électrotechnique, Automatique et Traitement du Signal (EEATS)**

JOINT RADIO AND POWER RESOURCE OPTIMAL MANAGEMENT FOR WIRELESS CELLULAR NETWORKS INTERCONNECTED THROUGH SMART GRIDS

Thèse soutenue publiquement le **08 octobre 2018**, devant le jury composé de :

Antonio Loria

Directeur de recherche CNRS, président

Lars Nordström

Professeur à l'université KTH, rapporteur

Patrice Mégret

Professeur à l'université de Mons, rapporteur

Patrick Leguillette

Fondateur de Beebryte, examinateur

Nouredine Hadjsaid

Professeur à Grenoble-INP, directeur de thèse

Raphael Caire

Maître de conférence HDR à Grenoble-INP, codirecteur de thèse

Antonio De Domenico

Docteur-ingénieur de recherche CEA, co-encadrant de thèse

Vincent Heiries

Docteur-ingénieur de recherche CEA, co-encadrant de thèse



ABSTRACT

Pushed by an unprecedented increase in data traffic, *Mobile Network Operators* (MNOs) are densifying their networks through the deployment of *Small-cell Base Stations* (SBSs), low-range radio-access transceivers that offer enhanced capacity and improved coverage. This new infrastructure –*Heterogeneous cellular Network* (HetNet)– uses a hierarchy of high-power Macro-cell Base Stations overlaid with several low-power SBSs.

The increasing deployment and operation of the HetNets raise a new crucial concern regarding their energy consumption and carbon footprint. In this context, the use of energy-harvesting technologies in mobile networks have gained particular interest. The environment-friendly power sources coupled with energy storage capabilities have the potential to reduce the carbon emissions as well as the electricity operating expenditures of MNOs.

The integration of renewable energy (solar panel) and energy storage capability (battery) in SBSs gain in efficiency thanks to the technological and economic enablers brought by the *Smart Grid* (SG). However, the obtained architecture, which we call *Green Small-cell Base Station* (GSBS), is complex. First, the multitude of power sources, the system aging, and the dynamic electricity price in the SG are factors that require design and management to enable the GSBS to efficiently operate. Second, there is a close dependency between the system sizing and control, which requires an approach to address these problems simultaneously. Finally, the achievement of a holistic management in a HetNet requires a network-level energy-aware scheme that jointly optimizes the local energy resources and radio collaboration between the SBSs.

Accordingly, we have elaborated pre-deployment and post-deployment optimization frameworks for GSBSs that allow the MNOs to jointly reduce their electricity expenses and the equipment degradation. The pre-deployment optimization consists in an effective sizing of the GSBS that accounts for the battery aging and the associated management of the energy resources. The problem is formulated and the optimal sizing is approximated using average profiles, through an iterative method based on the non-linear solver *fmincon*. The post-deployment scheme relies on learning capabilities to dynamically adjust the GSBS energy management to its environment (weather conditions, traffic load, battery status, and electricity cost). The solution is based on the fuzzy Q-learning that consists in tuning a fuzzy inference system (which represents the energy arbitrage in the system) with the Q-learning algorithm. Then, we formalize an energy-aware load-balancing scheme to extend the local energy management to a network-level collaboration. We propose a two-stage algorithm to solve the formulated problem by combining hierarchical controllers at the GSBS-level and at the network-level. The two stages are alternated to continuously plan and adapt the energy management to the radio collaboration in the HetNet.

Simulation results show that, by considering the battery aging and the impact of the system design and the energy strategy on each other, the optimal sizing of the GSBS is able to maximize the return on investment with respect to the technical and economic conditions of the deployment. Also, thanks to its learning capabilities, the GSBSs can be deployed in a plug-and-play fashion, with the ability to self-organize, improve the operating energy cost of the system, and preserves the battery lifespan.

RÉSUMÉ

Face à l'explosion du trafic mobile entraînée par le succès des smartphones, les opérateurs de réseaux mobiles (MNO) densifient leurs réseaux à travers le déploiement massif des stations de base à faible portée (SBS), capable d'offrir des services très haut débit et de remplir les exigences de capacité et de couverture. Cette nouvelle infrastructure, appelée réseau cellulaire hétérogène (HetNet), utilise un mix de stations de base hiérarchisées, comprenant des macro-cellules à forte puissance et des SBS à faible puissance.

La prolifération des HetNets soulève une nouvelle préoccupation concernant leur consommation d'énergie et empreinte carbone. Dans ce contexte, l'utilisation de technologies de production d'énergie renouvelable dans les réseaux mobiles a suscité un intérêt particulier. Les sources d'énergie respectueuses de l'environnement couplées à un système de stockage d'énergie ont le potentiel de réduire les émissions carbone ainsi que le coût opérationnel énergétique des MNOs.

L'intégration des énergies renouvelables (panneau solaire) et du stockage d'énergie (batterie) dans un SBS gagne en efficacité grâce aux leviers technologiques et économiques apportés par le smart grid (SG). Cependant, l'architecture résultante, que nous appelons Green Small-Cell Base station (GSBS), est complexe. Premièrement, la multitude de sources d'énergie, le phénomène de vieillissement du système et le prix dynamique de l'électricité dans le SG sont des facteurs qui nécessitent planification et gestion pour un fonctionnement plus efficace du GSBS. Deuxièmement, il existe une étroite dépendance entre le dimensionnement et le contrôle en temps réel du système, qui nécessite une approche commune capable de résoudre conjointement ces deux problèmes. Enfin, la gestion holistique d'un HetNet nécessite un schéma de contrôle à grande échelle pour optimiser simultanément les ressources énergétiques locales et la collaboration radio entre les SBSs.

Par conséquent, nous avons élaboré un cadre d'optimisation pour le pré-déploiement et le post-déploiement du GSBS, afin de permettre aux MNOs de réduire conjointement leurs dépenses d'électricité et le vieillissement de leurs équipements. L'optimisation pré-déploiement consiste en un dimensionnement du GSBS qui tient compte du vieillissement de la batterie et de la stratégie de gestion des ressources énergétiques. Le problème associé est formulé et le dimensionnement optimal est approché en s'appuyant sur des profils moyens (production, consommation et prix de l'électricité) à travers une méthode itérative basée sur le solveur non-linéaire *fmincon*. Le solution de post-déploiement repose sur des capacités d'apprentissage permettant d'ajuster dynamiquement la gestion énergétique du GSBS à son environnement (conditions météorologiques, trafic de données, état de la batterie et coût de l'électricité). Cette méthode s'appuie sur le Fuzzy Q-Learning qui consiste à combiner le système d'inférence floue avec l'algorithme Q-learning. Ensuite, nous formalisons un système d'équilibrage de charge capable d'étendre la gestion énergétique locale à une collaboration à l'échelle d'un réseau. Nous proposons à ce titre un algorithme en deux étapes, combinant des contrôleurs hiérarchiques au niveau du GSBS et au niveau du réseau. Les deux étapes s'alternent pour continuellement planifier et adapter la gestion de l'énergie à la collaboration radio dans le HetNet.

Les résultats de la simulation montrent que, en considérant le vieillissement de la batterie et l'impact mutuel de la conception du système sur la stratégie énergétique (et vice-versa), le dimensionnement optimal du GSBS est capable de maximiser le retour sur investissement. En outre, grâce à ses capacités d'apprentissage, le GSBS peut être déployé de manière plug-and-play, avec la possibilité de s'auto-organiser, d'améliorer le coût énergétique du système et de préserver la durée de vie de la batterie.

KEYWORDS

Green communications, Heterogeneous Mobile Networks, Renewable energy, Smart grid, Energy management, System sizing, Battery aging, Fuzzy Q-learning.

CONTENTS

Contents	5
List of Figures	7
List of Tables	9
Abbreviations and acronyms	10
Notations	12
1 Introduction	12
1.1 Background	12
1.2 General goals of the Thesis	13
1.3 Structure of the Thesis and Outline	13
1.4 Publications and Patents	14
1.5 Funding	15
2 Context and Research Problems	16
2.1 Introduction	16
2.2 Heterogeneous Cellular Networks	17
2.3 Evolution of the Energy Context	21
2.4 Research Problems	25
2.5 Research methodology and Contributions	29
2.6 Conclusion	31
3 The Green Small Cell Base Station	32
3.1 Introduction	32
3.2 The proposed Green Small Cell Base Station	34
3.3 Small Cell Base Station Model	36
3.4 Photo-voltaic Production and Ambient Temperature Model	38
3.5 Battery Model	40
3.6 Electricity Pricing Model	44
3.7 Conclusion	45
4 The sizing of a Green Small-Cell Base Station	46
4.1 Introduction	46
4.2 System Sizing and the Subsequent Energy Management Problem	48
4.3 Results	52
4.4 Conclusion	62
5 FQL-based energy management	63

5.1	Introduction	63
5.2	Fuzzy Q-Learning technique	64
5.3	Implementation of <i>Fuzzy Q-Learning</i> (FQL) for the GSBS Management	70
5.4	Kalman estimation-based method	73
5.5	Simulation Results	75
5.6	Conclusion	81
6	Towards a collaborative large scale energy management	82
6.1	Introduction	82
6.2	System Model	84
6.3	Energy-Aware Management of Green HetNets	88
6.4	Simulation results	89
6.5	Conclusion	93
	Conclusions	95
	Main conclusions	95
	Future Work	97
	Appendix A Appendices	99
	Appendices	99
	A.1 How to Further Reduce the Calendar Aging of the Battery: Artificial Cycling	99
	A.2 Non-Linear programming	102
	Bibliography	103

LIST OF FIGURES

2.1	General network architecture of mobile networks.	17
2.2	Hexagonal Cell Layout.	18
2.3	Mobile traffic trend according to Cisco VNI Mobile.	19
2.4	Illustration of a heterogeneous network with macro and small cells.	20
2.5	Conventional organization of electrical power systems.	21
2.6	Key factors of the SG [Fang 2012].	22
2.7	Classification of energy storage technologies [Luo 2015].	24
2.8	Energy density per battery Chemistry [EPEC].	24
2.9	Proposed framework for green HetNets.	25
2.10	Classification of state variable models [Ulukus 2015a].	26
2.11	Classification of mathematical techniques for optimization (adapted from [Riffonneau 2011]).	28
3.1	System architecture of GSBS.	34
3.2	Block diagram of a SBS transceiver (adapted from [Auer 2011]).	36
3.3	Profile of the average small cell load λ [Auer 2010].	37
3.4	Solar Cell I-V Characteristic Curve for a given solar irradiation.	38
3.5	Profile of the average solar irradiation μ_{irrad}	39
3.6	Profile of the average ambient temperature μ_{temp}	39
3.7	Equivalent circuit model of a battery cell.	40
3.8	Equivalent circuit of a battery pack.	41
3.9	Recommendations for the operating range of <i>State of Charge</i> (SoC) of Lithium-ion battery [MpowerUK].	43
3.10	Profile of the average electricity price μ_{price}	44
4.1	Normalized profiles of the average solar radiation, average ambient temperature [SOLAR], SBS load intensity (based on [Auer 2010]), and average energy price [Ameren].	53
4.2	Benefits for different battery and <i>Photo-Voltaic</i> (PV) sizing.	54
4.3	SOH loss during one year for different battery capacities using a PV panel of 0.25 m ²	55
4.4	SOH loss during one year for different PV surfaces.	56
4.5	Benefits for different battery and PV sizings in case 1	57
4.6	Benefits for different battery and PV sizings in case 2	57
4.7	Benefits for different battery sizes and PV conversion efficiencies.	58
4.8	Benefits for different battery sizes in different load scenarios.	58
4.9	Impact on the benefits of the price factor ($\psi = 0\%$).	59
4.10	Impact on the benefits of the financial aid factor ($\kappa = 100\%$).	60
4.11	Benefits gain with the ideal energy management compared to the average-based energy management.	61
4.12	Power flows in an off-grid GSBS.	61
5.1	Fuzzy Inference System.	65
5.2	The agent-environment interaction in <i>Reinforcement Learning</i> (RL).	67

5.3	Visualization of the Q-values.	67
5.4	The agent-environment interaction in FQL.	69
5.5	Graphic representation of FQL.	71
5.6	Linguistic variables membership functions.	72
5.7	Normalized profiles of the average solar radiation, average ambient temperature [SOLAR], SBS load intensity (based on [Auer 2010]), and average energy price [Ameren].	76
5.8	Average power flows with (a) unconstrained Kalman strategy (b) constrained Kalman strategy (c) unconstrained FQL strategy (d) constrained FQL strategy (e) SoC comparison between unconstrained Kalman and FQL strategies (f) SoC comparison between the SoC constrained Kalman and FQL strategies.	78
5.9	Convergence of the FQL algorithm.	79
5.10	(a) Average cycle aging for Kalman and FQL strategies (b) Average calendar aging for Kalman and FQL strategies (with and without SoC constraints).	79
5.11	Average battery internal temperature for Kalman and FQL strategies (with and without SoC constraints).	80
6.1	Two-tier green HetNet architecture.	84
6.2	Area \mathcal{A}_U partition.	85
6.3	Average number of users in area \mathcal{A}_U	90
6.4	Location of the network's components.	90
6.5	SBS 1 Bandwidth requirement per sub-area ($\bar{w}_{BS_1, \mathcal{A}_k}$).	91
6.6	Bandwidth requirement per sub-area.	91
6.7	Load balancing.	92
6.8	Cumulative energy consumption of the network in the collaborative and non-collaborative schemes.	92
6.9	Power consumption vs number of users	93
6.10	Average power flows for (A) SBS 1 (non-collaborative) (B) SBS 1 (collaborative) (C) SBS 2 (non-collaborative) (D) SBS 2 (collaborative).	94
A.1	Average SoC strategy under different sets of battery constraints.	100
A.2	Average evolution of the <i>State of Health</i> (SoH) due to calendar aging under different sets of battery constraints.	100
A.3	Average evolution of the SoH due to cycle aging under different sets of battery constraints.	101

LIST OF TABLES

- 2.1 Characteristics of Various Cell Types [Auer 2011]. 18
- 2.2 Renewable Energy Usages 21

- 3.1 SBS parameters for the power model [De Domenico 2014a]. 37

- 4.1 Simulation Parameters [Pilot 2013, IEA-PVPS 2015, Dusonchet 2015]. 53
- 4.2 Battery Aging Simulation Parameters [Uddin 2014] [Ecker 2012]. 53

- 5.1 Simulation Parameters [Pilot 2013]. 75
- 5.2 Normalized average *OPERating EXpenditures* (OPEX) for different strategies. 81

ABBREVIATIONS AND ACRONYMS

3GPP	· <i>3rd Generation Partnership Project</i>
AC	· <i>Alternating Current</i>
BB	· <i>BaseBand</i>
BS	· <i>Base Station</i>
CAPEX	· <i>CAPital EXpenditures</i>
CN	· <i>Core network</i>
DEM	· <i>Discrete Element Model</i>
DER	· <i>Distributed Energy Resource</i>
DES	· <i>Distributed Energy Storage</i>
DG	· <i>Distributed Generation</i>
DC	· <i>Direct Current</i>
DR	· <i>Demand Response</i>
EARTH	· <i>Energy Aware Radio and NeTwork TecHnologies</i>
ESS	· <i>Energy Supervision System</i>
EU	· <i>EUropean commission</i>
FC	· <i>Fixed Cost</i>
FIS	· <i>Fuzzy Inference System</i>
FQL	· <i>Fuzzy Q-Learning</i>
G	· <i>Gain from investment</i>
GSBS	· <i>Green Small-cell Base Station</i>
HetNet	· <i>Heterogeneous cellular Network</i>
ICT	· <i>Information and Communication Technology</i>
LBC	· <i>Load Balancing Controller</i>
LTE	· <i>Long Term Evolution</i>
MNO	· <i>Mobile Network Operator</i>

MPP	· <i>Maximum Power Point</i>
OCV	· <i>Open Circuit Voltage</i>
OPEX	· <i>OPerating EXpenditures</i>
OFDMA	· <i>Orthogonal Frequency-Division Multiple Access</i>
PV	· <i>Photo-Voltaic</i>
PA	· <i>Power Amplifier</i>
QoS	· <i>Quality of Service</i>
RAN	· <i>Radio Access Network</i>
RF	· <i>Radio Frequency</i>
RTP	· <i>Real Time Pricing</i>
RM	· <i>Reception Module</i>
RL	· <i>Reinforcement Learning</i>
RE	· <i>Renewable Energy</i>
RC	· <i>Running Cost</i>
SON	· <i>Self Organizing Networks</i>
SINR	· <i>Signal-to-Interference-plus-Noise Ratio</i>
SBS	· <i>Small-cell Base Station</i>
SG	· <i>Smart Grid</i>
SoC	· <i>State of Charge</i>
SoH	· <i>State of Health</i>
TS	· <i>Takagi-Sugeno</i>
ToU	· <i>Time of Use</i>
TM	· <i>Transmission Module</i>
TRX	· <i>Transceiver</i>
UE	· <i>User Equipment</i>

INTRODUCTION

1.1 BACKGROUND

Global warming is one of the biggest and critical challenges of our era. For many years, human and industrial activity sectors have relied on fossil fuel (such as coal, oil, and gas) as an energy source. However, in addition to be not sustainable, this energy supply is causing our climate to overheat. A major objective of the *EUropean commission* (EU) is achieve energy transition, *i.e.*, to decarbonize energy supplied by switching to renewable sources and reducing demand by means of greater efficiency [Morris 2016]. Specifically, the EU energy road-map 2020 (known commonly as the "3×20") aims to reduce 20% of the greenhouse gas emissions, increase the share of renewable energy to 20% of consumption, and achieve 20% or energy efficiency compared to 1990 levels. The 2030 EU road-map sets even more ambitious objectives (resp. 40%, 27%, and 27%) and the upward trend is expected to continue.

It is clear that the energy transition requires innovation throughout the whole energy chain, including production, distribution, and consumption. The power grid, important actor in the energy chain, is also undergoing major changes. The concept of *Smart Grid* (SG) combines the *Information and Communication Technology* (ICT) with new energy technologies and provide infrastructure to enable the technological integration of *Renewable Energy* (RE) systems and form new market mechanisms based on flexibility (such as varying electricity pricing).

If the ICT sector is a key enabler of the SG, it remains nevertheless a heavy energy consumer. The ratio of ICT energy consumption to the global electricity consumption is rapidly growing, from 7.1% in 2008 to 14.6% by 2020 [Vereecken 2010]. The direct carbon emissions are also expected to rise significantly over the coming years (from 40 Gt CO₂e in 2002 to 51 Gt CO₂e by 2020) [Webb 2008]. In particular, *Heterogeneous cellular Networks* (HetNets) are considered as large contributors with 15% of the ICT global energy consumption and 13% of the ICT emissions by 2020 [Webb 2008].

Historically, communication networks have been mainly designed with the aim of optimizing performance metrics such as the data-rate, throughput, and latency. HetNets have exactly been deployed to address such issues in a context of growing mobile data demand. However, energy consumption and carbon emissions have become a primary concern in the design and operation of mobile communication systems, and energy efficiency has emerged as a new prominent criterion for *Mobile Network Operators* (MNOs) [De Domenico 2014a].

Envisioning a "green" HetNet that relies on RE requires efficient deployment and operating strategies. In addition to the environmental benefit, MNOs need an attractive business model, which, in turn, necessitates a holistic management based on the adaptation of the local energy and radio resources to the SG market.

1.2 GENERAL GOALS OF THE THESIS

This thesis is built around the *Green Small-cell Base Station* (GSBS) architecture detailed in Chapter 3. Such architecture is connected to the SG, and contains a *Small-cell Base Station* (SBS), a *Photo-Voltaic* (PV) panel (RE system), and a battery (energy storage). The global purposes are to decrease the system's carbon footprint by optimizing its energy consumption from the power grid, reduce the energy *OPERating EXpenditures* (OPEX), and slow down the system aging, of which the battery degradation constitutes the dominant part.

These general purposes bring about the following concrete objectives:

1. The studied architecture is complex as it consists of a combination of several sub-systems. To understand how it operates, we want to model the behavior of each components and their interfaces. Then we require an optimization framework in which the global objective function is quantitatively evaluated.
2. The second objective is to determine the sizing of the PV panel and the battery before the deployment of the GSBS. This will enable the system to operate efficiently while avoiding economic and energy waste.
3. The third objective takes place after the deployment of the GSBS. The need is to determine an energy strategy that autonomously adapts to the evolution of the GSBS's environment variables (weather, data traffic, and electricity price). The local management is intended to reduce the electricity cost and the battery aging.
4. The last objective is introducing perspectives on how to extend local energy management framework to a large scale cooperation of GSBSs.

1.3 STRUCTURE OF THE THESIS AND OUTLINE

This thesis is composed of a brief introduction, five chapters, and a summary of conclusions and perspectives. We also have included 2 appendices. The main points of each part of the manuscript is presented in the following.

- *Chapter 2: Context and Research Problems.* We discuss the characteristics, advantages, and challenges of the HetNet. We also present the main key factors of the SG that support the energy transition in HetNets. Finally, we overview the main research problems that we address in this work.
- *Chapter 3: The Green Small-Cell Base Station.* We detail the architecture of the GSBS, composed of a SBS, RE system (PV panel), and energy storage (battery), and connected to the SG. The proposed energy management is centered around the battery and relies on the selected model for each system component. The objective function is then defined to jointly reduce the expenses related to electricity consumption and the system aging cost.
- *Chapter 4: Sizing of a Green Small-Cell Base Station.* We investigated the sizing problem of a GSBS in two configurations: on-grid (grid-connected) and off-grid. The sizing problem is formulated to include the fixed cost of the investment related to the equipment purchase/installation, the running cost due to system aging, and the cost saving achieved by the investment, obtained by solving the inherent energy management. The parametric approach we propose to solve the sizing problem relies on the average profiles of the state variables, *i.e.*, energy consumption, production, and cost. Extensive simulations show the existence of an optimal solution that depends on the system conditions. In addition, based on the off-grid sizing, we propose an analysis to evaluate the maximum acceptable connection cost and the critical distance from the grid after which the connection to the SG is not economically valuable.
- *Chapter 5: Fuzzy Q-Learning (FQL)-based energy management.* We propose a model-free energy

management controller based on FQL that jointly minimizes the operating energy cost and preserves the battery lifetime. We compare the proposed method with other approaches, namely an online technique from the literature based on Kalman filter [Leithon 2013] and what we refer to as the *ideal* strategy, which is aware of the future states of the system variables. System simulations show that the FQL controller achieves considerable cost reduction compared to the method based on Kalman filter and other baseline strategies. Furthermore, the obtained energy management policy performs very closely to the *ideal* strategy. Also, simulation results show that, because the proposed energy management strategy is aware of the battery aging processes, we are able to enhance the battery life span by 30% per year.

- *Chapter 6: Towards a collaborative large scale energy management.* We propose a simplified scenario that extends the local energy management to a network-level collaboration of the GSBS. The idea is to transfer the energy demand between several GSBSs by redistributing the mobile users with respect to the availability of the local energy resources and the *Quality of Service* (QoS) requirements. This energy-aware load-balancing problem is formulated and the solution is derived using a two-stage algorithm. The latter divides the action process into two steps. The first stage occurs at the GSBS level and consists in learning the optimal management of the energy resources. The second stage happens at the network level and implements a load balancing strategy with respect to the average profiles of the user's traffic, RE production, and the electricity price. The two stages are alternated to continuously plan and adapt the energy management to the radio collaboration in the HetNet. Simulation results show that the obtained solution is able to increase the energy efficiency of the network, reduce the energy cost, and decrease the battery aging.

1.4 PUBLICATIONS AND PATENTS

ARTICLES

- [J1] Mendil, M., De Domenico, A., Heiries, V., Caire, R. and Hadjsaid, N. Battery-Aware Optimization of Green Small Cells: Sizing and Energy Management. *IEEE Transactions on Green Communications and Networking* (2018).
- [J2] Mendil, M., De Domenico, A., Heiries, V., Caire, R. and Hadjsaid, N., 2017. Battery aging-aware energy management of green small cells powered by the smart grid. *EURASIP Journal on Wireless Communications and Networking*, 2017(1), p.127.
- [J3] De Domenico, A., Bonnefoi, R., Mendil, M., Gavriluta, C., Palicot, J., Moy, C., Heiries, V., Caire, R. and Hadjsaid, N., 2016. Une architecture intelligente pour l'amélioration de l'efficacité énergétique du réseau cellulaire 5G. *La Revue de l'Electricité et de l'Electronique*, (5).

PROCEEDINGS

- [C1] Mendil, M., De Domenico, A., Heiries, V., Caire, R. and Hadjsaid, N., 2016, September. Fuzzy Q-Learning based energy management of small cells powered by the smart grid. In *Personal, Indoor, and Mobile Radio Communications (PIMRC), 2016 IEEE 27th Annual International Symposium on* (pp. 1-6). IEEE.
- [C2] Mendil, M., De Domenico, A., Heiries, V., Caire, R. and Hadjsaid, N., 2016, May. Energy Management of Green Small Cells Powered by the Smart Grid. In *International Conference on Cognitive Radio Oriented Wireless Networks* (pp. 642-653). Springer, Cham.
- [C3] Bonnefoi, R., Mendil, M., Gavritula, C., Palicot, J., Moy, C., Heiries, V., De Domenico, A., Caire, R. and Hadjsaid, N., 2016, March. A Low Energy Consumption Wireless Cellular Network. In *Journées Scientifiques URSI France Energie et radiosciences* (pp. 201-205).

PATENT

- [P1] Mendil, M., De Domenico, A. Heiries, V., Caire, R. and Hadjsaid, N. Process for controlling electrical energy fluxes in a system for radio access to a communication network, and associated control device. U.S. Patent Application 15/583,004.

1.5 FUNDING

The research leading to these results is funded by the French Agence Nationale de la Recherche in the framework of the SOGREEN project (ANR-14-CE29-0025-01).

CONTEXT AND RESEARCH PROBLEMS

Contents

2.1	Introduction	16
2.2	Heterogeneous Cellular Networks	17
2.2.1	Mobile Networks and Cellular organization	17
2.2.2	Towards a Heterogeneous Structure of Cellular Networks: Objectives and Challenges	18
2.3	Evolution of the Energy Context	21
2.3.1	The smart grid	21
2.3.2	Distributed Generation and Renewable Energy Sources	22
2.3.3	Energy Storage	23
2.3.4	Demand Response and Electricity Pricing	24
2.4	Research Problems	25
2.4.1	Modeling Approach	26
2.4.2	Sizing and control	27
2.5	Research methodology and Contributions	29
2.6	Conclusion	31

2.1 INTRODUCTION

The ICT industry is seen as an increasingly important energy consumer from 7.1% in 2008 to 14.6 % of the worldwide power consumption expected by 2020 [Vereecken 2010]. In this context, the European Commission has acknowledged the opportunities ICT has to offer in reducing the energy intensity of the economy and pointed out that ICT needs to lead by example in increasing its energy efficiency [Communities 2008]. In particular, the power demand of mobile networks constitutes a substantial proportion of the total ICT consumption and is in continuous growth [Vereecken 2010]. In this chapter we will overview the opportunities brought by the energy transition to improve the energy usage in HetNets, which constitute the next generation of mobiles networks.

In Section 2.2, we define the mobile HetNet architecture and present the energy challenges of the mobile networks. In Section 2.3, we discuss the technological and economic enablers leveraged by the SG to support the energy transition in HetNets. Section 2.4 defines the major research problems that need to be addressed. Section 2.5 gives an overview about the adopted methodology to solve the research problems and presents the associated contributions. Finally, we summarize the Chapter in Section 2.6.

2.2 HETEROGENEOUS CELLULAR NETWORKS

2.2.1 MOBILE NETWORKS AND CELLULAR ORGANIZATION

The mobile network is a support of communication for wireless equipments. It allows several static or mobile wireless devices to access voice and data services such as telephony and Internet. The high-level architecture of mobile networks is illustrated in the Fig. 2.1. This schematic is general and aims to show the different components in the network, which are the following:

- *User Equipment (UE)*: any device used directly by an end-user to access voice and data services such as laptops, and smart-phones.
- *Radio Access Network (RAN)*: handles the radio communication between the UEs and the core network. It is composed of several radio-transceivers called *Base Stations (BSs)*, each connecting to a number of UEs.
- *Back-haul*: comprises the intermediate links between the core network, and the different components of the RAN. Generally, back-haul solutions can largely be categorized into wired (copper, fiber) or wireless depending of different parameters such as capacity, cost and reach.
- *Core network (CN)*: central part of a telecommunications network that provides various services (routing calls, internet ...) to customers who are connected by the access network.

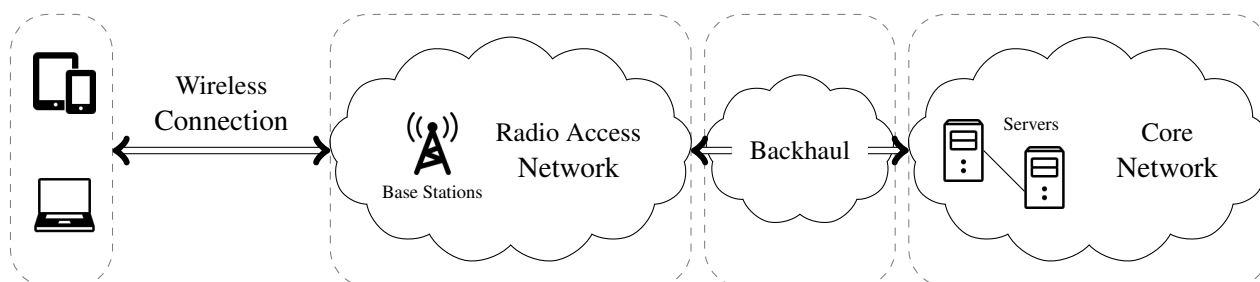


FIGURE 2.1: *General network architecture of mobile networks.*

In mobile networks, the wireless communication is based on *Radio Frequency (RF)* transmission of data. This kind of transmission relies on the usage of the radio spectrum, which is a limited and expensive resource. As a consequence, the majority of radio access technologies have to distribute as efficiently as possible the available radio spectrum between many users. This concern is addressed in the wireless part of mobile networks, which mainly corresponds to the RAN. As a matter of fact, the RAN is composed of a large number of BSs with limited power, each covering only a limited area called "cell". The limited power makes it possible to re-use the same frequency a few cells away from the BS without causing harmful interferences. In this way, a large geographic area can be covered with only a limited set of frequencies. This makes the "cellular" structure a very efficient manner of using the scarce frequency resources.

The BSs in the RAN provide radio communication (using radio transceivers) within one of several cells in order to enable UEs (e.g., cell phones, smart-phones) to communicate with each others and access various services. They also enable seamless wireless handover, *i.e.*, a continuous conservation of the QoS when UEs are moving through different cells. Fig. 2.2 represents a schematic view of a typical layout of a cellular network. The coverage area of a cell is normally illustrated as a hexagon, but in practice it has an irregular shape. Also, the coverage range depends on a number of factors (such as BS's height and transmit power), and defines four types of cells:

- *Macro-cells* (radius from 1 km to 10 km) have the widest coverage and are used in rural and urban areas or highways.
- *Micro-cells* (radius from 200 m to 1 km) are used in urban and high density areas.
- *Pico-cells* (radius from 100 m to 200 m) have smaller coverage than micro-cells and are used in

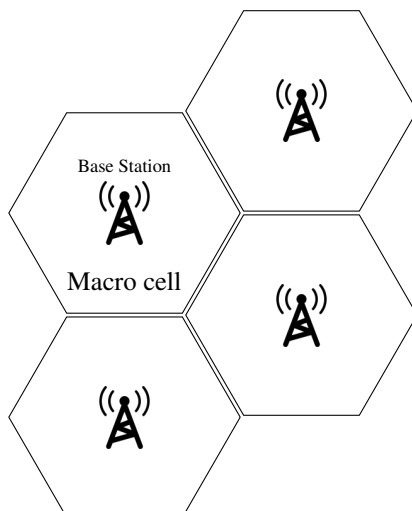


FIGURE 2.2: Hexagonal Cell Layout.

malls, subways, tunnels, or outdoor hot-spots.

- Femto-cells (radius less than 100 m) have the smallest coverage area and is used indoor for providing mobile access in homes or offices.

The term small-cell is used to designate a small cellular area, including femto-cells, pico-cells, and micro-cells. A SBS is a BS covering a small-cell. We regroup in Table 2.1 the characteristics of various cell types and their associated BSs.

TABLE 2.1: Characteristics of Various Cell Types [Auer 2011].

Cell Type	Deployment	Maximum Cell Radius	Maximum RF Output Power	Maximum Power Consumption
Femto	Indoor	100 m	50 mW	10.4 W
Pico	Indoor/Outdoor	200 m	130 mW	14.7 W
Micro	Outdoor	1 km	6.3 W	144.6 W
Macro	Outdoor	10 km	20 W	1350 W

In the rest of this dissertation, we use interchangeably the expressions macro-cell BS (respectively micro-cell BS, pico-cell BS, and femto-cell BS) and macro-BS (respectively micro-BS, pico-BS, and femto-BS) to designate a BS covering a macro-cell (respectively micro-cell, pico-cell, and femto-cell).

2.2.2 TOWARDS A HETEROGENEOUS STRUCTURE OF CELLULAR NETWORKS: OBJECTIVES AND CHALLENGES

In the traditional homogeneous network, composed only of macro-cells, all the BSs have similar transmit power levels and serve roughly the same number of UEs. The locations of the macro-BSs are carefully chosen through network planning, and the BS settings are properly configured to maximize the coverage and control the interference with neighboring cells.

As the traffic demand grows (Cisco forecasts an exponential increase in global mobile data traffic to achieve 24.3 Exabytes per month by 2019, see Fig. 2.3), the network needs to overcome capacity limitations and maintain uniform user experience. Historically, the MNOs used to improve the wireless coverage and capacity through additional carriers (bandwidth) and acquiring new cell sites. However, site and bandwidth

acquisition for macro-BSs is expensive and becomes more and more difficult in dense urban areas [Qualcomm 2011]. Therefore, it is only by finding flexible business and technical models that the MNOs can improve the network capacity in a ubiquitous and cost-effective way.

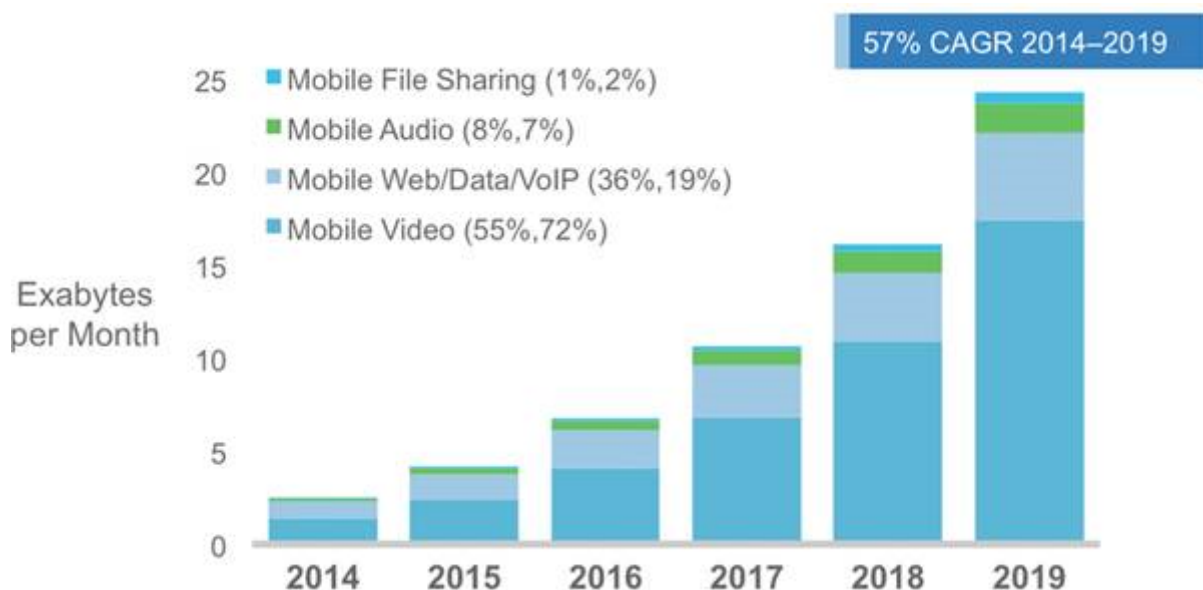


FIGURE 2.3: Mobile traffic trend according to Cisco VNI Mobile.

The concept of HetNets has emerged in the context of *Long Term Evolution* (LTE) and corresponds to a mobile network whose RAN comprises layers of different-sized cells. As represented in Fig. 2.4, this cellular system consists of regular (planned) placement of macro-BSs that transmit at high power level, overlaid with several SBSs, which transmit at substantially lower power levels and are typically deployed in a relatively unplanned manner. The low-power SBSs can be deployed to eliminate coverage holes in the macro-only system and improve capacity in hot-spots [Qualcomm 2011]. Contrarily to the deployment of macro-BSs that requires a careful network planning, the placement of SBSs is mostly ad-hoc, based only on a rough knowledge of coverage issues and traffic density (*e.g.*, hot-spots) in the network.

Small-cell deployment has garnered significant interest in the mobile industry and research communities due to the low cost of SBSs, the deployment flexibility, and the capacity enhancement benefits. Currently, the total number of the small cells deployed has already exceeded the number of installed macro-cells [Andrews 2012]. The multiplication of small-cells is also an important step towards the 5th Generation (5G) of mobile networks, which promises considerable improvements such as high data rate (1000 times more than 4G), lower latency (< 1 ms), and 100 times less energy consumption compared to 4G networks [Andrews 2014]. The low energy objective and the concerns about the network's carbon footprint have stimulated the interest of researchers in an innovative research area called "green cellular networks" [Hasan 2011a]. The European Commission has then started several projects within its seventh Framework Programme (FP7) [FP7] to address the energy efficiency of mobile communication systems such as *Energy Aware Radio and NeTwork TecHnologies* (EARTH) [EARTH], *Towards Real Energy-efficient Network Design* (TREND) [TREND], and *Cognitive radio and Cooperative strategies for POWER saving in multi-standard wireless devices* (C2POWER) [C2P].

In such projects and other studies [Koutitas et al. 2010], several concepts have been proposed to improve the energy consumption in mobile networks addressing different aspect such as network planning, protocols, and equipment. The proposed techniques can be classified in term of goals as follows:

- Minimizing the energy consumption by improving the technical characteristics of the equipment such as the efficiency of the power amplifier, which represents 50-80% on the entire power consumption of a macro-BS.

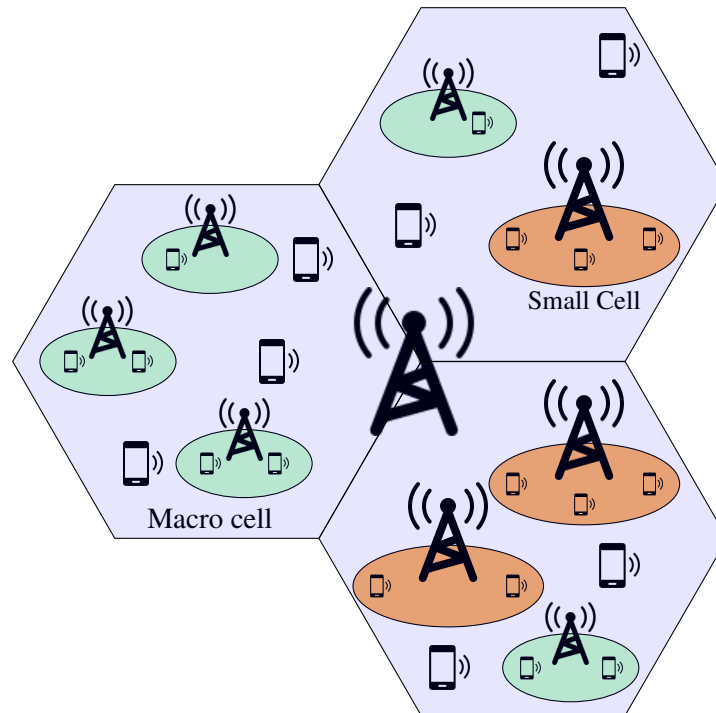


FIGURE 2.4: Illustration of a heterogeneous network with macro and small cells.

- Efficient and energy-aware power management based on the cooperation between BSs: The uneven nature of user distribution and traffic generates unbalanced loads on the neighboring BSs. Therefore, there will always be some cells under low load, while some others may be under heavy traffic load. The concept of *Self Organizing Networks* (SON) has been developed in multiple releases of the *3rd Generation Partnership Project* (3GPP) standards [3GPP 2010] to add network management and intelligence features in the network. According to Hasan *et al.* [Hasan 2011b], substantial amount of energy savings can be obtained through the usage of different mechanisms such load balancing, cognitive radio, cell zooming (a technique through which BSs can adjust the cell size according to the traffic load), and discontinuous transmission (intelligent switching scheme for the SBS during inactivity) [De Domenico 2014b].
- RE: Several recent works start taking explicitly into account the availability and the specificities of RE sources in the functioning of the cellular network infrastructure [Ulukus 2015b]. Adopting RE is necessary in off-grid schemes (desert, island, *etc.*) where the access to the power grid is not possible and the usage of diesel generators is expensive. The main objective is to replace the traditional energy sources by an environmental friendly solution, which firstly decreases the carbon footprint of mobile networks and, through efficient investment into RE technologies, enables substantial long term saving on the operating energy expenditures of the MNOs. The benefits of RE are summarized in the Table 2.2.

In this work, we concentrate on the RE integration in HetNets. Note that this approach is not restricted to energy harvesting and can be considered as a framework that overhauls the aforementioned energy efficient schemes targeting the network's equipment and protocols. Our choice is especially motivated by a context of energy transition in which the 5G is seen as an enabler of the SG; the latter offers many new technological and economic opportunities for the MNOs (such as the use of RE sources, storage technologies, and an open retail electricity market) to enable a green and energy-efficient HetNet. The impact of the energy context is developed in the following section.

TABLE 2.2: Renewable Energy Usages

Renewable Energy Usages	
Global Concerns	MNO Concerns
Decrease greenhouse gas emissions	Reduce the electricity Bill
Decrease the total energy consumption	Sell energy excess

2.3 EVOLUTION OF THE ENERGY CONTEXT

2.3.1 THE SMART GRID

The classical structure of the electric power system, displayed in Fig. 2.5, is characterized by a hierarchical architecture with the top layer represented by the central generation system, going down to the final consumers through the transmission (high-voltage) and distribution (medium-low voltage) networks. The existing electricity grid is a product of rapid urbanization and infrastructure developments in various parts of the world in the past century. Though they exist in many differing geographies, the utility companies have generally adopted similar technologies. Worldwide, the generation capacity was almost entirely ensured by large central power plants, usually based on fossil fuels, nuclear, and hydro power. The power grid, at the time, was specifically designed to transfer energy in one-way, from producers to consumers.

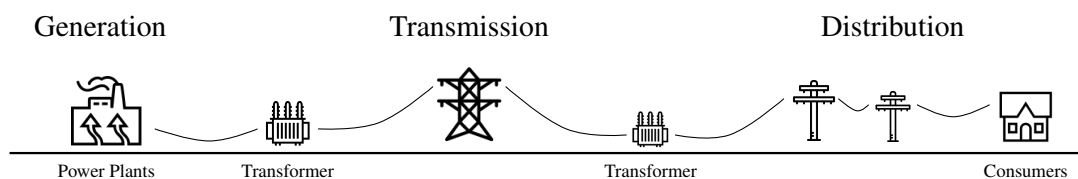


FIGURE 2.5: Conventional organization of electrical power systems.

However, even if the hierarchical structure of the grid remained unchanged for a long period of time, the electrical power system has undergone a continuous evolution (in terms of efficiency, security, and reliability), influenced by economic, political, and geographical factors. In the beginning of the 21st century, with the emergence, among others, of new energy usages, such as massive distributed generation and electric vehicles, the way of thinking the energy grid has shifted to a new concept called SG.

In the strategic deployment document for Europe's electricity networks of the future [Platform 2010], the European commission defines a SG as "an electricity network that can intelligently integrate the actions of all users connected to it - generators, consumers and those that do both - in order to efficiently deliver sustainable, economic, and secure electricity supplies". Other definitions have also been proposed; however, almost all of them stress the common objectives of SG deployment: providing secure, reliable, efficient, and sustainable electricity grid system. This initial concept of SG integrates the idea of a massive usage of advanced metering infrastructure with the aim of improving demand-side management, energy efficiency, and constructing self-healing reliable grid protection against malicious sabotage and natural disasters [Farhangi 2010]. With time, new requirements and demands drove the electricity industries, research organizations, and governments to rethink and expand the initially perceived scope of the SG. Eventually, the essential key factors for SG deployment converged to the following (Fig. 2.6): *Distributed Energy Resource* (DER), smart advanced metering, monitoring/control, and smart micro-grid [Fang 2012].

Without neglecting the impact of the other factors, we will focus on DERs because they offer a privileged ecosystem for RE integration in HetNets. Specifically, centralized generating facilities are giving

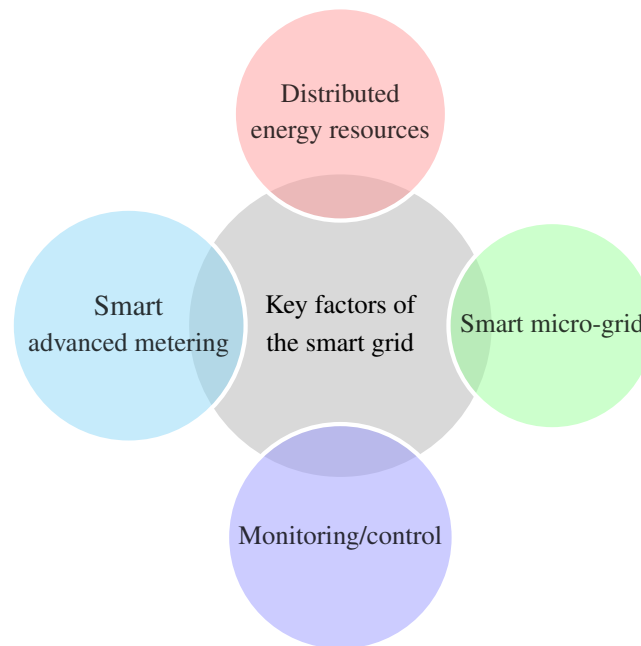


FIGURE 2.6: Key factors of the SG [Fang 2012].

way to smaller, more distributed energy resources partially due to the loss of traditional economies of scale. DER encompasses a wide range of technologies: *Distributed Generation* (DG), *Distributed Energy Storage* (DES), and *Demand Response* (DR) [Poudineh 2014]. The DERs emerging under the SG are especially targeted at the distribution level and present many potential opportunities for the development of green communications. In particular, we will describe the three aforementioned technologies of the DER and discuss how they could be beneficial to our objective: improve the energy usage in HetNets.

2.3.2 DISTRIBUTED GENERATION AND RENEWABLE ENERGY SOURCES

As mentioned before, energy generation in power grids was historically centralized and most electricity worldwide is produced within large (from 1 MW to 1,000 MW) power plants and delivered to electricity users via the transmission and distribution grid. With the growing number of consumers, utilities invested massively in expanding their generation capacity. This becomes problematic today since the planned new generating capacity is not keeping pace with the evolution of the transmission and distribution systems, which is expensive and subject to strict reliability and security constraints [Little 1999].

The DG is part of the answer, which consists in using smaller power plants located at or near electricity users. DG is a promising generating option to meet expected load growth and relieve transmission constraints. The most timely and economical sources of new power may indeed be smaller, strategically located facilities that avoid transmission and distribution infrastructure costs while offering unique benefits that grid power alone cannot provide [Fang 2012].

DG is mainly based on RE generating technologies that produce electricity at distributed levels, including distributed PV systems, micro hydro-power, and small wind turbines. Particularly, PV is one of the most important technology for DG [REN21 2017]. It uses solar cells assembled into solar panels to convert (static conversion) sunlight into electricity. The PV technology is growing rapidly, making solar panels more effective and less costly. The consequence is a fast increase of worldwide installed solar capacity, which doubles every couple of years [IAE 2015]. PV systems are usually deployed in residential, and commercial rooftop or as building integrated installations. The integration of distributed PV capacity in HetNets is therefore interesting given the ad-hoc deployment of SBSs.

As said earlier, the SG is an important enabler of DG. First, it offers the technological means for DG integration in the power grid [Fang 2012], which leads in particular to a two-way interconnection of the PV

installation to the distribution network. Also, the SG enables various business models for DG integration, given the regulation and degree of liberalization of the market environment: many countries have adopted different policies to accelerate investment in RE technologies, called feed-in-tariff [Couture 2010], that specify the benefit of using RE such as the payment of the electricity injected into the grid and even the production consumed locally. Historically, in France for example, it was economically uninteresting for households to consume their own production, as they would rather sell the energy produced and buy separately the electricity delivered by the utility to meet their demand. The regulation has changed and enables now a more favorable framework for self-consumption, which allows the consumers to freely manage their production (consume it locally or sell it back to the grid) [Ministériel 2017].

Basically, every consumer equipped with RE production is confronted with two possibilities, which can be more or less advantageous given the regulation, technological, and economic specificities of each country. The solar energy production that is not immediately consumed by the end-user can be either: 1) injected in the power grid to be delivered to another consumer or 2) stored for later use.

Storing the PV electricity produced enables a more flexible energy usage, which has several benefits especially in the context of dynamic electricity pricing. For example, the MNO can rely on energy storage during the peak price periods, when the electricity is expensive. Alternatively, the stored electricity can also be provided to the SG (in exchange of financial incentives), which can contribute, for example, to a better power grid management during peak energy demand. This flexibility is therefore interesting from both economic and environmental perspectives (see Section 2.3.4) and makes it essential for MNOs to choose a suitable technology of energy storage.

2.3.3 ENERGY STORAGE

Energy storage is the key component for creating flexible energy systems [Komor 2015]. With the integration of RE, energy storage can have multiple attractive value propositions to power network operation, load balancing, and local energy management such as:

- Reducing electrical energy import during peak demand periods, which is advantageous both for end-users (kWh price is generally expensive during peak periods) and the grid stability (some key component of the distribution network can be highly stressed during peak-load).
- Mitigating the intermittence of renewable source power generation: RE technologies can generate energy in a sustainable and environmentally friendly manner. However, their intermittent nature still prevents them from becoming a primary energy carrier. Energy storage technologies have the ability to virtually "offset" the RE production by storing it and making it accessible upon demand.
- Providing time varying energy management: energy storage offers flexibility in managing the consumption from the power grid. It enables to shift the energy consumption, or in the contrary, encourage it, depending on the electricity price and the availability of energy production.

There are many storage technologies including electro-chemical storage (such as batteries), kinetic storage (such as flywheels), mechanic storage (such as pumped hydro storage) and others (see Fig. 2.7). In this work, we concentrate on the battery storage, which is the most frequently used technology with PV installations at the distribution network level.

The battery is a specific storage technology that converts chemical energy directly to electrical energy. It can be based on different chemistries, which determine the battery energy density, load characteristics, maintenance requirements, self-discharge, and operational costs.

Lithium-based batteries are attractive in many sectors ranging from industry (electric vehicles) to consumer oriented applications (*e.g.*, appliances, laptop computers or any electronic device), due to their high energy densities (Fig. 2.8). With proper management, their life-span and performance are among the best electrochemical accumulators [Divya 2009]. The cost is still important compared to other technologies (such as lead-acid batteries) but a significant decrease in the next years is expected so that Li-ion is currently the most interesting technology for the PV applications [Sánchez Muñoz 2016].

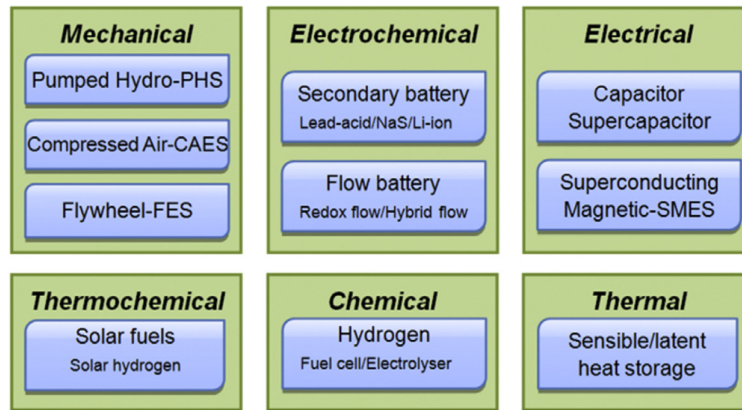


FIGURE 2.7: Classification of energy storage technologies [Luo 2015].

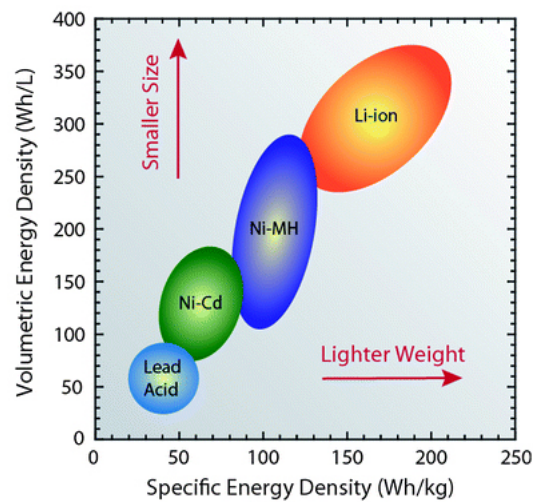


FIGURE 2.8: Energy density per battery Chemistry [EPEC].

2.3.4 DEMAND RESPONSE AND ELECTRICITY PRICING

DR is the capacity of shifting the electricity usage of consumers from their normal or current consumption patterns in response to electricity market signals [Rahimi 2010]. In contrast to energy efficiency, which aims at reducing the overall energy consumption, DR is mainly about shifting consumption to a different point in time. This enable to smoothen the electricity consumption during peak load hours and avoid backup energy production characterized by a high marginal cost and significant carbon footprint. Therefore, DR has the capacity to achieve significant economic and environmental benefits.

Torrìti *et al.* [Torrìti 2011] define two types of DR programs: explicit (automated) DR where the consumption is automatically shifted by a third party operator, and implicit (voluntarily) DR where the consumers change themselves their consumptions. Specifically, the varying electricity price is an implicit DR scheme, which targets to reflect the value and cost of electricity in different time periods. The consumers can decide to shift their electricity consumption away from times of high prices, accordingly. They are rewarded for their flexibility by reducing their electricity bill.

In an exhaustive survey, Borenstein *et al.* [Borenstein 2002] present in details the existing pricing schemes. Particularly, the most used one today is called *Time of Use* (ToU) pricing. Under such scheme, the day is composed of several time periods, each associated to a fixed electricity price. The prices paid for the energy consumed during these periods are pre-established and known by the consumers in advance, thus allowing them to plan their usage in response and manage their energy costs by shifting usage to a lower cost period

or reducing their consumption overall. However, with the technological opportunities brought by the SG, a more adaptive and flexible version of ToU is foreseen, called *Real Time Pricing* (RTP). With this scheme, the electricity prices may change hourly, or even sub-hourly, with price signals provided to the user shortly in advance, reflecting the utility's cost of generating and/or purchasing electricity at the wholesale level. In particular, such pricing, when correctly leveraged, represents an important opportunity for MNOs to reduce the electricity expenditures of the network operations.

2.4 RESEARCH PROBLEMS

The general aim of this work is improving the energy usage in HetNets through integration of RE. In the previous Section, we have discussed the role of the DERs interfaced by the SG, as major technological and economic enablers. The general proposal of a HetNet architecture leveraging DER is depicted in Fig. 2.9. Instead of being powered uniquely by the classical power grid, this architecture is based on an innovative energy framework composed of the following elements:

- The SG provides the technological overhaul for energy import and export on the distribution network.
- The PV panels are the RE source of the system. The energy production can be consumed instantaneously, stored in the battery, or sold to the SG.
- The Li-ion battery is the energy storage in the architecture. It enables to store electricity coming from the SG and/or the PV panel. The battery is discharged to feed the SBSs and/or to sell the energy to the power grid.

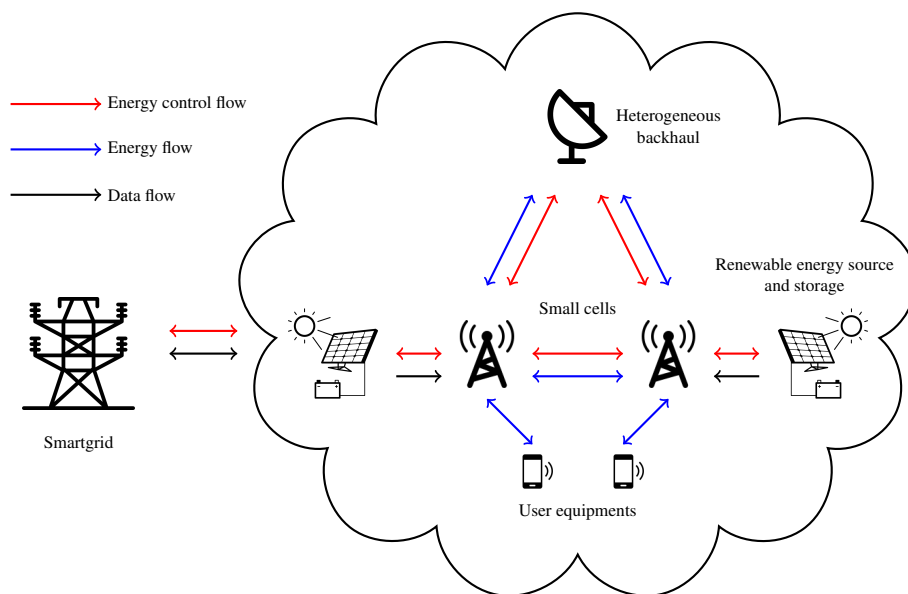


FIGURE 2.9: Proposed framework for green HetNets.

We will provide more details about such architecture in Chapter 3. However, we can already note two issues that need to be addressed: system sizing and control for an optimized OPEX and *CAPital Expenditures* (CAPEX). The OPEX corresponds to the cumulative cost of energy import/export to the SG by MNOs during a period of time. Reducing the OPEX is doubly beneficial: for the MNOs who reduce their electricity bill, and by doing so, participate to DR programs of the distribution system operator, which improves the network's stability and carbon footprint. The CAPEX corresponds to the funds used to acquire and maintain the system. It is therefore affected by the lifetime of the battery and PV panel starting from the moment they are first deployed. These components eventually deteriorate; however, the pace at which they age depends on how they are operated and the environment in which they are installed. With an extended life-span, the frequency of equipment replacement is lower, which makes the investment

economically-efficient and eco-responsible (lower manufacturing environmental footprint).

2.4.1 MODELING APPROACH

2.4.1.1 STATE VARIABLE RANDOMNESS

When dealing with any optimization problem, the obtained performances are systematically related to the representation of the state variables. In the current architecture, three state variables are subject to random phenomena:

- The SBS power consumption: related to the traffic demand of the users served by the SBS.
- The PV panel production: related to the solar irradiation.
- The electricity price in the SG: related to the evolution of retail electricity markets.

Fig. 2.10 shows the classification of various techniques to model such state variables [Ulukus 2015a].

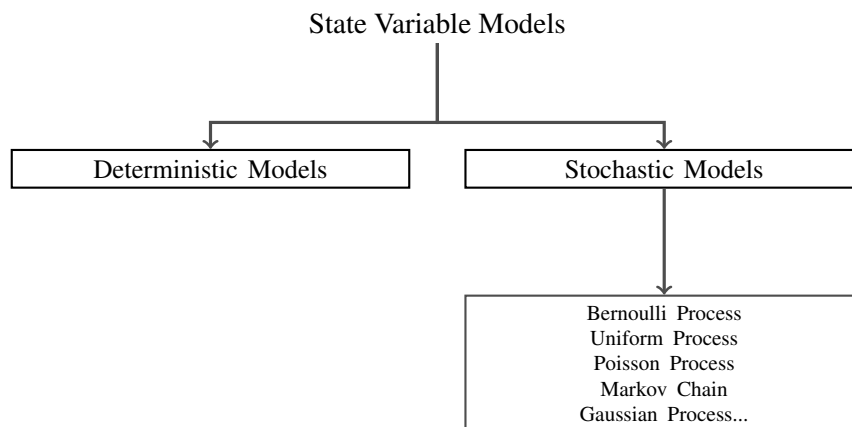


FIGURE 2.10: Classification of state variable models [Ulukus 2015a].

1. *Deterministic Models*: in deterministic models, full knowledge of the variables realization is provided in advance to the decision maker. By assuming that the non-causal information is acquired perfectly, deterministic models are useful to characterize the optimal energy scheduling strategies and to benchmark the fundamental performance limits of energy harvesting systems [Ulukus 2015a]. Nevertheless, such model can heavily limit the effectiveness of the energy management, which relies on accurate state prediction over the optimization time horizon. In general, the deterministic models can only be suitable for the applications in which the state variables are predictable or vary slowly.
2. *Stochastic Models*: in stochastic model, the knowledge of the state variables by the decision maker is subject to uncertainties due to some inherent randomness. In other words, the variable states are not described by unique values, but rather by probability distributions. This type of models is suitable for the applications where the state information cannot be perfectly predictable. However, it is crucial to properly tune the parameters of stochastic model, such as the probability of a UE arrival. In real applications, this should be closely related to real empirical data measured specifically in the environment in which the system is deployed [Ho 2010].

The complexity to represent each state variable lays on the choice and configuration of its model. The latter has to be accurate enough to capture the principal dynamics of the involved phenomena, and still be consistent with the time-scale of the decision making.

2.4.1.2 THE PROBLEM OF BATTERY AGING

The battery degradation is an important phenomenon that has usually been neglected when investigating energy-harvesting cellular networks [Khalilpour 2016] [Liu 2015a] [Leithon 2014] [Niyato 2012]. As a consequence, the economical and environmental impact of the battery aging in such networks is still unknown.

The research and industrial communities have been actively investigating the battery aging models for a large range of chemistries and technologies [Barré 2013]. These models can be classified into two categories, with varying degrees of complexity:

- *Fundamental approach*: the derived models account for particle movement and chemical reactions inside the cell using partial differential equations. They are highly accurate but are computationally consuming (see [Santhanagopalan 2006] for a review of the proposed works based on this approach).
- *Phenomenological approach*: instead of investigating the fundamental physics, this approach provides a representation of the input/output relationship of the system. This is a way of simplifying the behavior of complex systems into a topology consisting of discrete entities that approximate their functioning under certain assumptions. These models present less mathematical complexity, are simple to solve, and suitable for real-time simulation. However, they are not able to achieve an accuracy comparable to fundamental models.

Choosing an aging model enables to understand and quantify the way the battery utilization causes its degradation. The aging models have to be chosen, adapted to, and integrated into the proposed energy optimization framework.

2.4.2 SIZING AND CONTROL

Following the model selection, the optimization problems regarding the sizing of the system's components and the control of its energy resources are to be formulated to jointly optimize the CAPEX and the OPEX. They can be solved using several optimization methods and assuming different levels of correlation between the two problems.

2.4.2.1 OPTIMIZATION METHODS

There are many ways to solve the optimization problems related to energy-harvesting wireless networks, depending on the nature of the problem's parameters. We first distinguish between two optimization classes: off-line and on-line. The first category consists in solving the optimization problem assuming full knowledge of the state variables (deterministic model). The second category uses adaptive methods to take into account the uncertainty of electricity price, RE production, and the data traffic of UEs (stochastic model).

Each of the two classes integrates a set of mathematical tools, depending on the nature of the state variables. These methods are summarized in Fig. 2.11. For discrete-value states, the exact global optimum is found through exhaustive searches (high computational complexity) or graph-based approaches such as dynamic programming and branch & bound. These approaches have generally an exponential complexity and are substituted by less computation-demanding algorithms, such as reinforcement learning, to approximate the optimal solution. Concerning continuous-value states, linear programming provides exact solutions when the problems are linear while non-linear problems relies on numerical algorithms to approximate the optimal solution (more details about non-linear programming are provided in Appendix A.2).

When facing continuous state variables (such as in our case), it is usually more intuitive to recourse to convex optimization. However, the problem at hand can be complex (non-convex) and requires in that case relaxation to approximate (locally or globally) an acceptable solution. Besides, it is also possible to discretize the continuous variable, which enable the exploitation of the associate set of mathematical techniques.

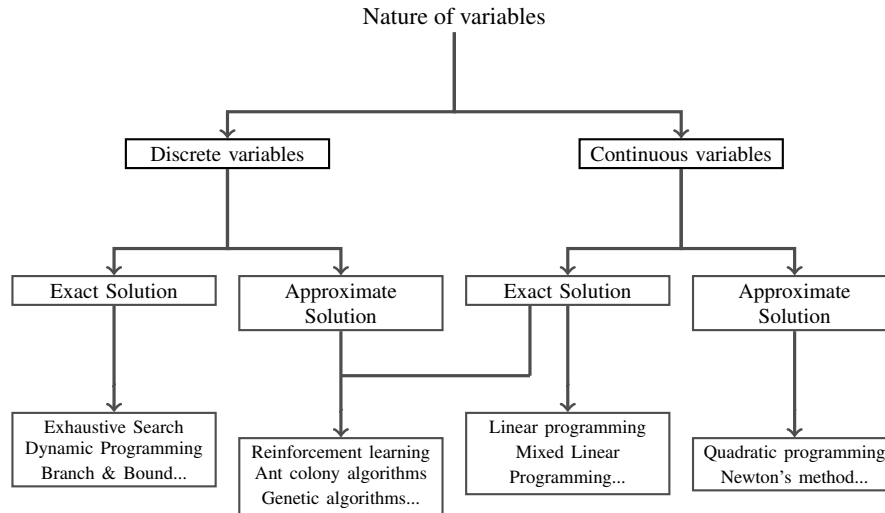


FIGURE 2.11: *Classification of mathematical techniques for optimization (adapted from [Riffonneau 2011]).*

In this work, the problems to solve are the sizing and control of energy-harvesting HetNets. The resolution method needs to be chosen in adaptation with the system model and the nature of the state variables.

2.4.2.2 SYSTEM SIZING/CONTROL CO-OPTIMIZATION

Sizing the energy-harvesting SBS enables to optimize the design of the system's electrical component in terms of CAPEX so it is able to operate with the expected QoS. A basic approach consists in establishing the minimal sizes and ratings of the PV panels and the batteries in order to meet the energy requirements of the SBSs and maintain the UEs' QoS. However, the sizing can be planned with a more developed approach to optimize the return on investment. It means that, in addition to guaranteeing the minimum mandatory service, the equipment characteristics can be tuned to fit their economic environment in the long term given the profile of energy consumption and production. This problem can be very complex, especially when accounting for the system aging in the cost/benefit study.

Also, the quality of the sizing is affected by the energy strategy implemented. As the architecture is marked by the diversity of energy sources and loads, it is nearly impossible to operate such system without an energy controller that dispatches energy from production units to consumption units. Besides, the energy arbitrage can be based on different metrics that orient the energy management strategy such as the network throughput [Ulukus 2015b], electricity operating cost [Liu 2015a], and energy efficiency metrics [De Domenico 2014b]. In general, the energy management is enhanced due to the battery usage, but it is also made more complex. One reason is that the battery offers flexibility by limiting the on-grid energy consumption. As for example, the energy demand of the system, from the power grid's perspective, can virtually be none if the battery covers the power consumption of the BS. Also, the battery permits a flexibility in the production usage. Specifically, instead of being immediately consumed, the energy produced at a certain moment can be stored to meet a later energy demand. The number of possible actions to manage the system is therefore increased and requires an awareness of the system evolution (such as future energy production and consumption, and electricity price).

Several studies have investigated the power control of energy harvesting BSs in the on-grid case and off-grid case (see Chapter 5) and showed that important cost savings can be realized with proper management. Regardless of the method used, we note that the energy management system needs a clear definition of the three following elements:

- System states: the variables that impact the decision making.

- System actions: the possible decisions taken by the controller.
- Objective function: what gives a purpose to the energy management. It is based on the two previously defined metrics.

In real conditions, the energy controller makes decisions with incomplete knowledge of the system evolution. In fact, prediction models are only suitable for a specific situation (geographic area or period of the year) and have inherent limits due to constant evolution of the energy production, consumption, and electricity price. Therefore more adaptive approaches are needed, which are able to tune the decision-making through a continuous interaction with the environment.

Generally, the design of energy harvesting systems uses pre-defined control policies of the energy resources. Such approach is sub-optimal, because of the lack of adaption with respect to the specific dynamics of the state variables. For example, adopting a strategy that completely discharges the battery by the end of the day might be good for a medium sized battery, but not necessarily for twice as much battery size. The reason is that a given energy management strategy is suitable only for a specific configuration of batteries and PV panels, and generalizing it is not optimized for other settings. This illustrates the trivial dependency of the control on the sizing, but also demonstrates that control policies can affect the sizing study. This close correlation between control and sizing makes the design of such architectures very challenging. The resulting framework combines two problems (sizing and control) with different complexities, which add up because of their interdependence.

Also, different from their traditional counterparts, wireless networks with energy harvesting can further optimize the management of their resources (such as power and spectrum allocation) through energy-aware schemes. However, such energy-aware radio cooperation policies gain in complexity, as they are affected by the already complex local energy resources management of the SBSs. Therefore, the design of a holistic resource optimization framework for energy-harvesting networks has to be addressed including the energy opportunities and trade-offs [Chia 2014].

2.5 RESEARCH METHODOLOGY AND CONTRIBUTIONS

Each of the previous research problems are discussed in a dedicated chapter. In each chapter, we present the related works from the literature and highlight the novelty brought by our study.

To answer the research problems, we propose an architecture connected to the SG that contains a SBS, a PV panel (RE source), and a battery (energy storage). The obtained architecture is called GSBS. We choose to simulate the randomness of the system environment (traffic of UEs, solar irradiation, ambient temperature, and electricity price) with realistic stochastic models. Also, the power model of each component of the GSBS is selected to find a good trade-off between the time scale of control and the involved physical dynamics. In particular, we detailed the battery model to capture its non-linear behaviors and aging mechanisms.

Accordingly, we elaborate optimization frameworks for the pre-deployment and post-deployment of GSBSs that allow the MNOs to jointly reduce their electricity expenses and the equipment degradation. The pre-deployment optimization consists in an effective sizing of the GSBS that accounts for the battery aging and the associated management of the energy resources. The problem is formulated and the optimal sizing is approximated using average profiles, through an iterative method based on the non-linear solver *fmincon*. The post-deployment scheme relies on learning capabilities to dynamically adjust the GSBS energy management to its environment (weather conditions, traffic load, and electricity cost). The solution is based on the fuzzy Q-learning that consists in tuning a fuzzy inference system (which represents the energy arbitrage in the system and discretize the state variables) with the Q-learning algorithm. Finally, we formalize an energy-aware load-balancing scheme to extend the local energy management to a network-level

collaboration. We propose a two-stage algorithm to solve the formulated problem by combining hierarchical controllers at the GSBS-level and at the network-level. The two stages are alternated to continuously plan and adapt the energy management to the radio collaboration in the HetNet.

The novelty of this PhD work is represented by the following main contributions:

- *Contribution 1:* We design a GSBS architecture composed of a SBS connected to the SG, integrating RE (PV panel) and energy storage (battery). The purpose of such architecture is to jointly improve the economical –OPEX and CAPEX– and environmental impacts of HetNets. The proposed energy management framework relies on the efficient use of RE and the battery, in a context of time-varying electricity price and two-way energy flow between the GSBS and the SG. Unlike existing works, the actual energy management considers realistic battery models that capture the non-linear behaviors and aging mechanisms.

The novelty of this contribution is based on one patent [P1], one journal article [J2], and a conference paper [C2].

- *Contribution 2:* We propose an approach to find the optimal capacity sizing of the PV panel and the battery in a GSBS. The related problem is formulated to include 1) the *Fixed Cost* (FC) of the investment related to the equipment purchase/installation, 2) the *Running Cost* (RC) due to system aging, and 3) the cost saving achieved by the investment, obtained by solving the associated energy management problem using the non-linear solver *fmincon*. We solve the sizing problem by using an iterative method, which relies on the average profiles of the state variables, *i.e.*, energy consumption, production, and cost. Extensive simulations show the existence of a unique optimal solution that depends on the system conditions. Following a similar approach, we formulate and solve the sizing problem for a stand-alone (*i.e.*, off-grid) GSBS. An analysis of the obtained results enables the evaluation of the critical connection distance between the GSBS and the SG as well as the economical value of this connection.

The novelty of this contribution is based on one journal article [J1].

- *Contribution 3:* We propose a model-free *Energy Supervision System* (ESS) for the GSBS based on FQL. The FQL combines the advantages of Q-Learning and *Fuzzy Inference System* (FIS) and enables to design a controller that does not need any prior knowledge on the energy consumption, energy production, and energy price. In other words, the actual proposal enable a plug-and-play deployment of GSBSs, with the ability to improve the operating energy cost of the system and preserves the battery lifetime.
- *Contribution 4:* We compare the FQL-based method with other approaches, namely: 1) the on-line Kalman filter technique from the literature [Leithon 2013] and 2) what we refer to as the *ideal* strategy, which is aware of the future states of the system variables. System simulations show that the FQL controller achieves considerable cost reduction compared to the method based on Kalman filter and other baseline strategies. Furthermore, the obtained energy management policy performs very closely to the *ideal* strategy. Simulation results also show that by taking into account the battery aging processes, the proposed energy management strategy enhances the battery life span by 30% per year. The battery aging awareness also leads to an increase in the OPEX, however negligible compared to the cost saving on the battery replacement.

The novelty of *Contribution 3* and *Contribution 4* is based one journal article [J2], and a conference paper [C1].

- *Contribution 5:* We formulate an energy-aware load-balancing problem for a network of GSBSs. The aim is to jointly reduce the total energy cost of the network and the system aging by combining hierarchical controllers at the GSBS-level (ESS) and at the network-level (*Load Balancing Controller*

(LBC)). We propose a two-stage algorithm to solve the formulated problem. The first stage occurs at the GSBS level and consists in learning the optimal strategy for managing the local energy resources. The second stage happens at the network level and implements a load balancing strategy with respect to the average profiles of the users' traffic, RE production, and the electricity price. The two stages are alternated to continuously plan and adapt the energy management to the radio collaboration in the HetNet. Simulation results show that the obtained solution is able to increase the energy efficiency of the HetNet, reduce the energy cost, and decrease the battery aging.

2.6 CONCLUSION

This chapter presents the importance of integrating PV energy in mobile networks to support the cost-efficient deployment of HetNets. We have seen that the SG offers many opportunities to this regard, especially thanks to the technological integration of distributed generation and energy storage in the distribution network as well as in a liberalized energy market that creates economic value through DR. At the end of this chapter, we drafted the general architecture that layouts the introduction of PV panels and batteries in HetNets. The associated research issues, namely system sizing and control, have been presented and we stressed the additional complexity due the interdependence between the two problems. In the next chapter, we will detail the proposed architecture and define the associated system model, which will serve to optimize the system sizing and energy management schemes.

THE GREEN SMALL CELL BASE STATION

Contents

3.1	Introduction	32
3.1.1	Motivation	32
3.1.2	Related Works	33
3.1.3	Contribution	33
3.2	The proposed Green Small Cell Base Station	34
3.2.1	System Architecture	34
3.2.2	Energy Management	35
3.3	Small Cell Base Station Model	36
3.3.1	Characteristics	36
3.3.2	Energy Consumption Model	37
3.4	Photo-voltaic Production and Ambient Temperature Model	38
3.4.1	Characteristics	38
3.4.2	Energy Production Model	38
3.5	Battery Model	40
3.5.1	Characteristics	40
3.5.2	Power Model	41
3.5.3	<i>State of Charge</i> (SoC) model	42
3.5.4	Aging Model	42
3.6	Electricity Pricing Model	44
3.6.1	Characteristics	44
3.6.2	Electricity Price Model	44
3.7	Conclusion	45

3.1 INTRODUCTION

3.1.1 MOTIVATION

In the previous chapter, we have discussed the economic and environmental benefits of integrating RE/storage into future mobile HetNets and using the advanced capabilities of the SG for a better management of the energy consumption at the small cells. In order to benefit from these advantages, it is required to

envison a system architecture that integrates all these elements, a clear description of the functions of each components, and the associated interfaces. In addition, to determine an appropriate management strategy, it is necessary to know the behavior of the system according to the data input. This is achievable through the knowledge of input data profile and the suitable operating model of each system component.

3.1.2 RELATED WORKS

Several studies have shown a particular interested to wireless communication devices with energy harvesting capabilities. They proposed different architectures considering various types of harvested energy and technologies of energy storage [Ku 2015]. Also, hybrid systems based on multiple energy sources and storage have been proposed to cope with the variability of RE production. For example, Alsharif *et al.* [Alsharif *et al.* 2016] and A. Kwasinski [Kwasinski 2013] have proposed two hybrid integrations schemes of wind power and solar energy for LTE cellular networks. Ozel *et al.* [Ozel 2014] have presented an energy-harvesting transmitter that has a hybrid energy storage unit composed of a battery and a super-capacitor. Aside from the selection of production and storage technologies, the usage of RE in cellular networks is either dedicated to feed off-grid BSs where the connection to the power grid is expensive [Wang 2015], or to reduce the OPEX related to energy consumption in the on-grid deployment [Ulukus 2015a].

In the majority of the works investigating the on-grid architecture, the main objective is to reduce the amount of the energy consumed from the power grid [Khalilpour 2016] [Liu 2015a] [Leithon 2014] [Niyato 2012]. To do so, they usually rely on energy-scheduling schemes, considering the characteristics and models of the architecture components. However, there are two limitations to be highlighted regarding these studies. First, the energy resource management does not integrate a variable pricing of the electricity coming from the power grid. Yet, with such pricing framework, the SG can enable larger environmental advances and cost reduction for the MNOs (see Chapter 2). Second, the battery is often represented as an energy-buffer that exchanges energy with the sources and loads. This model is unrealistic and too simple to capture the proper functioning of a battery. Some works have considered a non-ideal battery by including new aspects, such as the imperfect knowledge of the battery's SoC [Biaison 2016], energy leakage [Badia 2017], or battery degradation [Michelusi 2013]. However, they especially focused on the battery cycle aging and did not exhaustively analyze the contribution of the calendar aging that degrades the battery when inactive. In this chapter, we propose a GSBS architecture and a suitable system model, which is able to realistically capture the phenomena of interest (particularly the battery aging and the variable electricity price), considering a time-scale where the physical dynamics have to be consistent with the decision making.

3.1.3 CONTRIBUTION

Our main contributions in this chapter are as follows:

- *Contribution 1:* We propose a GSBS architecture connected to the SG that integrates both a PV panel and a battery. The objective of such architecture is to jointly minimizes the expenses related to electricity consumption and the battery aging. The proposed optimization framework relies on the efficient use of the RE and battery, which takes benefit from the time-varying electricity price offered by the SG.
- *Contribution 2:* Contrarily to other works that consider the battery as an energy buffer, we propose an energy management framework focused on the battery control, in which realistic battery models capture the non-linear behaviors and aging mechanisms.
- *Contribution 3:* We describe the operating models of each element of the architecture and the dynamics of their respective input data based on statistical and experimental measurements. The current design considers a time-scale where the physical dynamics of the system components are consistent with the decision making.

The novelty of this chapter is based on one patent [P1], one journal article [J2], and a conference paper [C2].

This chapter is organized as follow. In Section 3.2, we present the proposed green architecture and define the corresponding energy management framework. In Sections 3.3 to 3.6, we respectively describe the models of the SBS, PV panel, battery, and electricity pricing. Finally, we summarize the chapter in Section 3.7.

3.2 THE PROPOSED GREEN SMALL CELL BASE STATION

3.2.1 SYSTEM ARCHITECTURE

In this work, we propose an architecture inspired from Fig. 2.9, which we call GSBS. It corresponds to the multiple-sources multiple-loads system represented in Fig. 3.1, which is composed of three categories of components:

- **The energy sources:** are the components that can only provide electricity. In our architecture, it corresponds to the PV panel.
- **The energy loads:** are the components that can only consume electricity. In our architecture, it corresponds to the SBS.
- **The hybrid components:** are the components that can act like both energy sources and loads. In our architecture, it corresponds to the battery and the SG.

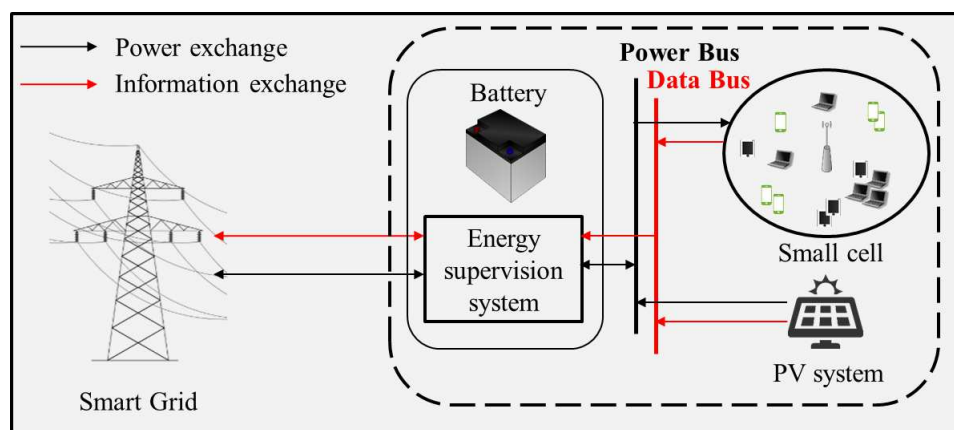


FIGURE 3.1: System architecture of GSBS.

The utility of the system is to offer high data rate services to mobile users. To do so, the power and electronic components of the SBS, namely the radio receiver/transmitter, require an energy supply (more details in Section 3.3.1), which can be provided by the aforementioned energy sources and the hybrid components. As discussed in Chapter 2, the use of RE provides several benefits compared with only-grid-powered SBSs such as long-term cost savings and reduced carbon emissions. Also, the battery is used to smoothen the variations of the PV production -which is known to be intermittent- and offers flexibility in the energy utilization, *i.e.*, energy is not necessarily consumed or sold to the SG right after it is produced.

Intuitively, as a first approach, it is possible to consider the SG as a backup energy source when the PV production is insufficient and the battery is depleted. Nevertheless, if the electricity price changes in real time (see Section 3.6), the cost of buying/selling energy will be more or less interesting at certain times of the day. In case the pricing dynamics are considered as a criterion in the energy management, it can be possible to dispatch the energy sources/hybrid components on the loads/hybrid components in a way

to optimize MNO's electricity expenditures. This is the role of the **ESS** that schedules the energy flows between the components of the GSBS to jointly reduce the electricity bill and improve the battery life span.

3.2.2 ENERGY MANAGEMENT

In the GSBS, the PV panels are cost-effective, due to their decades of lifetime and almost negligible maintenance expenditure. However, the battery is extremely impacted by the aging phenomenon compared to other GSBS components (*i.e.*, the PV panel and the SBS). Therefore, we assume that the system aging is only due to battery degradation.

Let's consider a SG context with RTP pricing. The purpose of the ESS is to jointly reduce the energy bill and the battery aging by efficiently using the energy produced by the PV sources and stored at the battery to optimize the power exchanged with the SG. To achieve this goal, it is necessary to define an energy management strategy that continuously determines the charge and discharge rates of the battery, taking into account the availability of PV energy, the SBS consumption, the prices of electricity, and the battery aging.

Important remark: Implementing an energy strategy with the ESS is essential when the GSBS is already deployed and in operation for achieving the aforementioned goals. Nevertheless, it is also vital to estimate the energy management policy during the study of the system sizing. This is due to the interdependence between the optimal dimensioning and the energy management strategy (refer to 2). Therefore, we distinguish between two types of energy management:

- Pre-operation energy management (ACT): estimated energy management policy to determine the optimal associated sizing;
- In-operation energy management (REACT): implemented energy management in a deployed and operating GSBS.

The proposed energy management framework is applied for both types.

In the existing works addressing energy management in green communication systems [Blasco 2013, Liu 2015b], the battery is not the main focus and the energy management is rather centered around the electricity exchange with the power grid. Contrarily, the main function of the ESS in this study corresponds to the battery control. Let \mathcal{S} be a finite set that describes the system state space, defined as $\mathcal{S} = \mathcal{C} \times \mathcal{B} \times \mathcal{R} \times \mathcal{P}$, where \mathcal{C} , \mathcal{B} , \mathcal{R} , and \mathcal{P} are the state sets related to the hourly average SBS power consumption (P_{BS}) [W], the SoC of the battery z , the RE production (P_{PV}) [W], and the electricity price (p) [\$/kWh], respectively. The set of actions \mathcal{A} is composed by the values of current rate C_{rate} [h^{-1}] at which the battery can be charged (positive rate) or discharged (negative rate).

Every hour, for the system state $\mathbf{s} = (P_{BS}, z, P_{PV}, p)$, the ESS performs an action $a \in \mathcal{A}$, and thereby an amount of energy is exchanged within the system elements, and between the system and the SG. As a matter of fact, by determining the battery action, all the consumed and produced energies are well-defined. It is noteworthy that the usage of the hour as a time step does not lead to loss of generality: we could consider another time scale (*e.g.*, minutes) for the power control and the dynamics of the energy variables without any changes in the current energy management framework.

We define the cost function associated with each state-action pair (\mathbf{s}, a) at time t as

$$c(\mathbf{s}, a) = p(t) \cdot E_b(t) + p_{sell}(t) \cdot E_s(t) + \Gamma, \quad (3.1)$$

where $E_b(t) = \max(0, (P_{BS}(t) + P_{batt}(t) - P_{PV}(t)) \cdot \Delta t)$ [Wh] is the quantity of energy bought from the SG at hour t , $E_s(t) = \min(0, (P_{BS}(t) + P_{batt}(t) - P_{PV}(t)) \cdot \Delta t)$ [Wh] is the energy sold to the SG at hour t , $P_{batt}(t)$ [W] is the power injected into or provided by the battery at time t , Δt is the duration of a time step, p_{sell} [\$/kWh] is the price of selling the energy back to the SG (p and p_{sell} are dependent as will be presented in Section 3.6), and Γ is a penalty function related to the battery aging, which is detailed in eq.

(4.8) and (4.12) of chapter 4 for the sizing problem and in eq. (5.11) of chapter 5 for the in-operation energy management problem. The system and data models required for the energy management are presented in the following sections.

Important remark: The analyses we present in this work rely on the input data of the system, namely: data traffic, solar irradiation, ambient temperature, and electricity price. A straightforward approach would be to consider time series of real measurement, to represent each of these variables in the simulation environment. However, we chose to build stochastic models based on their historical data to generate a high number of scenarios, which would be otherwise difficult given the limited amount of accessible data.

3.3 SMALL CELL BASE STATION MODEL

3.3.1 CHARACTERISTICS

We consider a SBS that consists of multiple *Transceivers* (TRXs), each one corresponding to an antenna element. Fig. 3.2 represents a block diagram of a TRX in a small cell BS. Each TRX comprises a *Power Amplifier* (PA), a radio frequency small-signal *Transmission Module* (TM) and *Reception Module* (RM), a *BaseBand* (BB) engine including a receiver (uplink) and transmitter (downlink) section, and an *Alternating Current* (AC)-*Direct Current* (DC) converter for the connection to the SG.

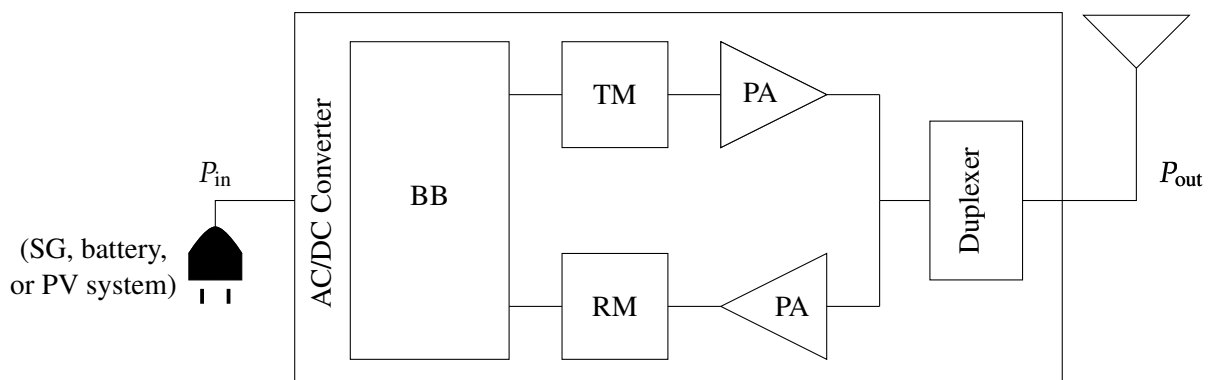


FIGURE 3.2: Block diagram of a SBS transceiver (adapted from [Auer 2011]).

We suppose that the SBS power consumption grows proportionally with the number of transceiver chains N_{TRX} . Therefore, the power consumption of the SBS, P_{BS} [W], at maximum load, *i.e.*, when the RF output power P_{RF} [W] reaches its maximum P_{max} [W], is expressed as a function of the power consumption of the TM/RM modules ($P_{\text{TM}} + P_{\text{RM}}$) and the power consumption P_{BB} [W] of the BB engine [Auer 2011]:

$$P_{\text{BS}} = \frac{N_{\text{TRX}}}{\eta_{\text{AC-DC}}} \cdot \left[\frac{P_{\text{max}}}{\eta_{\text{PA}}} + P_{\text{TM}} + P_{\text{RM}} + P_{\text{BB}} \right], \quad (3.2)$$

where $\eta_{\text{AC-DC}}$, and η_{PA} are the efficiencies of the AC-DC converter and the PA, respectively. Note that the RF power is considered at the input of the antenna, so that losses due to the antenna interface is not included.

The power model at maximum load can then be split into a term related to the maximum RF power output and a constant term P_0 :

$$P_{\text{BS}} = P_0 + \Delta_p \cdot P_{\text{max}}, \quad (3.3)$$

where P_0 [W] is the power consumption at the minimum non-zero output power and Δ_p is the slope of the input-output power consumption.

3.3.2 ENERGY CONSUMPTION MODEL

The power model describes the amount of energy needed at the SBS to satisfy the momentary traffic load. In this work, we suppose that the SBS load ρ varies according to a non-homogeneous Poisson process, whose intensity λ is time-dependent. Additionally, we assume that the SBS can be either in the active state ($\rho > 0$) or sleep state ($\rho = 0$). Fig. 3.3 represents the average daily load profile that we assume for the small cell, which shows a regular pattern during the day with low load periods early in the morning, medium loads during work-time, and high data rate in the late evening. This load is adapted from the network load profile in Europe [Auer 2010], where the SBS is supposed to be in a sleep state between 3:00 and 10:00, and that the traffic is handled by the under-layer macro-BS.

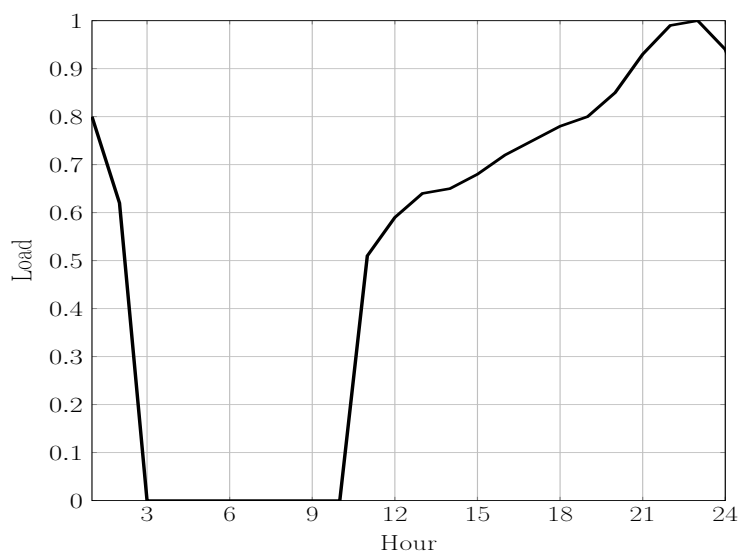


FIGURE 3.3: Profile of the average small cell load λ [Auer 2010].

Auer *et al.* demonstrates that there exists a nearly linear relation between the relative RF output power $P_{\text{RF}}(t)/P_{\text{max}}$ for a given load $\rho(t)$ and the SBS power consumption [Auer 2011]. Hence, we will consider the following linear approximation to represent the relation between the traffic load and the momentary SBS power consumption P_{BS} :

$$P_{\text{BS}}(t) = \begin{cases} P_0 + \Delta_p \cdot \rho(t) \cdot P_{\text{max}}, & \text{if } 0 < \rho(t) \leq 1 \\ P_{\text{sleep}}, & \text{if } \rho(t) = 0 \end{cases},$$

where P_{sleep} [W] is the power consumed in sleep mode. Table 3.1 shows the reference values of N_{TRX} , P_{max} , P_0 , Δ_p , and P_{sleep} for micro, pico, and femto BSs, respectively.

TABLE 3.1: SBS parameters for the power model [De Domenico 2014a].

SBS type	N_{TRX}	P_{max} (W)	P_0 (W)	Δ_p	P_{sleep} (W)
Micro	2	6.3	56	2.6	39
Pico	2	0.13	6.8	4	4.3
Femto	2	0.05	4.8	8	2.9

3.4 PHOTO-VOLTAIC PRODUCTION AND AMBIENT TEMPERATURE MODEL

3.4.1 CHARACTERISTICS

There exist several technologies of PV arrays, each one with different characteristics and performances [Parida 2011]. In this study, we consider a PV module composed of poly-crystalline cells, which is currently the most widely used technology since it offers the best trade-off between the cost and the performance.

The PV module is an electrical device that generates a current via the PV effect, *i.e.*, it absorbs the photons from sunlight and releases them as electrons (or other charge carrier), causing an electric current to flow when the module is connected to an external load. The main electrical characteristics of a PV module are summarized as an I - V curve, which represents the relation between the current produced and the voltage at the terminal of the module (Fig 3.4). The output power is then obtained by multiplying point by point the current and the corresponding voltage.

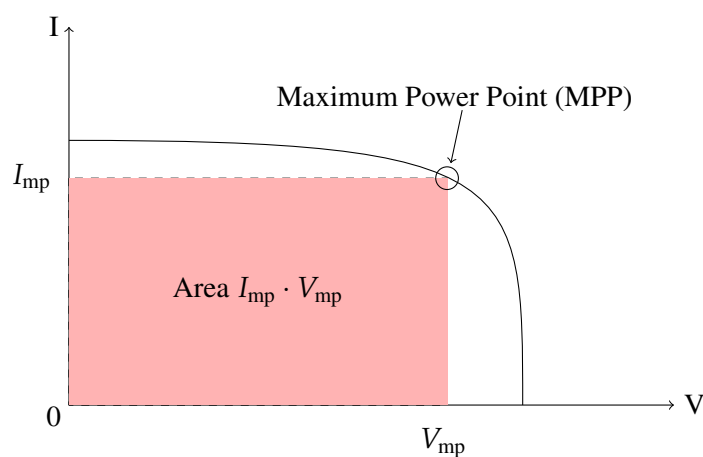


FIGURE 3.4: Solar Cell I - V Characteristic Curve for a given solar irradiation.

There is an important parameters on the PV characteristic called the *Maximum Power Point* (MPP), which corresponds to the point (I_{mp}, V_{mp}) at which the cell generates the maximum electrical power. The MPP is shown at the top right area of the red rectangle and it is the ideal operation point of a PV panel. Therefore, we can optimize the usage of the PV panel by operating at its MPP. This is achieved by always selecting the voltage that corresponds to the MPP at the terminals of the module V_{mp} .

Since the value of V_{mp} varies depending on the irradiation, an algorithm should be used to calculate the voltage to be imposed according to the weather conditions, called the MPP tracker. In our system, we consider the PV panel always works at his MPP regardless of the conditions. Therefore, we only model the behavior of the maximum power of the generator as a function of the irradiation.

3.4.2 ENERGY PRODUCTION MODEL

The energy production is generally obtained through a *Discrete Element Model* (DEM) of the PV module. It consists on proposing an equivalent electrical circuit that reproduces as accurately as possible the I - V characteristic [Dolara 2015]. The most used DEMs are the single diode and double diode, with some variants including resistive elements to increase the model precision. Other works considered more simplified model that describes the general behavior of the PV production regarding the solar irradiation [Rami 2004]. In the following, we use such simplified model for the output power of the considered PV module P_{PV} [W]:

$$P_{PV}(t) = \eta_{PV} \cdot S \cdot I_g(t), \quad (3.4)$$

where $\eta_{PV} \in [0, 1]$ is the energy conversion efficiency of the solar panel, S [m^2] is the module surface, and I_g [W/m^2] is the solar irradiation that depends on several factors including the geographical location and time of the day.

We want to use realistic models that capture the stochastic variation of the solar irradiation in a short time scale. This will enable to have insights on the energy management of the GSBS. Besides, the solar irradiation is a variable correlated to the ambient temperature, which we also need to assess the battery internal temperature, and the corresponding battery aging conditions (see Section 3.5). Therefore, we present in the following a joint model of the solar irradiation and temperature.

In this work, we consider a statistical model built from the time series of solar radiation and meteorological data provided by Solagis API [SOLAR]. Time series helps in understanding how much solar irradiation was falling on the solar panels in the past and by using real historical data, all the phenomena that influence the temperature and the solar irradiation are captured in the obtained stochastic process (such as clouds).

Let I_t [W/m^2] and T_t [$^\circ\text{C}$] be the random variables corresponding to the solar irradiation and the

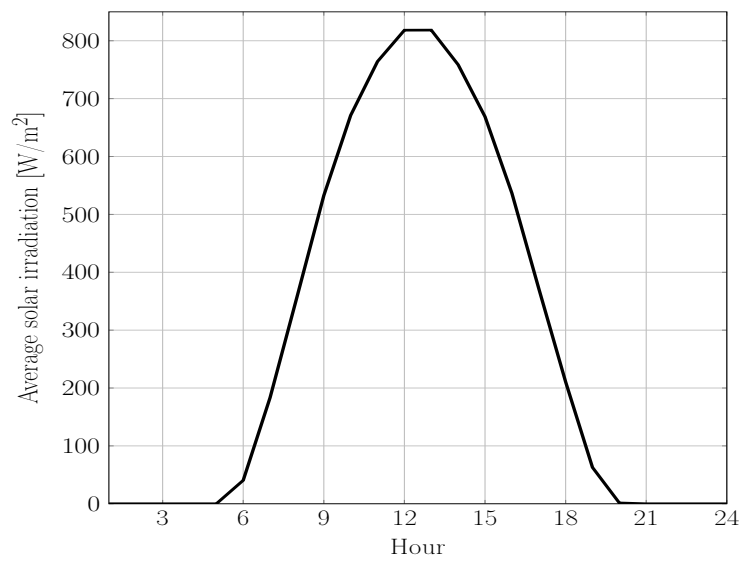


FIGURE 3.5: Profile of the average solar irradiation μ_{irrad} .

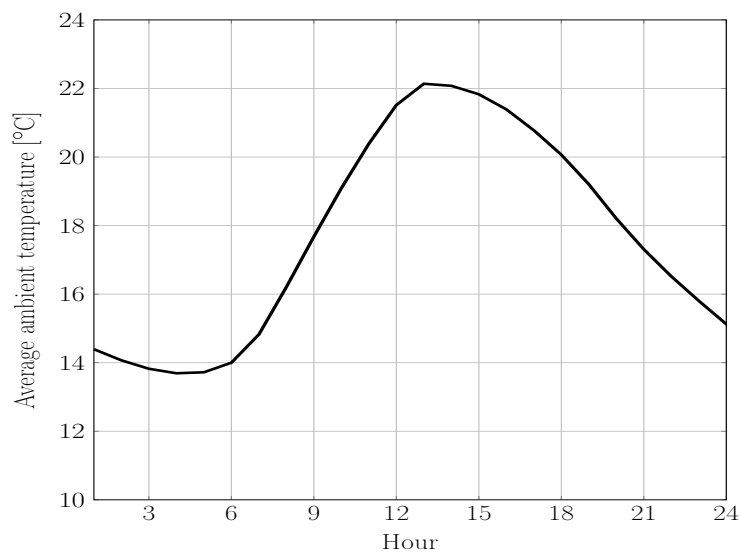


FIGURE 3.6: Profile of the average ambient temperature μ_{temp} .

ambient temperature at hour t , respectively. We suppose that the combined daily radiation-temperature vector $(I_1, \dots, I_{24}, T_1, \dots, T_{24})$ follows a multivariate Gaussian distribution $GP([\boldsymbol{\mu}_{\text{irrad}}, \boldsymbol{\mu}_{\text{temp}}], \boldsymbol{\Sigma}_{\text{irrad-temp}})$, where $\boldsymbol{\mu}_{\text{irrad}}$ (resp. $\boldsymbol{\mu}_{\text{temp}}$) is a vector of size 1×24 composed of the hourly average irradiances (resp. temperatures) of the day, and $\boldsymbol{\Sigma}_{\text{irrad-temp}}$ is the covariance matrix 48×48 . We compute $\boldsymbol{\mu}_{\text{irrad}}$, $\boldsymbol{\mu}_{\text{temp}}$, and $\boldsymbol{\Sigma}_{\text{irrad-temp}}$ as the means and the covariance of successive realizations related to historical measures of solar radiations and associated temperatures during five years [SOLAR].

The average profile of the solar irradiation is illustrated in Fig. 3.5. It has a bell shape characterized by a peak around midday, positive values during daytime, and the absence of sunlight during nighttime. Similarly, in Fig. 3.6, the temperature profile is bell-shaped and reaches the maximum between 12:00 and 14:00, which corroborates the existing correlation to the solar irradiation.

3.5 BATTERY MODEL

3.5.1 CHARACTERISTICS

A battery cell is an electrochemical system that converts chemical energy to electrical energy and delivers a voltage depending on the used chemistry. In this work, we consider the Li-ion chemistry for its many advantages such as high density, low self-discharge, and interesting cost evolution (see Chapter 2). Two main approaches, with varying degrees of complexity, have been adopted to capture the battery behavior for specific purposes, from battery design and performance estimation to circuit simulation:

- **Fundamental approach:** the derived models account for particle movement and chemical reactions inside the cell using partial differential equations. They are highly accurate but are computationally consuming (see [Santhanagopalan 2006] for a review of the proposed works based on this approach).
- **Phenomenological approach:** instead of investigating the fundamental physics, this approach provides a representation of the input/output relationship of the system. This is a way of simplifying the behavior of complex systems into a topology consisting of discrete entities that approximate their functioning under certain assumptions. These models present less mathematical complexity, are simple to solve, and suitable for real-time simulation. However, they are not able to achieve an accuracy comparable to fundamental models.

In this work, we focus on a specific phenomenological model based on equivalent electrical circuit. Quoting M. Muratori [Muratori 2010], the equivalent circuit model has a simple structure but can capture sufficient dynamics under both temperature and SoC variation, thus making it applicable for the real-time battery management in a GSBS. The considered circuit is represented in Fig. 3.7.

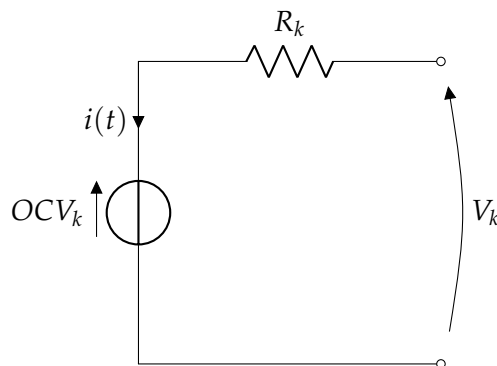


FIGURE 3.7: Equivalent circuit model of a battery cell.

The equivalent circuit is called a zero-order Randles circuit model. It consists of two elements, an ideal voltage source and a resistor. The resistor in this model represents the internal resistance, R_k [Ω], and the

voltage source represented the *Open Circuit Voltage* (OCV) OCV_k [V]. Therefore, the voltage between the terminals of the cell is:

$$V_k(t) = OCV_k(z_k(t)) + R_k \cdot i(t), \quad (3.5)$$

where $z(t)$ is the cell SoC at time t . In eq. 3.5, the OCV is expressed as a function of the SoC. This model is further detailed in Section 3.5.2. According to Barre *et al.* [Barre 2014], there are other parameters influencing the OCV such as the current intensity and the temperature. However, their impact is insignificant compared to the SoC in a way they are usually neglected even in high-precision energy management problems [Plett 2004]. Our simplification is therefore permitted.

3.5.2 POWER MODEL

A Li-ion battery pack is generally composed of several modules. Each module contains cells organized in series and parallel.

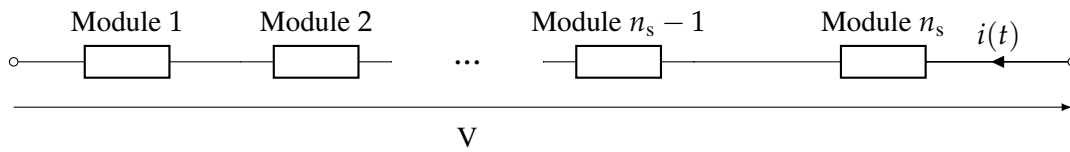


FIGURE 3.8: *Equivalent circuit of a battery pack.*

Without loss of generality, we suppose that the battery has n_s modules connected in series, where each cell module comprises one cell (see Fig. 3.8). In this configuration, the relation between the current $i(t)$ [A] and the voltage of the pack $V(t)$ [V] is the sum of the voltage of each module:

$$V(t) = \sum_{k=1}^{n_s} OCV_k(z_k(t)) + R_k \cdot i(t), \quad (3.6)$$

Important remark: We suppose that the battery is provided with a cell balancing system that ensures that no particular cell is stressed more than the others. This means that the SoC of each cell is the same. We define therefore the battery SoC z as the common SoC between all the cells.

The OCV-SoC dependency can be constructed experimentally by disconnecting the battery from any load for a long duration until reaching equilibrium and then measuring its voltage, for different SoC values [Chang 2013]. The obtained data can be used to build an analytical OCV model. In our work, we consider the following n -order polynomial approximation model for all cells:

$$OCV_k(z(t)) = \sum_{j=0}^n a_j \cdot z^j(t), \quad (3.7)$$

where n is a natural number and $(a_j)_{j=0..n}$ are the polynomial coefficients calculated from the experimental OCV-SoC dependency function.

As a sign convention, we assume that the charge (resp. discharge) current and power have a positive (resp. negative) sign. Consequently, the power P_{batt} of the battery is:

$$P_{\text{batt}}(t) = i(t) \cdot V(t). \quad (3.8)$$

By combining the equations (3.6) to (3.8), the battery power can be expressed as a function of two consecutive SoC values $z(t)$ and $z(t + \Delta t)$:

$$P_{\text{batt}}(t) = \sum_{k=1}^{n_s} \sum_{j=0}^n A_{j,k} z^j(t) z(t + \Delta t) - B_{j,k} z^{j+1}(t) + \alpha^2 \cdot R_k \cdot z^2(t + \Delta t), \quad (3.9)$$

where

$$\begin{aligned} A_{j,k} &= \alpha \cdot (a_j - 2\alpha \cdot R_k \cdot \delta_{1,j}), \\ B_{j,k} &= \alpha \cdot (a_j - \alpha \cdot R_k \cdot \delta_{1,j}), \\ \alpha &= \frac{3600 \cdot C_N}{\eta \cdot \Delta t}, \end{aligned}$$

and $\delta_{1,j}$ is the Kronecker symbol, equals to 1 when $j = 1$ or 0 otherwise.

3.5.3 SOC MODEL

We use the current integration method to estimate the variation of the battery storage level over time [Chang 2013]. The rate at which the battery is (dis)charged C_{rate} [h⁻¹] denotes the (dis)charge current intensity $i(t)$ relative to the nominal capacity C_N [Ah]:

$$C_{\text{rate}}(t) = \frac{i(t)}{C_N}.$$

Then, at each time step, we use the Ampere-Hour integral model to estimate the SoC variation:

$$z(t + \Delta t) = z(t) + \eta \int_t^{t+\Delta t} C_{\text{rate}}(u) du,$$

where η represents the battery Coulombic efficiency, which equals to η_{dis} when discharging and η_{chg} when charging.

3.5.4 AGING MODEL

The *State of Health* (SoH) degradation is inevitable in a battery life cycle. It is manifested as a loss of available capacity (energy loss) and/or an increase in impedance (power loss). In this work, we assume that the SoH reflects the capacity evolution:

$$SOH(t) = \frac{C_{\text{ref}}(t)}{C_N}, \quad (3.10)$$

where $C_{\text{ref}}(t)$ [Ah] is the reference capacity defined as the battery maximum storage capacity at time t . The degradation of the battery reference capacity can be caused by two aging situations: during use (cycle aging) and on storage (calendar aging) [Broussely 2005]. In the following, these two aging mechanisms are considered independent and thus additive.

In general, the performance of Li-ion cells is dependent on both the temperature and the operating voltage. Therefore, the battery constructors recommend to operate the cell within restricted temperature and voltage limits. Otherwise, the battery is subject to rapid capacity loss and decrease of the (dis)charge efficiency [MpowerUK]. The voltage restrictions necessary to avoid such problems can be translated into recommendations for the operating range of the battery SoC as shown in the Fig. 3.9.

3.5.4.1 CYCLE AGING

Cycle aging is modeled as reference capacity losses, which depends linearly on the battery SoC variations [Riffonneau 2011]. At each time step, the new SoH is obtained by eq. (3.11):

$$SOH(t + \Delta t) = SOH(t) - Z \cdot [z(t) - z(t + \Delta t)]. \quad (3.11)$$

The experimental results of [Lemaire-Potteau 2008] determine the linear aging coefficient Z for different battery technologies. However, because the cycle aging is amplified outside the recommended operating

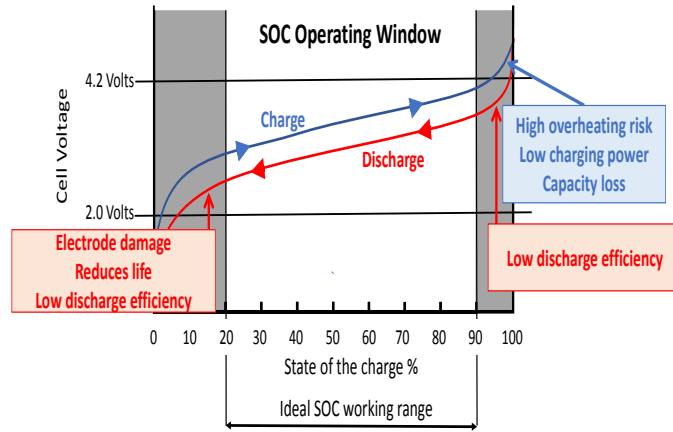


FIGURE 3.9: Recommendations for the operating range of SoC of Lithium-ion battery [MpowerUK].

range $\Delta_{\text{soc}} = [20\%, 90\%]$ of the battery SoC (see Fig. 3.9 [MpowerUK]), we define the aging coefficient Z as:

$$Z = \begin{cases} 85 \cdot 10^{-6}, & \text{if } 20\% \leq \text{SOC}(t) \leq 90\% \\ \chi \cdot 85 \cdot 10^{-6}, & \text{otherwise} \end{cases} \quad \forall t, \quad (3.12)$$

where χ is a scalar strictly greater than one.

3.5.4.2 CALENDAR AGING

The battery temperature is an important parameter to model calendar aging, especially for Li-ion technology. The thermal model is used to estimate the cell temperature in response to the current, voltage, and ambient temperature. According to the energy conservation law, the temperature change for a battery cell is given by [Cordoba-Arenas et al. 2015]:

$$m_c \cdot c_h \frac{dT}{dt} = Q_g - Q_r, \quad (3.13)$$

where m_c [g] is the mass of the cell, c_h [J/(g K)] is specific heat capacity at constant pressure, T [°C] is the temperature within the cell, Q_g [W] is the rate of heat generated by the single cell, and Q_r [W] is the rate of heat removed from the cell by the cooling. The heat generation for a battery cell k can be approximated by the Joule heating law:

$$Q_g = R_k \cdot i^2. \quad (3.14)$$

For simplicity, the heat generation and temperature within the battery are assumed to be uniformly distributed. The single-cell thermal model is thus supposed to represent the overall internal battery temperature.

Ecker *et al.* [Ecker 2012] have proposed a calendar lifetime prediction model describing the degradation of the battery C_{ref} over time. The model shows exponential dependency with the battery voltage V and temperature T , and square root dependency with the time of rest. The degradation of SoH after a time rest Δt (expressed in weeks in eq. (3.15)) is defined as follows:

$$\frac{\text{SOH}(t + \Delta t)}{\text{SOH}(t)} = 1 + c_a \cdot c_V^{\frac{V-V_0}{\Delta V}} \cdot c_T^{\frac{T-T_0}{\Delta T}} \cdot \sqrt{\Delta t}, \quad (3.15)$$

where T_0 and V_0 are reference temperature and voltage, ΔT and ΔV are reference temperature and voltage variation, and c_a , c_V , and c_T are fitting parameters based on accelerated calendar aging test data. Given this

model, we can conclude that high voltages, and therefore high SoCs (eq. (3.5)), contribute to an accelerated battery degradation during rest. Also, the calendar aging grows exponentially with the temperature. By considering the relation between the current intensity and the heat generated within the battery (eq. (3.14)), it is clear that a high current rate increases the internal temperature. Therefore, disconnecting the battery after a high-current (dis)charge leads to faster calendar aging.

3.6 ELECTRICITY PRICING MODEL

3.6.1 CHARACTERISTICS

In Chapter 2, we defined the DR as the capacity of changing the electricity usage from their normal or current consumption patterns in response to electricity market signals. In contrast to energy efficiency, which aims at reducing the overall energy consumption, DR is mainly about shifting consumption to a different point in time. This enable to smoothen the electricity consumption during peak load hours and avoid backup energy production characterized by a high marginal cost and significant Carbon footprint. Therefore, DR can achieve significant economic and environmental benefits.

Recall that RTP is an implicit DR scheme, which targets to reflect the value and cost of electricity in different time periods. The consumers can decide to shift their electricity consumption away from times of high prices, accordingly. They are rewarded for their flexibility by reducing their electricity bill. The majority of studies interested in RTP in power grids have modeled it by investigating unit commitment problems [Zheng 2015]. It consists on determining the electricity price based on the optimal scheduling of the generating units at every hour interval with varying loads under different constraints and environments. This level of understanding is not needed for the energy management of the GSBS. As a matter of fact, our management framework can be extended to any price signal, depending on the DR objectives. Therefore, in the following, we will consider a specific but yet realistic model of the electricity price.

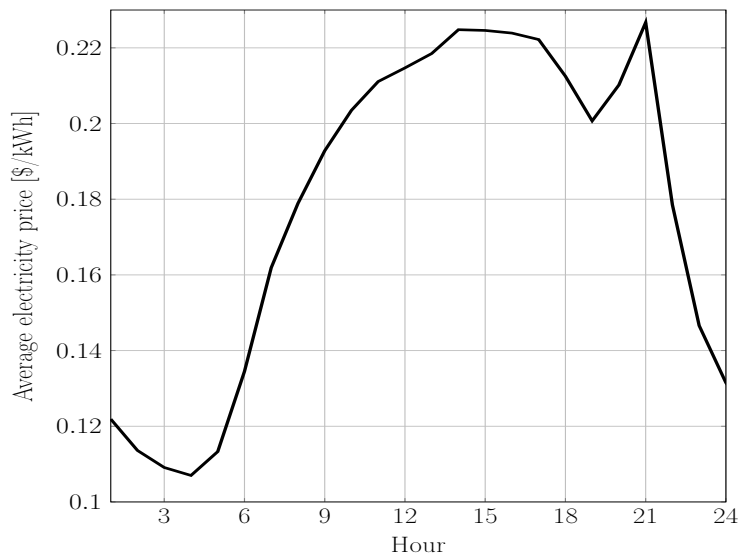


FIGURE 3.10: Profile of the average electricity price μ_{price} .

3.6.2 ELECTRICITY PRICE MODEL

Let $p(t)$ be the random variable corresponding to the buying price (i.e., the price at which electricity is bought from the SG) at hour t . The vector $(p(1), \dots, p(24))$ of the daily energy buying price is supposed to follow a multivariate Gaussian distribution $GP(\mu_{\text{price}}, \Sigma_{\text{price}})$, where μ_{price} is a vector of size 1×24 composed of the hourly average buying price of the day, and Σ_{price} is the covariance matrix 24×24 . We

compute μ_{price} and Σ_{price} as the mean and the covariance of successive realizations related to historical data of electricity pricing for residential customers during five year [Ameren]. Moreover, the price at which energy is sold back to the SG is set proportional to the buying electricity price such that $p_{\text{sell}} = \kappa \cdot p$, where κ is the price factor.

Fig. 3.10 represents the profile of the average electricity buying price. It is marked by an increasing trend from low prices late at night to high values attained during the afternoon and the evening.

3.7 CONCLUSION

In this chapter, we have presented the proposed GSBS architecture that relies on a PV panel as RE source, a battery as energy storage, and the SG, all of which supply the SBS to serve the momentary traffic load. We have observed that the multitude of power sources, the battery being subject to the aging phenomena, and the price signal of the SG are factors that require a management to efficiently control the energy production and consumption. Accordingly, we proposed an energy management framework for the GSBS centered around the battery, to jointly reduce the electricity expenses of the MNOs and the battery degradation. This energy management framework requires an understanding of how the system operates, which we achieved by selecting the models of each component of the system and the associated input data. In particular, and contrarily to other works that consider the battery as an energy buffer, the battery model is detailed to capture its non-linear behaviors and aging mechanisms. In the following chapter, we investigate the sizing problem of the GSBS with respect to the proposed optimization framework.

THE SIZING OF A GREEN SMALL-CELL BASE STATION

Contents

4.1	Introduction	46
4.1.1	Motivation	46
4.1.2	Related work	47
4.1.3	Contribution	47
4.2	System Sizing and the Subsequent Energy Management Problem	48
4.2.1	Problem Presentation	48
4.2.2	Energy Management Strategy Estimation	48
4.2.3	Proposed Resolution Approach	50
4.2.4	Off-grid System Analysis	51
4.3	Results	52
4.3.1	Optimal Sizing	54
4.3.2	Sizing Sensitivity to the Optimization Parameters	56
4.3.3	Sizing Sensitivity to the Energy Management Estimation	59
4.3.4	Practical Insights on the Sizing Procedure	60
4.3.5	Off-grid GSBS Analysis	61
4.4	Conclusion	62

4.1 INTRODUCTION

4.1.1 MOTIVATION

When designing a GSBS, it is critical to establish the sizes and ratings of the major components needed to meet the energy requirements of the SBS and maintain the users' QoS. Nevertheless, these resources come with a cost, and they need to be optimized to avoid any wastage. Specifically, the battery and the PV panel need to be sized such that their investment cost is beneficial for the MNO in the long term. There are two considerations to keep in mind to attain this objective: 1) the sizing performance depends on the energy strategy that will be implemented when the GSBS becomes operational, and needs to be adapted to it 2) the cost savings achieved by the system are reliant on the performance and the durability of the battery. Many characteristics of the battery can cause an accelerated aging when used in a certain manner and should be

chosen to maximize the battery life span as much as possible.

These two considerations need to be addressed in a joint framework. The battery and the PV panel are thereby selected to maximize the achieved cost saving relatively to the investment cost.

4.1.2 RELATED WORK

Several research efforts have been made to determine the optimal storage and production capacities in energy-harvesting mobile communication. Alsharif *et al.* have studied the sizing problem for various hybrid renewable sources to supply on-grid mobile SBSs sites [Alsharif *et al.* 2016]. In particular, the RE that is most commonly gathered in mobile networks is the solar energy using PV panels [Ulukus 2015b]. Depending on the type of deployment (off-grid or grid-connected), the PV panel and the battery dimension is determined based on system specifications such as the battery capacity and the PV panel surface. For off-grid applications, the battery storage capacity and the PV panel have to be large enough to supply the energy use during the most unfavorable conditions for RE production (longest cloudy period and nighttime). In his study [Wang 2015], H. Wang *et al.* have selected the solar panel and the battery size via simulations to optimize the operation of a standalone BS, which considers reliability metrics in terms of service outage probability, the energy loss, and the total cost. In contrast, if the PV system is grid-connected, the autonomy is a secondary goal and the batteries are used instead to reduce the fluctuation of RE production and provide economic benefits. Khalilpour and Vasallo [Khalilpour 2016] have investigated multi-period mixed-integer linear programming techniques to find the optimal sizing among a finite PV/battery combinations set. A limited number of researchers, however, have considered a non-trivial energy management estimation in the sizing problem, that is aware of the battery aging. For example, Ru *et al.* have studied the optimal storage capacity considering battery cycle aging [Ru 2013]. However, in all these works, the impact of both cycle and calendar aging processes has not been integrated in the OPEX and CAPEX study. Hence, the contributions of this chapter.

4.1.3 CONTRIBUTION

Our main contributions in this chapter are as follows:

- *Contribution 1:* We propose an optimization framework for the optimal sizing of a GSBS that integrates the estimation of the energy management strategy. The sizing problem is formulated to include the fixed cost of the investment related to the equipment purchase/installation, the running cost due to system aging, and the cost saving achieved by the investment, obtained by solving the inherent energy management problem. The parametric approach we propose to solve the sizing problem relies on the average profiles of the state variables, *i.e.*, energy consumption, production, and cost. Extensive simulations show the existence of an optimal solution that depends on the system conditions.
- *Contribution 2:* We assess the economical attractiveness of connecting an off-grid SBS to the SG. To do so, we formulate the off-grid sizing problem. Afterwards, we propose an analysis to evaluate the maximum acceptable connection cost and the critical distance from the grid after which the connection to the SG is not economically valuable.

The novelty of this chapter is based on one journal article [J1].

The rest of this chapter is organized as follow. In Section 4.2, we formulate and analyze the sizing problem of a GSBS and the corresponding energy management sub-problems in the on-grid and off-grid scenarios. In Section 4.3, we provide simulation results and discuss the obtained performances. Finally, we summarize the chapter in Section 4.4.

4.2 SYSTEM SIZING AND THE SUBSEQUENT ENERGY MANAGEMENT PROBLEM

4.2.1 PROBLEM PRESENTATION

We are interested in the sizing problem of a GSBS, that is, determining the characteristics of the battery and the PV panel used for the GSBS deployment. The objective is to enhance the efficiency of the investment by achieving the largest benefit, which is defined as follows:

$$\text{Benefit} = G - FC - RC. \quad (4.1)$$

In the above formula, the *Gain from investment* (G) refers to the expenses saving (or incomes) generated thanks to the investment, by reducing the energy consumption from the SG and selling the electricity. The cost of investment corresponds to a FC of purchasing and installing the equipments, and a RC due to system maintenance and replacement. The PV panels are cost-effective, due to their decades of lifetime (the actual warranties are covering around 20 years) and almost negligible maintenance expenditure. However, the battery is extremely impacted by the aging phenomenon compared to the other GSBS components (*i.e.*, the PV panel and the SBS). Therefore, we consider that the system life L corresponds to the lifespan of the PV panel and that the RC of investment is only due to battery aging.

The characteristics of the battery and the PV panel to be select in the sizing problem are the capacity and the surface, respectively. The influence of other attributes will be later discussed in the results section. Additionally, we suppose that:

1. The maximum PV panel dimension S_{PV}^{max} is constrained by the space allocated to the GSBS.
2. The maximum battery capacity C_N^{max} is set such that the GSBS equipped with a PV panel of maximum size can autonomously operate for a given period of time in the off-grid mode – the system is disconnected from the SG – without power outage or PV energy wastage.

The objective of the sizing procedure is to maximize the benefit with respect to the battery capacity and the PV panel surface:

$$\mathbf{P}_1 : \max_{(C_N, S_{PV}) \in [0, C_N^{max}] \times [0, S_{PV}^{max}]} [G - RC](C_N, S_{PV}) - FC(C_N, S_{PV}); \quad (4.2)$$

As discussed in Section 2.4 of Chapter 2, the gain from the investment and the running cost due to the battery aging are dependent on the energy management foreseen for the GSBS over a duration N . In eq. (4.1), the only term that is independent of the energy strategy is FC :

$$FC(C_N, S_{PV}) = \frac{N}{L} [(1 - \psi) \cdot UC_{Batt} \cdot C_N + UC_{PV} \cdot S_{PV}], \quad (4.3)$$

where $\psi \in [0, 1]$ is the financial aids for the battery investment, UC_{Batt} [\$/Ah] and UC_{PV} [\$/m²] are the unit cost of purchasing and installing the battery and the PV panel, respectively. The FC is weighted by the ratio N/L to adjust the investment lifespan to the time scale of the energy management.

4.2.2 ENERGY MANAGEMENT STRATEGY ESTIMATION

To estimate $(G - RC)$, it is required to consider an energy management strategy that will be used for each sizing, when the GSBS is deployed and operational.

Let's suppose a GSBS equipped with a battery of capacity C_N and a PV panel of surface S_{PV} . The quantity $(G - RC)$ is calculated by finding the energy management strategy that jointly maximizes the gain from the investment and minimizes the battery aging in a GSBS. This is achieved by controlling the power flow

between the energy sinks and sources as presented in Chapter 3-1, over a time horizon discretized into N decision periods:

$$[G - RC](C_N, S_{PV}) = \max_{\mathbf{z} \in [0,1]^{N+1}} \underbrace{\sum_{t=1}^N p(t) \cdot P_{BS}(t)}_{\text{Term } a} - \underbrace{\sum_{t=1}^N p(t) \cdot (E_b(t) + \kappa \cdot E_s(t))}_{\text{Term } b} - \Gamma_s(1 \rightarrow N), \quad (4.4)$$

where $\mathbf{z} = (z(1), \dots, z(N+1))$ is the multivariable vector that represents the battery SoCs over the optimization horizon, $P_{BS}(t)$ is the energy consumed by the SBS at time t , $p(t)$ is the unit electricity cost at time t , $E_b \geq 0$ (resp. $E_s \leq 0$) is the amount of energy bought from (resp. sold to) the SG, κ is the selling price factor, and $\Gamma_s(1 \rightarrow N)$ is the RC of the investment due to battery aging during N decision periods. In the above formula, the term a corresponds to the electricity cost of feeding the SBS exclusively from the SG. Term b is the electricity cost generated by the GSBS when operated according to the energy strategy \mathbf{z} . Therefore, the cost saving realized when implementing \mathbf{z} is the difference between term a and term b . Notice however the system electricity cost expressed by term a does not rely on the battery, which makes it independent of \mathbf{z} . According to this, the previous optimization problem is equivalent to:

$$\max_{\mathbf{z} \in [0,1]^{N+1}} - \sum_{t=1}^N p(t) \cdot (E_b(t) + \kappa \cdot E_s(t)) - \Gamma_s(1 \rightarrow N),$$

which is equivalent to:

$$\mathbf{P}_2 : \min_{\mathbf{z} \in [0,1]^{N+1}} \sum_{t=1}^N p(t) \cdot (E_b(t) + \kappa \cdot E_s(t)) + \Gamma_s(1 \rightarrow N).$$

The optimal energy policy \mathbf{z}^* is found by solving the problem \mathbf{P}_2 subject to the following constraints:

$$E_b(t) = \max(0, P_{BS}(t) + P_{Batt}(z(t), z(t+1)) - P_{PV}(t)), \quad 1 \leq t \leq N, \quad (4.5)$$

$$E_s(t) = \min(0, P_{BS}(t) + P_{Batt}(z(t), z(t+1)) - P_{PV}(t)), \quad 1 \leq t \leq N, \quad (4.6)$$

$$- \sum_{t=1}^N E_s(t) \leq \sum_{t=1}^N P_{PV}(t), \quad (4.7)$$

$$\Gamma_s(1 \rightarrow N) = UC_{Batt} \cdot \Delta SOH(1 \rightarrow N). \quad (4.8)$$

At all time steps, the balance between the power supply and demand is expressed by the constraints 4.5 and 4.6. When the energy consumed is greater than the energy provided by the PV system and the battery (*i.e.*, $P_{BS}(t) + P_{Batt}(z(t), z(t+1)) - P_{PV}(t) \geq 0$), the ESS perceives a cost $p(t) \cdot E_b(t) \geq 0$ corresponding to the energy bought from the SG. In contrast, when the energy available exceeds the energy consumption (*i.e.*, $P_{BS}(t) + P_{Batt}(z(t), z(t+1)) - P_{PV}(t) \leq 0$), the ESS receives a negative cost $\kappa p(t) \cdot E_s(t) \leq 0$ associated to the energy sold to the grid by the energy locally produced as expressed in 4.7 to avoid over-speculation on the energy price. Finally, the RC generated by the battery aging $\Gamma_s(1 \rightarrow N)$ is defined in 4.8 as the product of the unitary battery investment cost UC_{Batt} and the SoH loss due to the cycle and calendar aging $\Delta SOH(1 \rightarrow N)$ during the N decision steps.

Important remark:

To make the equation less cluttered, we voluntarily omit in the notation the dependency of the following variables to C_N and S_{PV} :

- The energy bought E_b from and sold E_s to the SG. Actually, we note from the definition of these variables in (4.5) and (4.6) that they are expressed as a linear combination of P_{Batt} , which depends on C_N (see Section 3.5 Chapter 3), and P_{PV} , which depends on S_{PV} (see Section 3.4 Chapter 3).
- The energy management strategy of the battery \mathbf{z} is correlated to E_b and E_s . Transitively, it depends on C_N and S_{PV} .
- $\Gamma_s(1 \rightarrow N)$, defined in (4.8), is linked to the energy management \mathbf{z} . Therefore, it depends on C_N and S_{PV} .

To conduct the sizing study, we need to estimate the realizations of the stochastic variables involved in the sizing problem (*i.e.*, the SBS consumption, the PV production, and the electricity price) from the moment the GSBS is deployed until the end of the optimization horizon. We consider two possible scenarios:

1. Ideal energy management: in this ideal case we suppose that the ESS is able to perfectly predict the realization of all the system variables. The obtained energy strategy is optimal and enables to upper-bound the achievable benefits of the sizing problem.
2. Average-based energy management: this strategy is obtained using the average profiles of the state variables.

The resulting problem in the both cases is non-linear. It is solved using a Matlab's non-linear solver called *fmincon* that combines, amongst others, the trust region and interior point methods [Byrd 2000] (we invite the reader to refer to Appendix A.2 for more details).

4.2.3 PROPOSED RESOLUTION APPROACH

We propose a parametric approach to solve the sizing problem as described in Algorithm 1. The problem \mathbf{P}_2 is solved to estimate the energy management strategy for different battery capacities and PV surface, up to the maximum dimensions. Then, we compute the benefit based on the estimated strategies (using the objective function of \mathbf{P}_2) corresponding to each possible sizing. Once all the combinations are explored, the optimal characteristics (C_N^*, S_{PV}^*) are chosen such that the benefit is maximal.

Algorithm 1: GSBS sizing algorithm

Data: Profiles of the energy consumption, energy production, ambient temperature, and electricity price

Result: (C_N^*, S_{PV}^*)

for $C_N \in [0, C_N^{max}]$ **do**

for $S_{PV} \in [0, S_{PV}^{max}]$ **do**

 Solve \mathbf{P}_x ;

 compute Benefit(C_N, S_{PV});

$(C_N^*, S_{PV}^*) \leftarrow \arg \max_{C_N, S_{PV}} \text{Benefit}(C_N, S_{PV});$

4.2.4 OFF-GRID SYSTEM ANALYSIS

4.2.4.1 PROBLEM PRESENTATION AND FORMULATION

In the previous section, we supposed that the GSBS is connected to the SG (on-grid mode), such that the objective of the sizing study is to maximize the benefit from the installation. However, when the access to the electricity grid is intermittent or entirely nonexistent, such as is some rural areas, the electrical autonomy of the GSBS becomes the main priority. If the GSBS is in such off-grid mode, be it temporarily or permanently, the sizing problem must focus on finding the optimal battery capacity and PV panel surface that guarantee a continuous energy autonomy of the system while being the most efficient in terms of investment cost.

In a completely off-grid mode, the energy strategy (*i.e.*, the battery use) is imposed by the system's environment. Specifically, if the energy production is higher than the energy consumed, the excess is stored in the battery. Conversely, the battery is discharged when the PV production is not sufficient to cover the SBS needs. Therefore, unlike the on-grid mode, there is no "gain" per say from the investment other than guaranteeing the energy balance of the GSBS. As a consequence, the sizing problem of an off-grid GSBS is to jointly reduce the FC and RC of the investment:

$$\mathbf{P}_3: \min_{C_N, S_{PV}} \frac{N}{L} [(1 - \psi) \cdot UC_{\text{Batt}} \cdot C_N + UC_{\text{PV}} \cdot S_{\text{PV}}] + \Gamma_s(1 \rightarrow N)$$

Subject to

$$P_{\text{Batt}}(z(t), z(t+1)) = P_{\text{BS}}(t) - P_{\text{PV}}(t), \quad 1 \leq t \leq N, \quad (4.9)$$

$$0 \leq z(t) \leq 1, \quad 1 \leq t \leq N + 1, \quad (4.10)$$

$$z(1) = z_0, \quad (4.11)$$

$$\Gamma_s(1 \rightarrow N) = UC_{\text{Batt}} \cdot \Delta SOH(1 \rightarrow N). \quad (4.12)$$

In \mathbf{P}_3 , the first term indicates the investment FC as defined in (4.3) and the second term is the RC due to the aging of the battery over N decision steps. The constraint (4.9) describes the balance between production and consumption in the system at each time step. Since the GSBS is not connected to the SG, we here express the necessity to invest in a battery and a PV panel that cover the SBS consumption over the optimization horizon. The constraints (4.10) and (4.11) correspond to the definition of the SoC and its initialization, respectively. Finally, $\Gamma_s(1 \rightarrow N)$ is defined in (4.12) as the product of the unitary battery investment cost UC_{Batt} and the SoH loss due to the cycle and calendar aging $\Delta SOH(1 \rightarrow N)$ during the N decision steps. Again, for simplification purposes, we do not express the dependency on C_N and P_{PV} in the notations.

4.2.4.2 COST ANALYSIS OF THE CONNECTION TO THE SG

In the previous section, we exposed how to size an off-grid GSBS to meet the energy autonomy. Nevertheless, in the context of evolving energy markets approaching RTP, we have showed that it can be economically interesting to enhance the flexibility offered by the local energy storage and production by combining it with the SG services. In particular, the cost saving achieved from connecting an already-existing off-grid GSBS to the SG can surpass the cost of the connection.

To connect a GSBS to the SG, we need to take into account two types of costs:

- The device connection cost, noted DC [\$], which is the cost of connecting the PV panel the SG.
- The cost of the electricity-supply cabling, noted EC [\$], when the physical link between the GSBS and the SG is non-existent.

Now, suppose an off-grid GSBS equipped with a battery and a PV panel, which characteristics C_N and S_{PV} have been optimized according to the sizing study. The utility U of connecting the system to the SG is determined by: 1. the efficiency of the return on investment, calculated as difference between the cost

saving realized with the on-grid system $G_{\text{on-grid}}$ and the connection fees $CC+EC$, and 2. the improvement of the system lifespan, which is difference of the RC due to battery maintenance in the two deployment scenario: $RC_{\text{on-grid}} - RC_{\text{off-grid}}$. The utility U is expressed in eq. (4.13):

$$U(C_N, S_{PV}) = G_{\text{on-grid}} - (CC + EC) - (RC_{\text{on-grid}} - RC_{\text{off-grid}}) \quad (4.13)$$

In algorithm 2, we list the steps to take a decision regarding the connection to the SG:

Algorithm 2: Decision-making algorithm for connecting a off-grid GSBS to the SG

Data: Profiles of the energy consumption, energy production, ambient temperature, and electricity price

Result: Decision whether to connect an off-grid GSBS to the SG

$(C_N, S_{PV}, RC_{\text{off-grid}}) \leftarrow \text{Solve } \mathbf{P}_3;$

$(G_{\text{on-grid}}, RC_{\text{on-grid}}) \leftarrow \text{Solve } \mathbf{P}_2 \text{ for } (C_N, S_{PV});$

compute $U(C_N, S_{PV});$

if $U(C_N, S_{PV}) > 0$ **then**

 | Connect the GSBS to the SG;

else

 | Keep the GSBS off-grid;

4.3 RESULTS

In this section, we consider a pico-cell BS, which is typically deployed to cover small areas like squares, train stations, and malls. For this analysis, we assume that $UC_{\text{Batt}} = 6$ \$/Ah [Pillot 2013] and $UC_{\text{PV}} = 1200$ \$/m² [IEA-PVPS 2015] [Dusonchet 2015], both including the purchase and installation fees. Also, we suppose that the economical context enables a battery financial aid of $\psi = 50\%$ [Truong 2016] and that the PV production is not subsidized, *i.e.*, the energy fed into the grid is purchased at the same price as the electricity sold to the final consumer $\kappa = 100\%$. The simulation settings are summarized in Table 4.1 and 4.2.

The profiles illustrated in Fig. 4.1 describe the cell load intensity λ , the average solar radiation μ_{irrad} , the average ambient temperature μ_{temp} , and the average energy buying price μ_{price} . We note that:

- The traffic load grows progressively and reaches the maximum around 21:00. In addition, we assume that the traffic between 3:00 and 10:00 is handled by the under-layer macro base station, such that the SBS load in this period is zero,
- the average profiles of the solar radiation and the ambient temperature are characterized by a peak around midday and positive values during daytime, and
- the energy price is marked by an increasing trend from low prices late at night to high values attained during the afternoon and the evening.

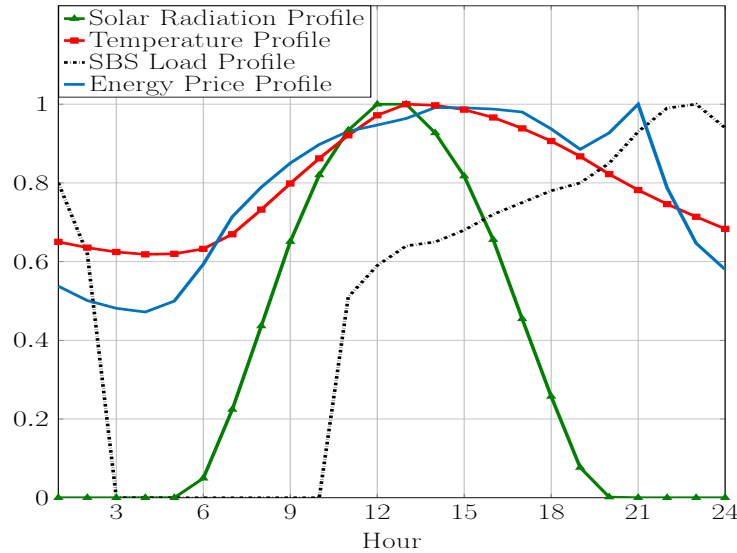
Given the periodic characteristics of the daily profiles, we suppose that the optimization horizon is $N = 24$ h.

TABLE 4.1: *Simulation Parameters [Pillot 2013, IEA-PVPS 2015, Dusonchet 2015].*

	Parameter	Value	Parameter	Value
SBS	P_0	13.6 W	Δ_p	4
	P_{\max}	0.13 W	P_{sleep}	8.6 W
Battery	R	250 m Ω	C_N^{\max}	50 A h
	η_{dis}	98%	η_{chg}	98%
	ψ	50%	UC _{Batt}	6 \$/Wh
Solar panel	η_{PV}	14%	S_{PV}^{\max}	1 m ²
	UC _{PV}	1200 \$/m ²	L	20 years
Energy price	κ	100%		

TABLE 4.2: *Battery Aging Simulation Parameters [Uddin 2014] [Ecker 2012].*

Parameter	Value	Parameter	Value
c_h	1900 J/(kg K)	V_0	3.5 V
c_a	-0.0064	T_0	25 °C
c_V	1.1484	ΔV	0.1 V
c_T	1.5479	ΔT	10 °C
λ	5	m_c	200 g

FIGURE 4.1: *Normalized profiles of the average solar radiation, average ambient temperature [SOLAR], SBS load intensity (based on [Auer 2010]), and average energy price [Ameren].*

Besides, to the best of our knowledge, and even if the regulation is slowly moving toward self-consumption schemes, the cost of connecting RE energy to the power grid is generally subsidized by governments. For example, the connection cost of photo-voltaic in low voltage grid in several European

countries constitutes between 0% and 5% of the total PV purchase and installation cost [Swider 2008]. Consequently, we neglect DC in this study and focus on the cabling expenses. We suppose that EC in low voltage grids is proportional to distance d between the system to connect and the power grid [Nerini 2015]:

$$EC(d) = \zeta \cdot d, \quad (4.14)$$

where ζ [\$/km] is the low voltage line cost for a unit distance.

In the following, we first present the sizing results of the GSBS in urban areas. We suppose that the electrical infrastructure is well-developed and enables the connection to the SG with no additional cost ($EC = 0$). Next, we highlight some structural insights of the solution by evaluating the sensitivity of the sizing with respect to the system characteristics. We also assess the impact of the estimation of the energy management strategy on the results. Finally, we analyze the scenario of an autonomous GSBS deployed in a rural area with underdeveloped electrical infrastructure, and study the profitability of connecting the system to the power grid.

4.3.1 OPTIMAL SIZING

We apply Algorithm 1 to find the optimal sizing for the considered GSBS. Through system simulations, we obtain Fig. 4.2 that illustrates the benefit for different battery and PV settings. Notice that the benefit is positive or negative, depending on the profitability of the investment. For a given battery capacity, increasing the solar panel dimensions will result in a linear growth of the benefits. On the one hand, the additional production diminishes the amount of energy bought from the grid, which reduces the electricity bill. On the other hand, the limit on energy speculation set in constraint (4.7) is increased, which enables the system to sell larger amount of energy to the SG. Hence, the cost savings and the cash flow received from the utility make the investment cost-efficient.

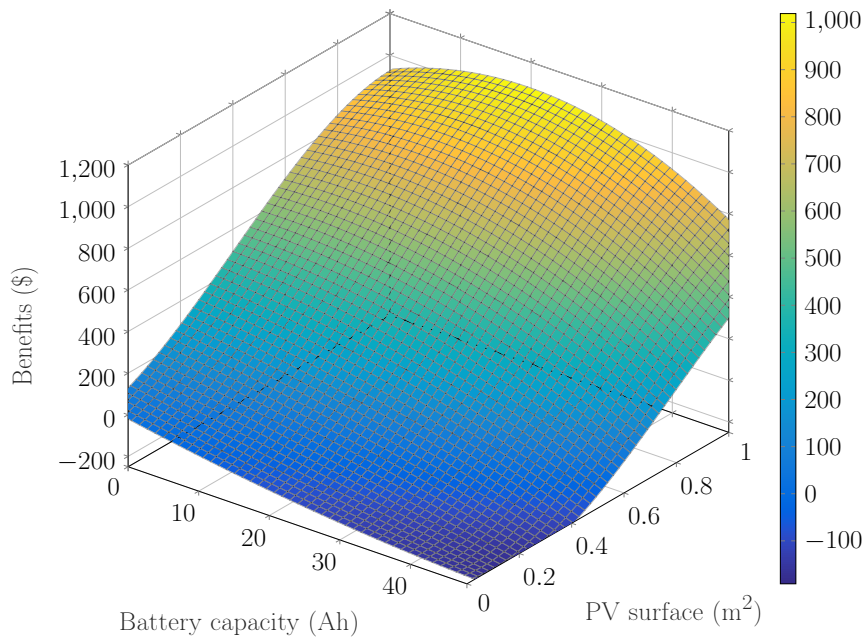


FIGURE 4.2: Benefits for different battery and PV sizing.

Similarly, increasing the battery capacity for a given PV surface enhances the system flexibility, which enables more profitable energy management strategies. Specifically, the GSBS does not buy electricity only to match the momentary energy demand, but also stores it in the battery to feed the SBS (or sell the energy back to the SG) when the energy price becomes expensive. However, when the battery capacity is too high, the storage surplus cannot be used make profits because of the limitation (4.7). Therefore, increasing the

battery size from a certain point will have no effect on the cost saving, but will still require a larger investment cost. This partially explains the parabolic shape of the benefit, which drops starting from a given battery capacity.

The other reason behind the parabolic shape of the benefit is linked to the influence of the RC of the investment. To demonstrate this, we evaluate the SoH loss (see the left y-axis in Fig. 4.3) and the corresponding capacity loss (right y-axis) during one year for a PV panel of 0.25 m^2 and different battery capacities. First, we can see that very small and very large batteries are more affected by the aging mechanisms. More specifically, the battery SoH loss for capacities less than 4 A h and more than 11 A h is higher than 20%. Also, the larger the battery capacity, the higher the SoH loss. This can lead to lose more than half of the storage capability in only one year for capacities higher than 30 A h.

Generally, the type and severity of aging depends on the battery size. Indeed, small batteries are rapidly charged and discharged due to the relatively large amounts of energy produced by the PV panel and consumed by the SBS. These batteries are likely to be cycled frequently and more consistently, so that they rarely go through inactivity periods. Therefore, small batteries are more concerned by cycle aging. In contrast, if the battery is over-sized compared to the system needs, it is lightly cycled and more likely to be unused for long time intervals. Therefore, large batteries are more subject to calendar aging. We can see then that the RC of the investment increases with very large or very small batteries, which explains the parabolic shape of the benefit with respect to the battery capacity. Eventually, some of these battery sizes do not efficiently pay off their investment, *i.e.*, they result in negative benefits, as shown in Fig. 4.2. Then, we can observe that the optimal sizing is ($S_{PV}=1 \text{ m}^2$, $C_N=16 \text{ A h}$), with a benefit of \$983.

Also, we want to investigate whether the PV panel surface has an influence on the battery aging. Fig.

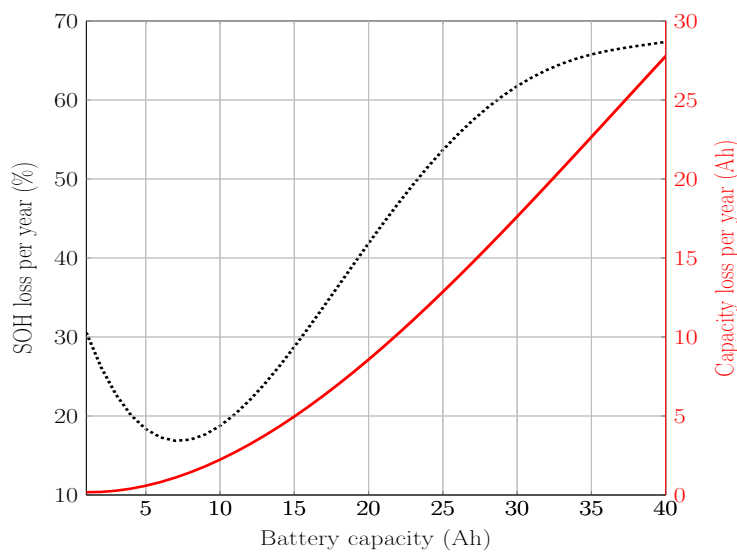


FIGURE 4.3: SoH loss during one year for different battery capacities using a PV panel of 0.25 m^2 .

4.4 represents the SoH loss during one year for three battery capacities and different PV surfaces. First, notice that the minimum SoH loss is achieved for $C_N=7 \text{ A h}$ as shown in Fig. 4.3. Then, we observe that there is a negligible dependency between the battery aging and the PV surface. In fact, the battery aging variation is at most 0.3% per year, which is very small considering that the overall aging is superior to 18%. Moreover, at a certain point, the battery aging is constant because all the additional production from a larger PV system is sold to the grid without impacting the SoC of the battery. Therefore, for the current economic framework, we can conclude that the surface of the PV panel has only a minor impact on the battery aging.

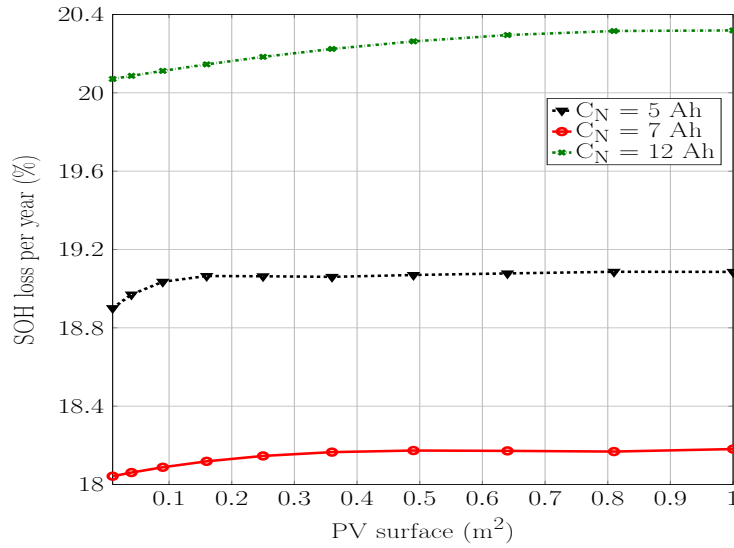


FIGURE 4.4: SOH loss during one year for different PV surfaces.

4.3.2 SIZING SENSITIVITY TO THE OPTIMIZATION PARAMETERS

The results of the sizing study is related to several parameters that characterize the battery (temperature and voltage), the PV panel (conversion efficiency), the SBS (traffic load), and the SG (financial aid and electricity pricing). In this section, we investigate how the sizing results are affected when the behavior of these parameters is taken into account.

4.3.2.1 SENSITIVITY TO BATTERY PARAMETERS

In this work, we employed a detailed battery model involving several parameters, namely the voltage and internal temperature, to realistically describe the aging process. The sensitivity study, which we present in this section, aims to justify the used calendar aging model by demonstrating that the considered parameters cannot be neglected. To do this, we suppose two cases in which we ignore the temperature and the voltage variation, respectively:

1. **Case 1:** the energy strategy is obtained assuming a constant battery temperature, equal to the average ambient temperature of 15 °C.
2. **Case 2:** the energy strategy is obtained assuming a constant voltage, equal to the average voltage 2.5 V.

The benefits in these two cases are represented in Fig. 4.5 and 4.6. In the first case, the optimal sizing is (1 m², 23 A h), for an expected benefit of \$1055. In the second case, it is (1 m², 20 A h), for an expected benefit of \$1005. Note that the optimal battery size increases to 23 A h in **case 1** (resp. 20 A h in **case 2**) from the 16 A h of the optimal sizing results where the battery temperature and voltage are not fixed (see Section 4.3.1). The choice of a larger battery capacity is due to the underestimation of the calendar aging process and hence, its RC. Indeed, for the sizing of 23 A h (resp. 20 A h), the expected benefit in **case 1** (resp. **case 2**) is higher compared to the benefit reached in realistic conditions, which is \$960 (resp. \$963), according to Fig. 4.2. Given these simulation results, 2.3% (resp. 2%) of the benefit is lost if the battery temperature (resp. voltage) is supposed constant when computing the system sizing. The benefit loss could be even larger if these two parameters are neglected simultaneously.

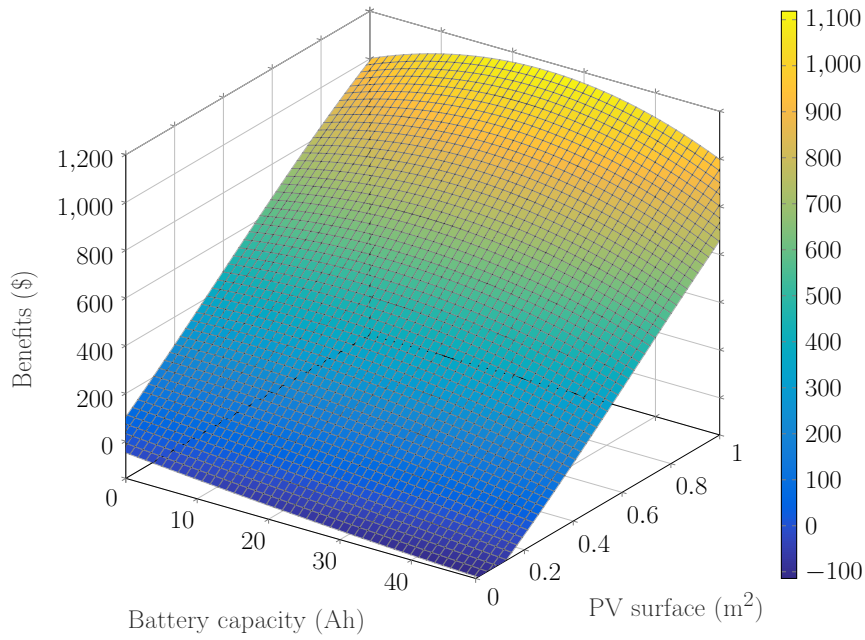


FIGURE 4.5: *Benefits for different battery and PV sizings in case 1.*

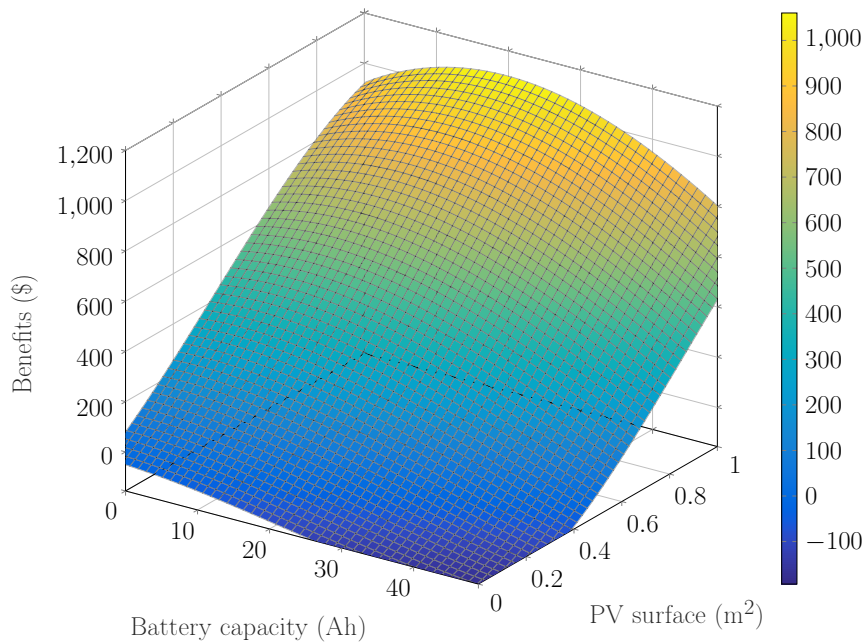


FIGURE 4.6: *Benefits for different battery and PV sizings in case 2.*

4.3.2.2 SENSITIVITY TO PV PARAMETERS

According to Section 3.4 in Chapter 2, besides the panel surface, the PV production depends on the energy conversion efficiency η_{PV} and the solar radiation. The latter is a consequence of the geographical location and cannot be tuned during the sizing study. Therefore, in the following, we are interested in how the PV conversion efficiency impacts the optimal sizing.

In the successive technologies, PV design has been improved to achieve higher efficiencies. As an approximation, we consider that the cost of improving the PV conversion efficiency is equivalent to the cost of increasing the PV size, *e.g.*, doubling the conversion efficiency costs as much as doubling the PV size.

Fig. 4.7 illustrates the benefits achieved by the GSBS, equipped with a 0.25 m^2 PV panel, for different PV conversion efficiencies and battery capacities. We see that improving the PV efficiency enables higher benefits. In particular, the maximum benefit reached with a higher η_{PV} increases linearly with the battery size.

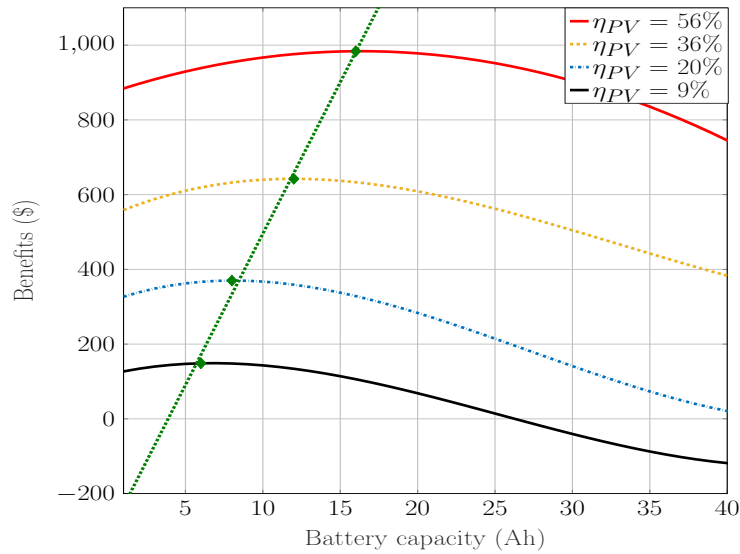


FIGURE 4.7: Benefits for different battery sizes and PV conversion efficiencies.

4.3.2.3 SENSITIVITY TO SBS PARAMETERS

In this part, we investigate the trade-off between the SBS load and the battery capacity in the three following scenarios:

1. **Scenario 1:** the daily SBS load is the average daily profile (Fig. 4.1).
2. **Scenario 2:** the daily SBS load is the 75% of the average daily profile.
3. **Scenario 3:** the daily SBS load is the 25% of the average daily profile.

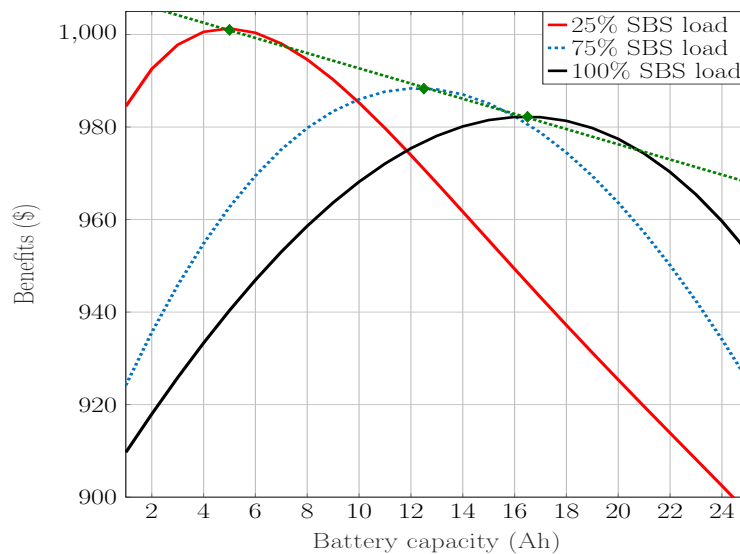


FIGURE 4.8: Benefits for different battery sizes in different load scenarios.

Fig 4.8 represents the benefits obtained in these three scenarios with 1 m^2 PV panel and different battery capacities. First, we can observe that the maximum achievable benefit increases when the SBS daily load is

reduced. Also, we see that the optimal battery capacity is 16 A h in **scenario 1**, 12 A h in **scenario 2**, and 5 A h in **scenario 3**. Therefore, the evolution of the optimal battery sizing is quasi-linear with respect to the BS load. This is an important finding for the holistic management of a cellular network. First, if we consider the SBS energy consumption instead of the SBS load (the two being linearly dependent), it is possible to dimension the optimal battery for other BS types (macro, micro, and femto cell BSs). In addition, a load balancing scheme aware of the battery state can be imagined. On the one hand, the battery sizing does not need to be optimized on the peak requirement of a single SBS but rather on the overall requirements of neighboring SBSs by exploiting statistical multiplexing gains. Indeed, due to the unbalanced distribution of the mobile traffic between neighboring cells, the load could be efficiently shared (or even the energy resources), leading to larger resource utilization efficiency and lower battery investments. On the other hand, this approach can be used to protect the battery from fast aging by transferring the traffic to the cells that gather the right conditions for the battery use.

4.3.2.4 SENSITIVITY TO ECONOMIC PARAMETERS

The following section examines the impact of the price factor and battery financial aid on the battery sizing solution. To do this, we consider a PV surface of 0.5 m^2 . As it is shown in Fig. 4.9, increasing the selling price factor contributes to achieve higher benefits. Additionally, the optimal battery size corresponding to the maximum benefit shifts to the right as the selling price factor grows. The reason behind this is that larger battery capacity allows more energy storage, which in turn increases the profit related to the energy sold to the grid. A similar behavior is illustrated in Fig. 4.10 as the optimal battery capacity increases with higher financial aid. Indeed, the cost of larger batteries is reduced through financial aid while more energy OPEX saving is achieved. In conclusion, the economic framework and the electricity market need to be taken into consideration during the GSBS sizing.

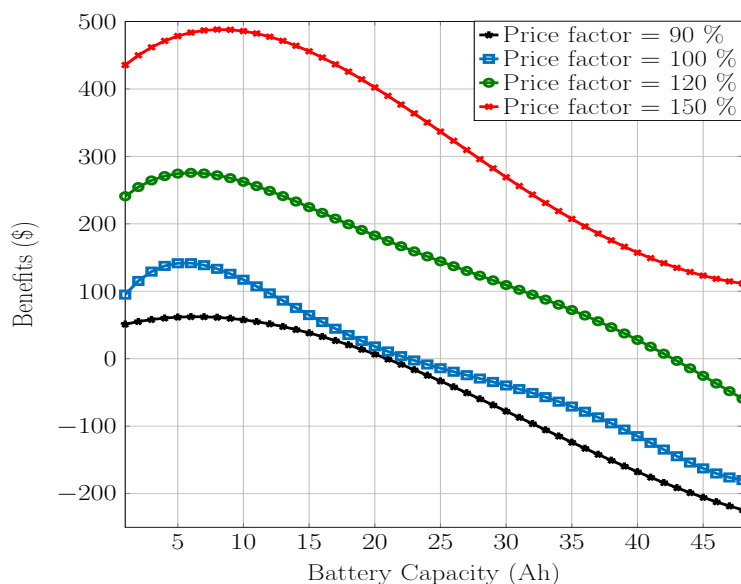


FIGURE 4.9: Impact on the benefits of the price factor ($\psi = 0 \%$).

4.3.3 SIZING SENSITIVITY TO THE ENERGY MANAGEMENT ESTIMATION

As presented in Section 4.2.2, the sizing problem requires an estimation of the energy management strategy over the optimization horizon. The average awareness of several inputs (the ambient temperature, the solar radiation, the SBS load, the battery SoC, and the electricity price) is enough to elaborate the average-based energy management and solve the sizing problem as we did in Section 4.3.1. In reality,

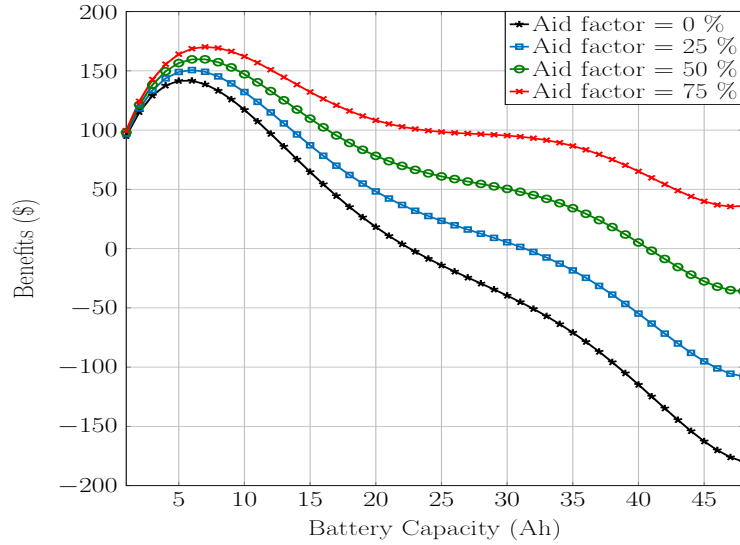


FIGURE 4.10: *Impact on the benefits of the financial aid factor ($\kappa = 100\%$).*

the realizations of the system variables are different each day and do not necessarily overlap with their respective average profiles. This raises the following question: by how much the gap between the estimated and real values impacts the sizing solution?

To answer this question, we compare the sizing results evaluated with the average-based energy strategy (imperfect knowledge) and the ideal energy strategy (perfect knowledge). Fig. 4.11 represents the benefit gain of the ideal energy strategy with respect to a realistic policy with imperfect knowledge, considering different pairs of PV surface and battery capacity. As expected, in the long term, the management based on perfect knowledge performs better economically than the one based on the average profile estimations. More specifically, the benefit gap increases linearly with the PV surface and the battery capacity. In fact, the uncertainty on the system parameters, namely the PV production and the battery internal temperature, is larger when the system sizing increases. Overall, the uncertainty on the optimization parameters can generate a reduction up to 4.5% on the benefit.

However, we notice that the two approaches lead to the same result in term of system sizing. When we integrate the benefit gain given by the perfect knowledge of the stochastic variables (Fig. 4.11) to the benefit obtained with the imperfect knowledge policy (Fig. 4.2), the battery-PV pair that achieves the global maximal benefit does not change. This result is very important because it is impossible to perfectly forecast in the long term the variables related to the PV production, SBS energy consumption, and the SG pricing. Therefore, planning for a GSBS deployment can reliably use statistical knowledge about the system variables to find the optimal sizing.

4.3.4 PRACTICAL INSIGHTS ON THE SIZING PROCEDURE

Following the previous analyses in the given economic framework, we observed that the PV panel size linearly increases the system benefits (see Fig. 4.2) while its effect on the battery aging is negligible (see Section 4.3.1). Consequently the PV surface can be selected prior to the sizing study, which simplifies Algorithm 1 by determining only the optimal battery capacity. Specifically, it is profitable to deploy a PV panel with a surface equal to all the available space dedicated at the GSBS. Thereafter, the battery capacity can be efficiently selected with respect to the chosen PV panel surface and technology (see Fig. 4.2 and 4.7), the SBS load (see Fig. 4.8), and the economic conditions (see Fig. 4.9 and 4.10).

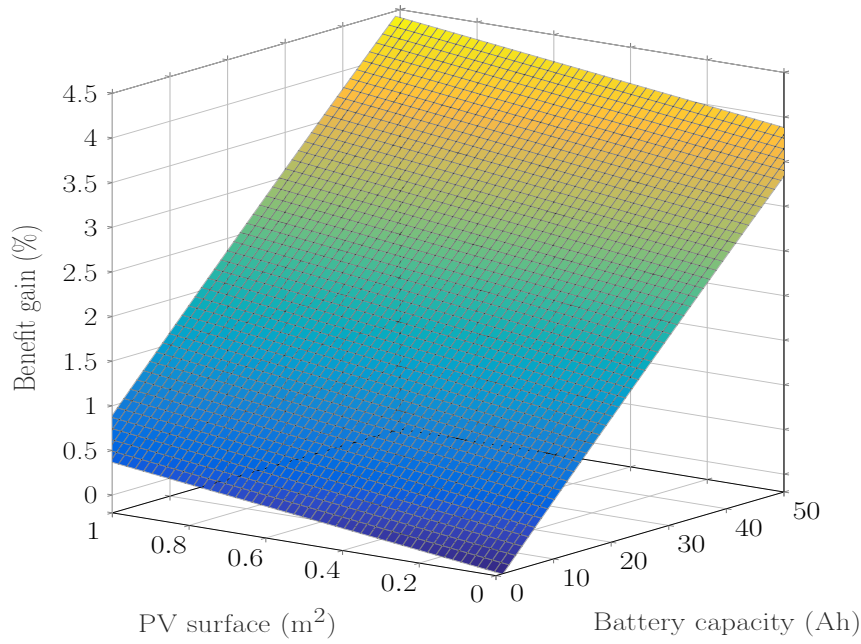


FIGURE 4.11: Benefits gain with the ideal energy management compared to the average-based energy management.

4.3.5 OFF-GRID GSBS ANALYSIS

In this part, we briefly discuss the results related to the off-grid sizing problem presented in Section 4.2.4. This problem is solved by adopting the average-based energy management, accordingly to the profiles of the state variables (Fig. 4.1). The obtained optimal sizing is (0.24 m², 15 A h) and corresponds to an investment cost of \$423, which includes the FC and the RC. Fig. 4.12 represents the SBS energy consumption, PV energy production, and the battery energy storage. The energy strategy simply consists on charging the battery using the RE production and discharging it to feed the SBS. Based on Algorithm

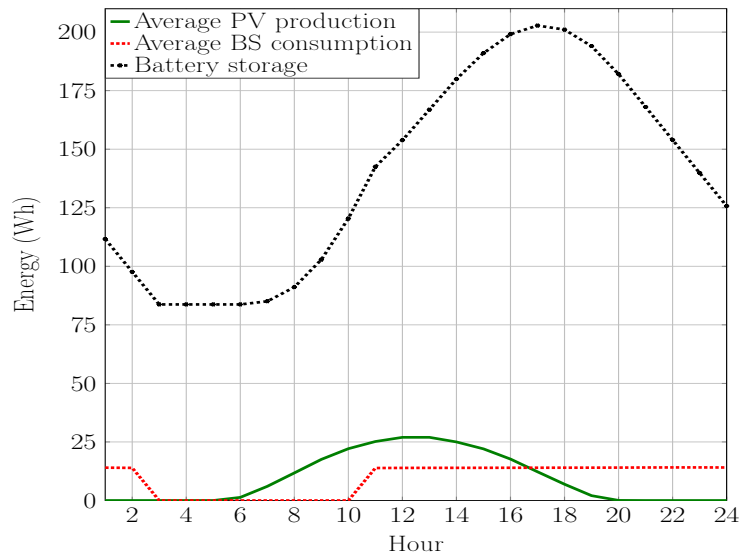


FIGURE 4.12: Power flows in an off-grid GSBS.

2, and by neglecting DC, we obtain the utility generated by connecting the GSBS the SG compared to the off-grid case:

$$U = \$163 - EC. \quad (4.15)$$

Accordingly, we can highlight that whenever the costs to connect the GSBS to the grid is below \$163,

the investment is economically feasible. Depending on the economic environment, the EC cost can change drastically. For example, assume the power line construction cost in low voltage grids of $\zeta = 5000$ \$/km [Nerini 2015]. Therefore, in order for the connection to the grid to be valuable, the distance separating the off-grid GSBS from the nearest connection point of the SG should be at most 33 m.

4.4 CONCLUSION

In this chapter, we investigated the sizing problem of a GSBS, which relies on the estimation of the energy management strategy. Our results showed that there is a unique battery size that optimizes the investment, which depends on the deployed PV panel, the SBS power consumption, and the economical market condition. Specifically, the dependency between the benefit and the battery storage capacity is a bell-shaped function. This is due to the fact that very large and very small batteries (compared to the optimal size) are more affected by the aging mechanisms. Especially, the calendar aging has a notable impact on large batteries while cycle aging particularly degrades small batteries. We also proposed a practical sizing approach based on the fact that the system benefits increase linearly with the PV panel size. As a consequence, the optimal PV size (in on-grid scenario) should be set equal to all available physical surface. Then, the battery capacity is optimally defined according to the system conditions. Besides, the hypothesis of average knowledge of the system parameters used to estimate the energy management strategy is not constraining when dimensioning the system since it results in the same optimal sizing as for the ideal knowledge case, in which the future states of the system variables are known. Finally, we evaluated the profitability of connecting an off-grid GSBS to the SG. Our simulation results allow to define the maximum acceptable connection cost and the critical distance from the grid after which the connection is not economically valuable.

Once the GSBS sized and deployed, the energy management strategy need to be adapted to real conditions, that differs from the average profiles considered in the sizing study. The next Chapter exposes in detail an adaptive approach based on machine learning that enables the ESS to efficiently adjust the energy strategy to the GSBS's environment (weather, traffic load, and electricity price).

FQL-BASED ENERGY MANAGEMENT

Contents

5.1	Introduction	63
5.1.1	Motivation	63
5.1.2	Related Works	63
5.1.3	Contribution	64
5.2	Fuzzy Q-Learning technique	64
5.2.1	Fuzzy Inference System	65
5.2.2	Q-Learning	67
5.2.3	Tuning the FIS by Q-learning	68
5.3	Implementation of FQL for the GSBS Management	70
5.4	Kalman estimation-based method	73
5.5	Simulation Results	75
5.5.1	Energy Management Strategy	76
5.5.2	Battery aging	77
5.5.3	Economic performance	80
5.6	Conclusion	81

5.1 INTRODUCTION

5.1.1 MOTIVATION

In the sizing method discussed in chapter 4, we have assumed a pre-operation energy management prior to the system deployment, based on the estimated average profiles of the SBS energy consumption, PV production, and electricity price. Once the GSBS is sized and deployed, the performance of the energy management strategy may suffer from inaccurate forecast of the traffic load and RE generation. An adaptive approach is therefore needed to enable the ESS to adjust the energy strategy to real operational conditions. The final goal is to optimally reduce the energy OPEX and enhance the battery conservation.

5.1.2 RELATED WORKS

Early works on energy cost optimization for on-grid energy-harvesting SBSs have used offline approaches, which consider traffic load profiles and long-term statistics of the PV energy production and

electricity price [Zhang 2016]. Amongst these works, Michelusi *et al.* [Michelusi 2013] have derived, by using Markov chains, an energy policy for sensor networks equipped with batteries, which captures cycle aging. However, although these methods are easy to implement, they are not effective in responding to the load, production, and price changes. To tackle the offline approach limitations, online policies have also been proposed. In this context, stochastic optimization has been implemented by assuming that the statistics of the energy processes are known and that past observations can correct the energy forecasts [Kaewpuang 2012] [Mao 2016]. Kaewpuang *et al.* have investigated an online stochastic approach based on multi-period recourse [Kaewpuang 2012]. Mao *et al.* have mapped an energy cost minimization problem into a discrete Markov decision process and derived specific solution properties to develop an algorithm based on monotone backward induction [Mao 2016]. To optimize the on-grid cost of energy-harvesting SBSs, Blasco *et al.* developed an energy controller, which is trained with statistical data and uses dynamic programming. Similarly, Leithon *et al.* [Leithon et al. 2016] have developed prediction models by using an auto regressive integrated moving average time series and Markov chains to optimize the energy decision variables on real-time basis.

All the energy management techniques mentioned before have systematically required a minimum knowledge of RE, BS load, and price models. However, some of these models are too complex and need to be continuously updated, since they only fit to a specific environment. While other approaches are too simple to capture the realistic behavior of the stochastic variables. The contributions of this chapter address this limitation.

5.1.3 CONTRIBUTION

Our main contributions in this chapter are as follows:

- *Contribution 1:* We propose a model-free energy management controller based on FQL that jointly minimizes the operating energy cost and preserves the battery lifetime. The FQL combines the advantages of Q-Learning [Watkins 1992] and FIS [Busoniu 2007] and enables to design a controller that does not need any prior knowledge on the energy consumption, energy production, and energy price.
- *Contribution 2:* We compare the proposed method with other approaches, namely an online technique from the literature based on Kalman filter [Leithon 2013] and what we refer to as the *ideal* strategy, which is aware of the future states of the system variables. System simulations show that the FQL controller achieves considerable cost reduction compared to the method based on Kalman filter and other baseline strategies. Furthermore, the obtained energy management policy performs very closely to the *ideal* strategy.
- *Contribution 3:* Simulation results show that by taking into account the battery aging processes, the proposed energy management strategy enhances the battery life span by 30% per year. The battery aging awareness also leads to an increase in the OPEX; however, this is negligible compared to the cost saving on the battery replacement.

The novelty of this chapter is based one journal article [J2], and a conference paper [C1].

The rest of the chapter is organized as follow. In Section 5.2, we define the theoretical framework of FQL. In Section 5.3, we present the proposed FQL based energy controller. In Section 5.4, we give an overview about the Kalman-based optimization. In Section 5.5 we provide and analyze the simulation results. Finally, we, summarize the chapter in Section 5.6.

5.2 FUZZY Q-LEARNING TECHNIQUE

FQL is the technique we use to solve the in-operation energy management problem presented in Chapter 3. This technique relies on a FIS provided with learning capabilities. In this preliminary section, we first give a general idea about the formulation of control-command problems with the FIS approach.

Then, we present the Q-learning algorithm, which belongs to a specific class of machine learning called *Reinforcement Learning* (RL). Finally, we explain the functioning of FQL that consists on tuning a FIS by Q-learning.

5.2.1 FUZZY INFERENCE SYSTEM

Fuzzy logic is an approach to computing, introduced by Zadeh [zad 1965], based on "degrees of truth" rather than the usual "true or false" (1 or 0) in Boolean (or crisp) logic. In fact, fuzzy logic considers 0 and 1 as extreme cases of truth and also includes the various states of truth in between so that, for example, the result of a comparison between two things could be not "large" or "small" but "20% of smallness". By introducing the notion of degree in the verification of a condition, fuzzy logic provides a very valuable flexibility for reasoning, which makes it possible to take into account inaccuracies and uncertainties.

The FIS employs fuzzy logic to elaborate a nonlinear mapping of an input data set to a scalar output data. This operation is achieved following three steps: fuzzification, inference based on fuzzy rules, and defuzzification. These components and the general architecture of a FIS is shown in Fig. 5.1.

The process of the FIS is explained in Algorithm 3: Firstly, a crisp set of input data are gathered

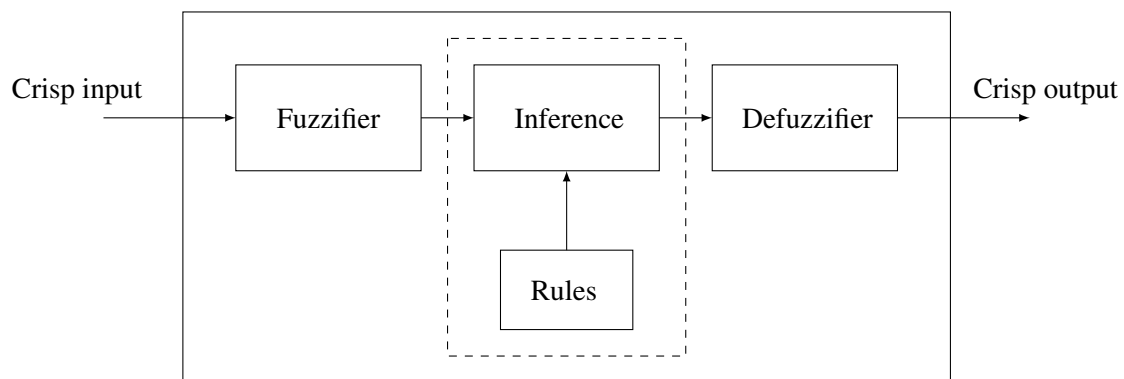


FIGURE 5.1: *Fuzzy Inference System.*

and converted to a fuzzy set using fuzzy linguistic variables (see Section 5.2.1.1), fuzzy linguistic terms (see Section 5.2.1.1), and membership functions (see Section 5.2.1.2). This step is known as fuzzification. Afterwards, an inference is made based on a set of rules (see Section 5.2.1.3). Lastly, the resulting fuzzy output is mapped to a crisp output using the membership functions, in the defuzzification step.

Algorithm 3: FIS algorithm

1. Define the linguistic variables and terms (initialization);
 2. Construct the membership functions (initialization);
 3. Construct the rule base (initialization);
 4. Convert crisp input data to fuzzy values using the membership functions (fuzzification) ;
 5. Evaluate the rules in the rule base (inference);
 6. Combine the results of each rule (inference);
 7. Convert the output data to non-fuzzy values (defuzzification);
-

5.2.1.1 LINGUISTIC VARIABLES

Linguistic variables are the inputs and outputs of the inference block. Their values are words or sentences from a natural language such as "high" and "low" [Zadeh 1974], instead of numerical values. Each

linguistic variable ξ is associated with a term set $T(\xi)$ that includes all the fuzzy sets corresponding to the names of the linguistic values of ξ . For example, in Section 5.3, we will associate to the electricity price the linguistic variable p^1 . To qualify the price, terms such as "high", "medium", or "low" are used in real life. These are the linguistic values of the price. Then, $T(p^1) = \{\text{Low, Medium, High}\}$ can be the set of decompositions for the linguistic variable price. Each member of this decomposition is called a linguistic term and can cover a portion of the overall values of the price.

5.2.1.2 MEMBERSHIP FUNCTIONS

Membership functions are used in the fuzzification steps of a FIS that maps the crisp (non-fuzzy) input values to fuzzy linguistic terms. A membership function is used to quantify a linguistic term. For instance, in Fig. 5.6, the membership functions that we used for the linguistic terms of the price variable are illustrated. Note that a numerical value does not have to be fuzzified using only one membership function. In other words, a value can belong to multiple sets at the same time.

5.2.1.3 TAKAGI-SUGENO INFERENCE

In a FIS, a fuzzy rule is a simple IF-THEN rule with a condition and a conclusion. It is constructed to control the output variable based on the input data.

Takagi-Sugeno (TS) rules have fuzzy inputs and a crisp output, which is a linear combination of the inputs. It is computationally efficient and suitable to work with optimization and adaptive techniques, so it is very adequate for control problems, mainly for dynamic nonlinear systems [Cavallaro 2015]. In particular, we consider the following TS rule structure that links a crisp output action a_j to the membership condition of the linguistic variable ξ to the fuzzy set $S_j \in T(\xi)$:

$$R_j : \mathbf{IF} \xi \text{ is in } S_j \mathbf{ THEN the action is } a_j.$$

The degree of truth of the condition of the j th rule is defined by the membership function μ_j .

For the input ξ the total output a of the TS model is computed by aggregating the individual rules contributions:

$$a = \sum_{j=1}^{|T(\xi)|} u_j(\xi) \cdot a_j,$$

where u_j is the normalized degree of fulfillment of the condition of rule R_j :

$$u_j(\xi) = \frac{\mu_j(\xi)}{\sum_{i=1}^{|T(\xi)|} \mu_i(\xi)}.$$

Note that TS inference approach integrates a defuzzification step such that the output of aggregating the inference rules is crisp.

Important remark: The condition of fuzzy rules can also apply to a vector of linguistic variables. Suppose a vector $\mathbf{v} = (v_1, v_2)$ composed of the two linguistic variable v_1 and v_2 . The term set associated to \mathbf{v} is constructed from the term sets of v_1 and v_2 such that $T(\mathbf{v}) = T(v_1) \times T(v_2)$. In the following, we consider that the condition:

$$\mathbf{IF} \mathbf{v} \text{ is in } V \mathbf{ THEN ...}$$

is equivalent to:

$$\mathbf{IF} v_1 \text{ is in } V_1 \mathbf{ AND } v_2 \text{ is in } V_2 \mathbf{ THEN ...}$$

where $V = (V_1, V_2) \in T(v_1) \times T(v_2)$.

5.2.2 Q-LEARNING

Q-learning is a model-free RL technique. Generally, RL techniques assume that, during the learning process, no supervisor is present to directly judge the quality of the selected control action and instead, the final evaluation of a process is known after along sequence of actions. Although the correct actions are not provided, the direct consequence of an action is given by the reinforcement signal. The learning system then has to discover by itself what actions lead to a better overall performance. It is therefore a trial-and-error-based method, in which the actions that improve the performance, when triggered in the presence of certain input signals, become associated with these input signals. Fig. 5.2 illustrates the agent-

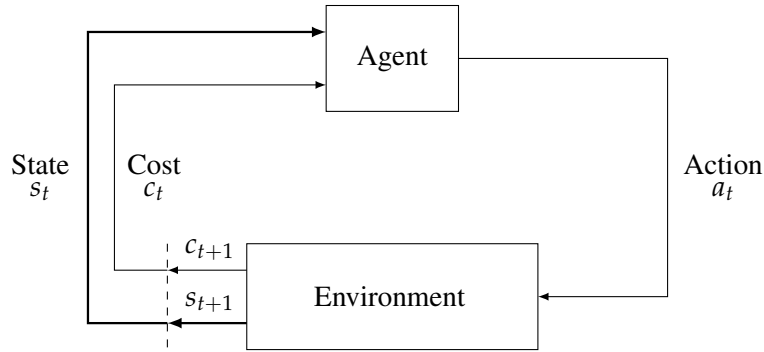


FIGURE 5.2: The agent-environment interaction in RL.

environment interaction on which RL is based [Sutton 1998]. The agent (decision-maker) and environment interact during a sequence of discrete time steps $t = 1, 2, 3, \dots$. At each time step t , the agent receives a representation of the environment's state s_t , and on that basis selects an action a_t . One time step later, in part as a consequence of its action, the agent receives a numerical cost $c_{t+1} \in \mathbb{R}$, and finds itself in a new state s_{t+1} . During the learning process, the agent visits a finite number of states and collects the transition cost each time an action is taken. The goal is to find an optimal policy, *i.e.*, a state-action mapping that minimizes the expected cumulative cost of the agent when visiting the state space. As represented in Fig.

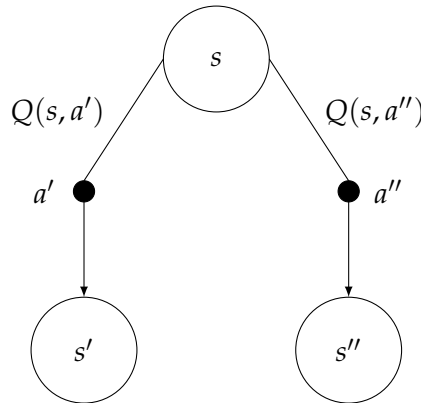


FIGURE 5.3: Visualization of the Q-values.

5.3, each pair state-action is defined by a Q-value $Q(\mathbf{s}, a)$, which represents the expected total discounted cost counting from the state-action pair (\mathbf{s}, a) over an infinite time:

$$Q(\mathbf{s}, a) = \mathbb{E} \left\{ \sum_{t=0}^{\infty} \gamma^t c(\mathbf{s}_t, a_t) \mid \mathbf{s}_0 = \mathbf{s}, a_0 = a \right\}, \quad (5.1)$$

where $\gamma \in [0, 1]$ is the discount rate that determines the current value of future costs.

In the Q-learning algorithm [Watkins 1992], the Q-values are first arbitrarily initialized, and then the optimal Q-values are computed in a recursive method. In each iteration, after the execution of an action a

in a state \mathbf{s} , the agent receives an immediate cost, perceives a new state \mathbf{s}' , and updates the value of $Q(\mathbf{s}, a)$ as :

$$Q(\mathbf{s}, a) \leftarrow Q(\mathbf{s}, a) + \alpha \cdot \Delta Q(\mathbf{s}, a), \quad (5.2)$$

$$\Delta Q(\mathbf{s}, a) = c(\mathbf{s}, a) + \gamma \min_{a' \in \mathcal{A}} Q(\mathbf{s}', a') - Q(\mathbf{s}, a), \quad (5.3)$$

where $\alpha \in [0, 1]$ is the learning rate, a' is the next state optimal action, and $Q(\mathbf{s}', a')$ is the next state Q-value. Watkins et al. [Watkins 1992] have proven that if each admissible state-action pair is visited infinitely often and the learning rate is decreased in a suitable way, then the Q-value (eq. (5.2)) will converge to an intermediate minimal $Q^*(\mathbf{s}, a)$ with probability 1. Therefore, we can determine the optimal action a^* with respect to the current state such that $Q^*(\mathbf{s}, a)$ is minimal as

$$a^* = \arg \min_{a \in \mathcal{A}} Q^*(\mathbf{s}, a). \quad (5.4)$$

Finally, the optimal state-action pairs are stored into a look-up-table, which is used for the optimal control of the system.

5.2.3 TUNING THE FIS BY Q-LEARNING

The FIS and Q-learning techniques, when used independently, suffer from limitations that reduce their scope of application. First, the Q-learning requires a discretization of the state and action spaces, which has to be rather fine to cover all possibly relevant situations and the wide variety of actions to choose from. As a consequence, there exists a combinatorial explosion problem when trying to explore all possible actions from all possible states. This is what Bellman called "the curse of dimensionality" [Sutton 1998]. Also, selecting discrete sets for states and actions introduces the subjectivity and human intervention in the algorithm design, which can lead to sub-optimal or/and non-generalizable solutions. In addition, the FIS system requires a prior knowledge to set the correct control action for each state. This necessitates a thorough awareness of the system dynamics and the evolution of the stochastic variables involved in the control, which is hardly realizable in the case of complex problems.

To overcome these limitations, the FQL provides the FIS with learning capabilities. On the one hand, the FIS framework makes it possible to formulate the control problem for a continuous space of states and actions, so that no discretization is required. On the other hand, instead of providing a prior state-action mapping to the inference engine of the FIS, the optimal actions associated to the fuzzy control rules are learned online.

Let's consider an input state vector \mathbf{x} , represented by L fuzzy linguistic variables; the set of state vectors of the L linguistic variables is denoted $\bar{\mathcal{S}} = \{\bar{\mathbf{s}}_1, \dots, \bar{\mathbf{s}}_N\}$, and for each state $\bar{\mathbf{s}}_j$, the set of actions is $\mathcal{A} = \{a_1, \dots, a_K\}$. As shown in Fig. 5.4, the agent in FQL corresponds to a FIS. The FIS receives a crisp state vector \mathbf{x} and infers the action based on control fuzzy rules, which consist of the TS rules tuned by the Q-learning algorithm:

$$\begin{aligned} R_j : \mathbf{IF} \mathbf{x} \text{ is in } \bar{\mathbf{s}}_j \text{ THEN} & \quad \text{action } a_1 \text{ with } q(\bar{\mathbf{s}}_j, a_1), \\ & \quad \mathbf{or} \quad \dots, \\ & \quad \mathbf{or} \quad \text{action } a_K \text{ with } q(\bar{\mathbf{s}}_j, a_K), \end{aligned}$$

where $q(\bar{\mathbf{s}}_j, a_i)$ is the fuzzy Q-value of the state-action pair $(\bar{\mathbf{s}}_j, a_i)$, $1 \leq j \leq N$, $1 \leq i \leq K$.

Note that these fuzzy rules only involves the Q-values associated to the linguistic variables and not the crisp state vector \mathbf{x} .

Typically, the practical implementation of the Q-learning requires that the Q-values are stored and updated explicitly for each state/action pair. This can be realized as long as the number of states and actions is reasonably large. When the combination of state-action space contains an infinite number of elements (as

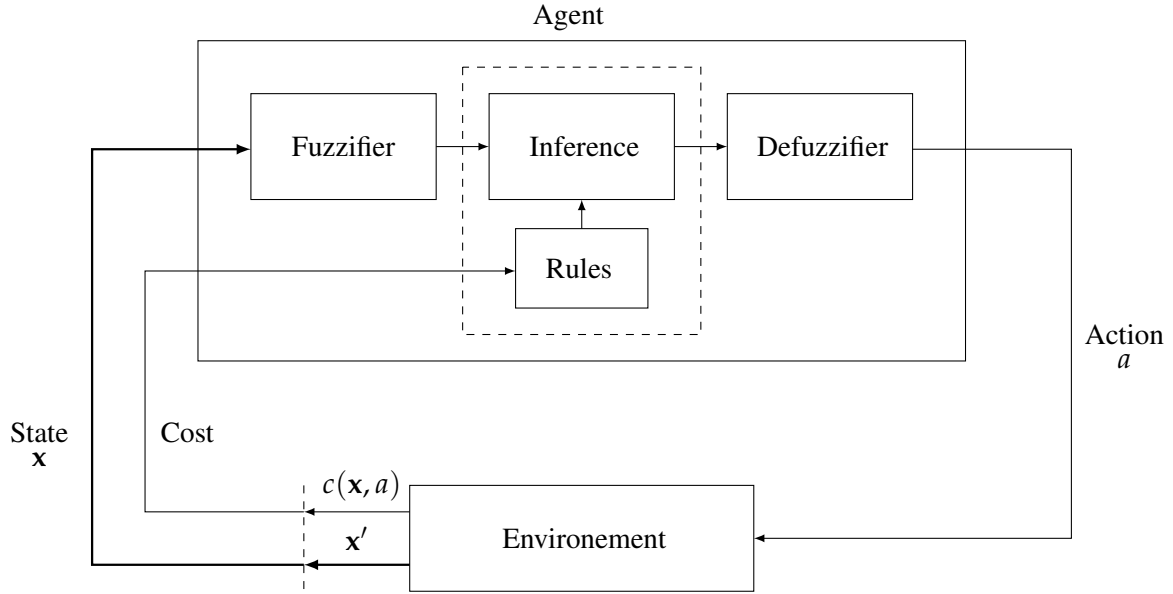


FIGURE 5.4: The agent-environment interaction in FQL.

in our case where the state space is continuous), approximate function are used to estimate the Q-value for each pair of continuous-state-vector and action. Many different methods of function approximation have been considered, such as the nearest neighbour, Fourier base, and neural networks [Sutton 2017]. However, there is no convergence guarantee for an arbitrary approximator of the Q-Learning. In the following, the Q-value associated to each state-action pair is approximated using a finite representation based on fuzzy logic rules. One advantage of the fuzzy Q-function approximation is the proved convergence, demonstrated by Busoniu et al. [Busoniu 2007].

Similarly to a classic FIS presented in Section 5.2.1, the FQL consists of three parts: *fuzzification* of the input variables, computation of *truth values*, and *defuzzification*. The first step takes the fuzzy input vector x and determines to which degree its elements belong to each of the appropriate fuzzy sets via membership functions. Then, the fuzzy-AND operator is applied to the membership degrees in order to obtain the truth value of the considered rule. Finally, the defuzzification process takes the computed true value w_j of each rule $1 \leq j \leq N$ and the associated optimal action a_j , and elaborates the inferred action for x as

$$a = \frac{\sum_{j=1}^N w_j \cdot a_j}{\sum_{j=1}^N w_j}. \quad (5.5)$$

Furthermore, the approximate of the Q-value for the state-action pair (x, a) is computed for the Q-value update (eq. (5.8)) as follows:

$$Q(x, a) = \frac{\sum_{j=1}^N w_j \cdot q(\bar{s}_j, a_j)}{\sum_{j=1}^N w_j}. \quad (5.6)$$

Then, after the execution of the action a , the agent receives an immediate cost $c(x, a)$, perceives the new state x' , and N Q-values can be updated as for the classic Q-learning scheme (see eq. (5.7))

$$q(\bar{s}_j, a_j) \leftarrow q(\bar{s}_j, a_j) + \alpha \cdot \Delta q(\bar{s}_j, a_j), \quad (5.7)$$

$$\Delta q(\bar{s}_j, a_j) = \frac{w_j}{\sum_{i=1}^N w_i} (c(\mathbf{x}, a) + \gamma Q(\mathbf{x}', a') - Q(\mathbf{x}, a)). \quad (5.8)$$

$Q(\mathbf{x}', a')$ is the next-state Q-value, which can be computed as

$$Q(\mathbf{x}', a') = \frac{\sum_{i=1}^N w_i \cdot q(\bar{s}_i, a_i^*)}{\sum_{i=1}^N w_i}, \quad (5.9)$$

where $a_i^* = \arg \min_{a_k \in \mathcal{A}} q(\bar{s}_i, a_k)$ is the optimal action for the next state \bar{s}_i , after the execution of action a_j in the previous fuzzy state \bar{s}_j .

5.3 IMPLEMENTATION OF FQL FOR THE GSBS MANAGEMENT

In this section, we present the proposed FQL based energy controller that jointly minimizes the electricity bill of the MNO and preserves the battery lifetime.

Let's consider the state representation $\bar{\mathbf{s}} = (P_{BS}^1, z^1, P_{PV}^1, p^1) \in \bar{\mathcal{S}}$ composed of four linguistic state variables that describe the hourly average SBS power consumption, battery SoC, RE production, and buying price, respectively.

We remind the cost function (defined in chapter 3) associated with each state-action pair (\mathbf{s}, a) at time t :

$$c(\mathbf{s}, a) = p(t) \cdot E_b(t) + p_{\text{sell}}(t) \cdot E_s(t) + \Gamma, \quad (5.10)$$

where $E_b(t) = \max(0, (P_{BS}(t) + P_{\text{batt}}(t) - P_{PV}(t)) \cdot \Delta t)$ is the quantity of energy bought from the SG at hour t , $E_s(t) = \min(0, (P_{BS}(t) + P_{\text{batt}}(t) - P_{PV}(t)) \cdot \Delta t)$ is the energy sold to the SG at hour t , $P_{\text{batt}}(t)$ is the power injected into or provided by the battery at time t , Δt is the duration of a time step, p_{sell} is the price of selling the energy back to the SG, and Γ the penalty function associated to the battery aging.

For the pre-operation energy management in chapter 4, the battery aging penalty has been modeled as a cost for replacing the lost capacity. Here, for the in-operation energy management, we define a penalty which depends on the operating SoC range Δ_{soc} (see the cycle aging model Section 3.5 in Chapter 3). The penalty function, noted Γ_m , increases as the distance between the SoC and Δ_{soc} grows:

$$\Gamma_m(z(t)) = \begin{cases} \chi \cdot (z(t) - 0.9), & \text{if } z(t) \geq 90\% \\ \chi \cdot (0.2 - z(t)), & \text{if } z(t) \leq 20\% \end{cases}, \quad (5.11)$$

where $\chi \geq 1$ is the penalty factor. This constraint enables to avoid intensive battery usage, which increases the cycle aging. Moreover, through the existing correlation between the SoC and voltage, it prevents high voltage during battery inactivity, which intensifies the calendar aging.

Also, we want to avoid using high (dis)charge current rates that cause accelerated calendar aging due to heat generation. Accordingly, we constrain the actions set such that the battery is operated only with low current rates. Each element of the action set corresponds to a C_{rate} limited in the interval $[-30\%, 30\%]$: $\mathcal{A} = \{0.01 \cdot k, k \in \{0, \pm 1, \pm 2, \pm 3, \dots, \pm 30\}\}$. The functionalities of the proposed FQL are represented in Fig. 5.5 and consists of a four layer FIS:

Layer 1: This layer has as input the four linguistic variables defined by the term sets $T(P_{BS}^1) = \{\text{Off, Idle, Low-Medium, High}\}$, $T(SOC^1) = \{\text{Very Low, Low, Medium, High, Very High}\}$, $T(P_{PV}^1) = \{\text{Low, Medium, High}\}$ and $T(p^1) = \{\text{Low, Medium, High}\}$. Then, we have $N_{\mathcal{L}} = |T(P_{BS}^1)| + |T(SOC^1)| + |T(P_{PV}^1)| + |T(p^1)| = 15$ nodes in the first layer, each one corresponding to a fuzzy set of a linguistic

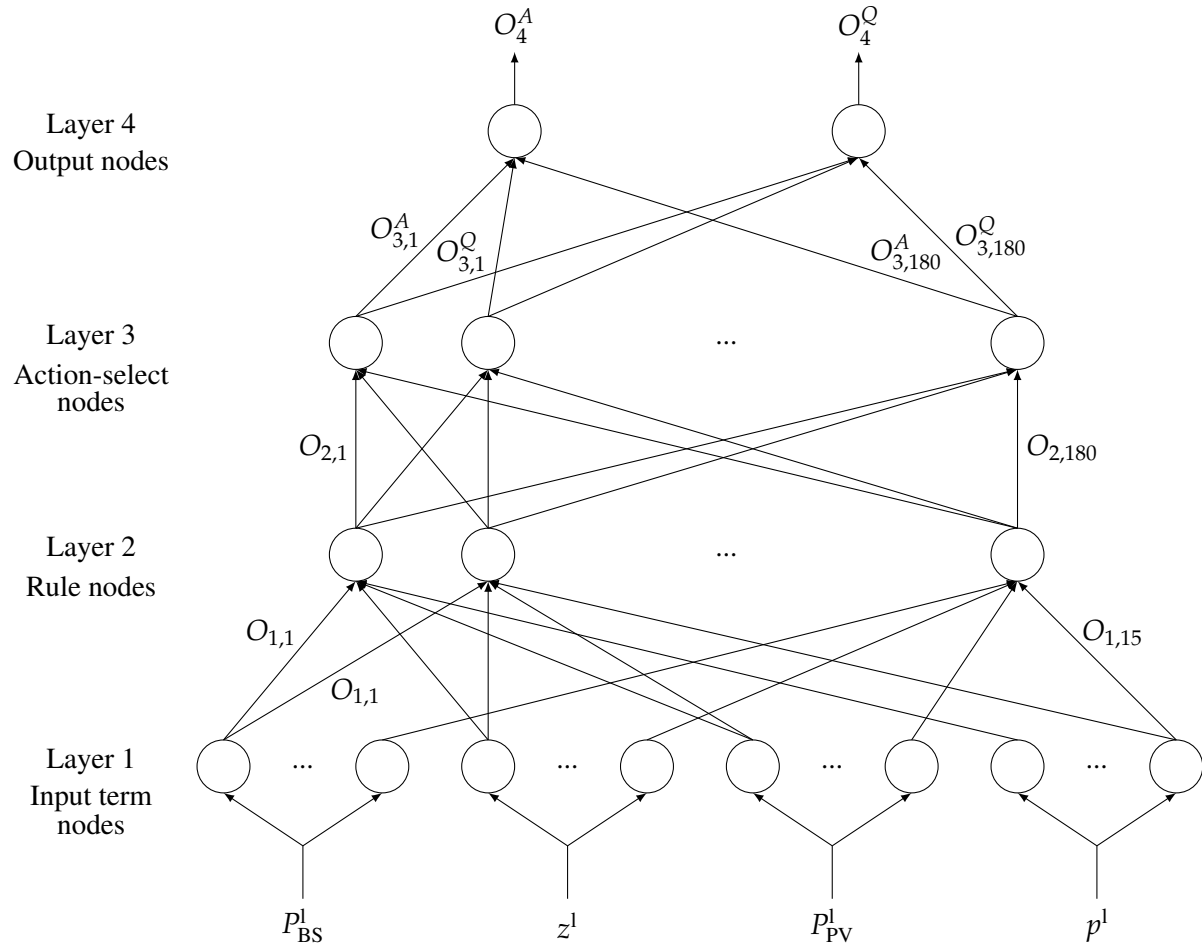


FIGURE 5.5: Graphic representation of FQL.

variable. Every node is defined by a trapezoid membership function. Finally, for a generic component s of the state vector \bar{s} , the output $O_{1,i}$ of the i th node of this layer is given by :

$$O_{1,i} = \begin{cases} 1, & \text{if } u_{\text{left}}^i \leq s \leq u_{\text{right}}^i \\ \frac{l_{\text{right}}^i - s}{l_{\text{right}}^i - u_{\text{right}}^i}, & \text{if } u_{\text{right}}^i < s \leq l_{\text{right}}^i \\ \frac{s - l_{\text{left}}^i}{u_{\text{left}}^i - l_{\text{left}}^i}, & \text{if } l_{\text{left}}^i \leq s < u_{\text{left}}^i \\ 0, & \text{otherwise} \end{cases} \quad i = 1, \dots, N_{\mathcal{L}}.$$

where l_{right} and l_{left} (resp. u_{right} and u_{left}) are the right and left terminals of the lower (resp. right and left upper) side of the trapezoid. Fig. 5.6 illustrates the membership functions defined in this work.

Layer 2: This layer is the rule nodes layer. It is composed by $|\bar{\mathcal{S}}| = |T(P_{BS}^l)| \times |T(SOC^l)| \times |T(P_{PV}^l)| \times |T(p^l)| = 180$ nodes, which compute the truth values of the fuzzy rules. Each node has four input values, one from one linguistic variable of each of the four components of the input state vector. Then the i -th rule node output $O_{2,i}$ is the product of the four membership values corresponding to the inputs:

$$O_{2,i} = \prod_{j \in \Phi_i} O_{1,j}, \quad i = 1, \dots, |\bar{\mathcal{S}}|,$$

where Φ_i is the set of the four nodes of the first layer used at the i -th rule node.

Layer 3: This layer is composed by $|\bar{\mathcal{S}}|$ action-select nodes. During the learning phase, each of these nodes

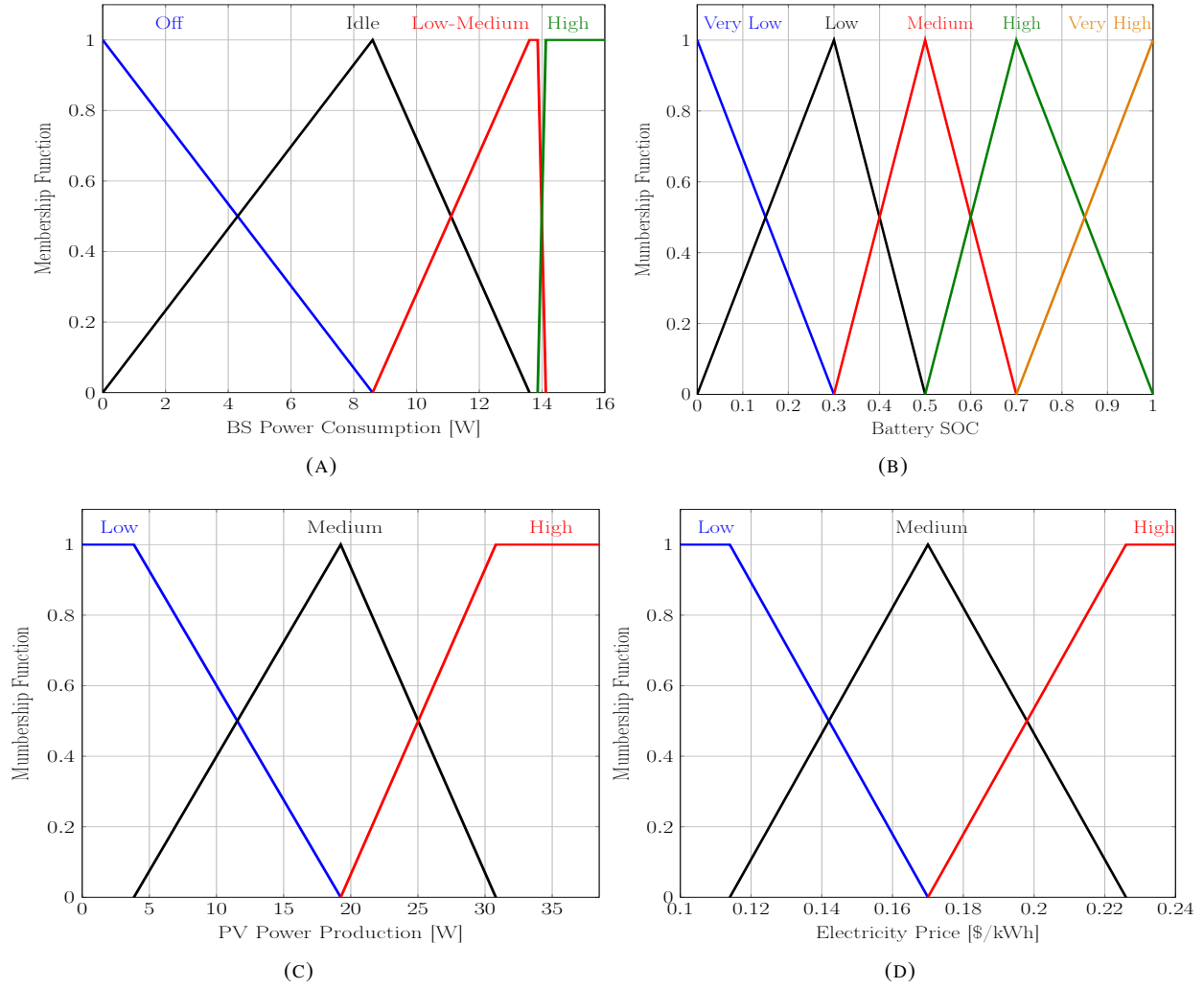


FIGURE 5.6: Linguistic variables membership functions.

selects the corresponding action (the battery charge or discharge rate) based on the ϵ -greedy policy, *i.e.*, it selects with probability $1 - \epsilon$ the action associated with the minimum Q-value, and with probability ϵ selects a random action:

$$a_i = \begin{cases} \arg \min_{a \in \mathcal{A}} q(\bar{\mathbf{s}}_i, a), & \text{if } y > \epsilon \\ \text{rand}(\mathcal{A}), & \text{otherwise} \end{cases} \quad i = 1, \dots, |\bar{\mathcal{S}}|,$$

where ϵ is a small positive value, y is a random value uniformly distributed between 0 and 1, and the function $\text{rand}(\mathcal{A})$ randomly chooses an action from the action set. By implementing the ϵ -greedy policy, the layer 3 aims to explore all possible actions and avoid local minima. Each node of the third layer outputs a weighted action and a Q-value as

$$O_{3,i}^A = \frac{O_{2,i} \cdot a_i}{\sum_{j=1}^{|\bar{\mathcal{S}}|} O_{2,j}}, \quad O_{3,i}^Q = \frac{O_{2,i} \cdot q(\bar{\mathbf{s}}_i, a_i)}{\sum_{j=1}^{|\bar{\mathcal{S}}|} O_{2,j}}, \quad i = 1, \dots, |\bar{\mathcal{S}}|.$$

Layer 4: This layer has two output nodes, action node O_4^A and Q-value node O_4^Q , which represent the

deffuzification step. The final outputs are given by:

$$O_4^A = \sum_{i=1}^{|\bar{\mathcal{S}}|} O_{3,i}^A, \quad O_4^Q = \sum_{i=1}^{|\bar{\mathcal{S}}|} O_{3,i}^Q. \quad (5.12)$$

Thereafter, the controller selects for the state \mathbf{s} the action $a = O_4^A$, which indicates how to charge or discharge the battery, and perceives an associated cost (see eq.(5.10)). Then, the fuzzy Q-values are updated by using the output of the Q-value node:

$$q(\bar{\mathbf{s}}_j, a_j) \leftarrow q(\bar{\mathbf{s}}_j, a_j) + \alpha \cdot \Delta q(\bar{\mathbf{s}}_j, a_j), \quad j = 1, \dots, |\bar{\mathcal{S}}|$$

where $\alpha \in [0, 1]$ is the learning rate and

$$\Delta q(\bar{\mathbf{s}}_j, a_j) = \frac{w_j}{\sum_{i=1}^N w_i} (c(\mathbf{s}, a) + \gamma Q(\mathbf{s}', a') - Q(\mathbf{s}, a)). \quad (5.13)$$

In eq. (5.13), $Q(\mathbf{s}, a) = O_4^Q$ and $Q(\mathbf{s}', a')$ is the next-state Q-value, which can be computed as

$$Q(\mathbf{s}', a') = \frac{\sum_{i=1}^N w_i \cdot q(\bar{\mathbf{s}}_i, a_i^*)}{\sum_{i=1}^N w_i},$$

where $a_i^* = \arg \min_{a_k \in \mathcal{A}} q(\bar{\mathbf{s}}_i, a_k)$ is the optimal action for the next state $\bar{\mathbf{s}}_i$, after the execution of action a_j in the previous fuzzy state $\bar{\mathbf{s}}_j$. At the end of the learning phase, each fuzzy state-action pair has been visited sufficiently often, and the $|\bar{\mathcal{S}}|$ Q-values converge to an intermediate minimum, from which the related optimal action can be computed. Then, the optimal state action pairs can be stored in a table, which can be used at the ESS for the battery management.

Note that the output of eq. (5.12) is not necessarily one of the discrete rates of the actions set, but a real value limited by the maximum charge and discharge rates. In fact, the subjectivity in the definition of actions, as well as the four term sets, is partially absorbed by the natural learning capability of FQL, in particular by the third layer process. Algorithm 4 summarizes the steps of the FQL.

5.4 KALMAN ESTIMATION-BASED METHOD

The approach we compare FQL to is an online Kalman-based optimization method proposed by Leithon *et al.* [Leithon 2013]. In the current literature, this solution is representative of the adaptive energy OPEX optimization methods for GSBS based on the estimation/correction scheme. Precisely, it makes use of the Kalman filter [Grewal 2011] to forecast the power consumption, RE production, and electricity price. The observation of the actual realization of the stochastic variables is used to progressively correct the predictions. This way, the algorithm requires solving a linear program every time a new observation is made for the remaining optimization period.

Unlike FQL, this approach requires prediction models of the stochastic variables, which are generally inferred from historical data. Besides, few changes have been introduced to the Kalman-based optimization problem characterized in details in [Leithon 2014] to include the SoC constraints.

The optimization problem is briefly described in the following:

$$\min_{E_c, E_d, E_s} p \cdot (P_{BS} - \eta_{dis} \cdot E_d + E_c - \eta_{dis} \cdot \kappa \cdot E_s)^\top \quad (5.14)$$

Algorithm 4: FQL algorithm

```

Initialization: for  $\bar{s} \in \bar{\mathcal{S}}$  and  $a \in \mathcal{A}$  do
  | initialize  $q(\bar{s}, a)$ ;
Learning: while no convergence do
  observe current state  $s$ ;
  for  $j \in \{1, \dots, N_{\mathcal{L}}\}$  do
    | compute the membership value  $O_{1,j}$  regarding the fuzzy sets;
  for  $i \in \{1, \dots, |\bar{\mathcal{S}}|\}$  do
    | compute the truth value  $O_{2,i}$  of the fuzzy rule  $R_i$ ;
  for  $i \in \{1, \dots, |\bar{\mathcal{S}}|\}$  do
    generate a random number  $y$  between 0 and 1;
    if  $y \leq \epsilon$  then
      |  $a_i \leftarrow \text{rand}(\mathcal{A})$ 
    else
      |  $a_i \leftarrow \arg \min_{a \in \mathcal{A}} q(\bar{s}_i, a)$ 
    compute the weighted action  $O_{3,i}^A$  and Q-value  $O_{3,i}^Q$ ;
  compute the defuzzified Q-value  $O_4^Q$  and action value  $O_4^A$ ;
  execute the action, receive an immediate cost, and observe the next state  $s'$ ;
  Update the fuzzy Q-values: for  $i \in 1..|\bar{\mathcal{S}}|$  do
    |  $q(\bar{s}_i, a_i) \leftarrow q(\bar{s}_i, a_i) + \alpha \cdot \Delta q(\bar{s}_i, a_i)$ ;
   $s \leftarrow s'$ ;

```

such that for $t = 1, 2, \dots, n$,

$$\eta_{\text{dis}} \cdot \sum_{i=1}^t E_c(i) - \sum_{i=1}^t E_d(i) - \sum_{i=1}^t E_s(i) \leq s_M - s_0 - \eta_{\text{chg}} \cdot \sum_{i=1}^t P_{\text{PV}}(i), \quad (5.15)$$

$$- \eta_{\text{dis}} \cdot \sum_{i=1}^t E_c(i) + \sum_{i=1}^t E_d(i) + \sum_{i=1}^t E_s(i) \leq s_0 - s_m + \eta_{\text{chg}} \cdot \sum_{i=1}^t P_{\text{PV}}(i), \quad (5.16)$$

$$E_c(t) \leq q_c - P_{\text{PV}}(t), \quad (5.17)$$

$$E_d(t) + E_s(t) \leq q_d, \quad (5.18)$$

$$\eta_{\text{dis}} \cdot E_d(t) \leq P_{\text{BS}}(t). \quad (5.19)$$

The decision variables correspond to the hourly vector of energy injected into the battery E_c , extracted from the battery E_d , and sold back to the grid E_s during the day; s_M (resp. s_m) represents the maximum (resp. minimum) energy that can be stored into the battery and s_0 is the energy initially stored in the battery; the battery maximum charging and discharging energy rates are respectively q_c and q_d . Note that $E_c, E_d, E_s, p, P_{\text{BS}}, P_{\text{PV}} \in \mathbf{R}_+^n$. The first constraint in (5.15) ensures that the maximum battery energy state is not surpassed, whereas the second constraint (5.16) ensures that the energy left in the battery is always above the minimum allowed. The third (5.17) and fourth (5.18) constraints impose the limited charging and discharging rates. The last constraint (5.19) ensures that the energy drawn from the battery to power the SBS is at most the energy required at every point in time.

The energy consumption P_{BS} , RE generation P_{PV} , and electricity price p processes are considered to follow a first-order Markovian model in which the current state depends only on the previous:

$$Y^{(i+1)} = \zeta^{(i)} \cdot Y^{(i)} + w, \quad (5.20)$$

where $Y^{(i)}$ is the state value of SBS power consumption, PV power production, or energy price at time step i , $w \sim N(0, \sigma_w^2)$ is an i.i.d. process noise, and $\zeta^{(i)}$ is the model slope at time step i . As the Kalman prediction model is supposed to be a linear relation between the next state and the current, it is assumed that every stochastic variable is represented by a piece wise linear system whose coefficients during each time step are computed from the profiles in Fig. 5.7:

$$\zeta^{(i)} = \frac{\bar{Y}^{(i+1)}}{\bar{Y}^{(i)}}, \quad (5.21)$$

where \bar{Y} denotes the recorded mean of the process.

In each time step, the estimation of the future state $\tilde{Y}^{(i+1)}$ is predicted using the linear model and corrected by the observation $Z^{(i)}$ of the current state as follows:

$$\tilde{Y}^{(i+1)} = \zeta^{(i)} \cdot Y^{(i)} + K^{(i)}(Z^{(i)} - Y^{(i)}), \quad (5.22)$$

where $K^{(i)}$ is the Kalman gain and the measurement is subject to an i.i.d. noise $v \sim N(0, \sigma_v^2)$ such that:

$$Z^{(i)} = Y^{(i)} + v. \quad (5.23)$$

At the beginning of the day, the stochastic processes are supposed to match their respective averages and the optimization problem is solved for these values. Once the next observation at time $(i + 1)$ is made, the current estimation of the process is updated from the $(i + 1)$ th element onward, and the values of $E_c^{(i+1)}$, $E_d^{(i+1)}$, and $E_s^{(i+1)}$ are computed using the updated estimation $\tilde{Y}^{(i+1)}$. This strategy requires thus solving a linear program every time a new observation is made for the remaining optimization period.

5.5 SIMULATION RESULTS

In this section, we consider a pico-cell base station, which is typically deployed to cover small areas like squares, train stations, and malls. Given the type of the SBS, we assume that the maximal available space for PV installation is 0.25 m^2 . In chapter 4, we have shown the optimal PV size should be set equal to all available physical surface, that is $S_{PV} = 0.25 \text{ m}^2$. Finally, according to the sizing results, the optimal battery capacity is $C_N = 7 \text{ Ah}$. The simulations have been accomplished for an optimization horizon of five years. To properly characterize their daily behavior, and without loss of generality, the stochastic variables are generated each hour of the day according to their respective models. In the simulation, we have considered the Kalman-based strategy such that the variance of the process noise for P_{BS} , for RE P_{PV} , and for electricity price p are extracted from the co-variance matrix of their respective models (see chapter 3). Furthermore, we have assumed that the measurement process is noiseless $\sigma_v^2 = 0$, which is a valid assumption given the accuracy of the sensors used nowadays. Other simulation parameters are summarized in Tables 5.1 and 4.2.

TABLE 5.1: *Simulation Parameters [Pillot 2013].*

	Parameter	Value	Parameter	Value
SBS	P_0	13.6 W	Δ_p	4
	P_{\max}	0.13 W	P_{sleep}	8.6 W
Battery	R	250 m Ω	C_N	7 A h
	η_{dis}	98%	η_{chg}	98%
	ψ	50%		
Solar panel	η_{PV}	14%	S_{PV}	0.25 m^2
Energy price	κ	100%		

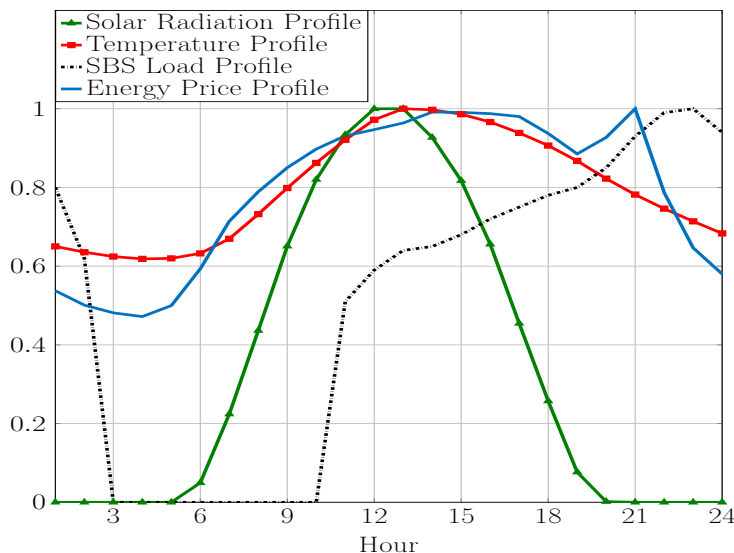


FIGURE 5.7: Normalized profiles of the average solar radiation, average ambient temperature [SOLAR], SBS load intensity (based on [Auer 2010]), and average energy price [Ameren].

In the following, we compare the energy management results obtained with the proposed FQL solution presented in Section 5.3 and the Kalman filter-based scheme presented in Section 5.4. Specifically, we show the differences in terms of energy management policies and their impact on both the OPEX saving and the battery aging. Also, to evaluate the trade-off between the cost saving on the energy bill and battery life span preservation, we implement the FQL and Kalman schemes in the two following cases:

1. The SoC constrained case, where the power flow strategy includes as constraints the recommended battery operating SoC interval $\Delta_{SoC} = [20\%, 90\%]$ and maximum charge/discharge rates $C_{rate} \in [-30\%, 30\%]$.
2. The unconstrained case, where the decision making does not take into consideration the battery life span preservation. In other words, all the possible values of the SoC between $[0\%, 100\%]$ and the charge/discharge rates in the interval $[-100\%, 100\%]$ are allowed. The penalty Γ_m in the cost function 5.11 is redefined as follows:

$$\Gamma_m(z(t)) = \chi, \text{ if } z(t) < 0\% \text{ or } z(t) > 100\%. \quad (5.24)$$

In addition, we analyze the energy cost savings achieved by the FQL and Kalman based schemes in the light of three baseline solutions:

1. The *reference* strategy that systematically buys energy from the SG, in which the battery and the solar panel are not used.
2. The *naive* strategy that seeks to reduce the immediate energy cost. At each decision period, if the PV production is sufficient to feed the SBS, the energy surplus is sold. Otherwise, the missing energy is purchased from the SG. Consequently the battery is never used.
3. The *ideal* strategy that has a perfect knowledge of the stochastic variables (SBS load, energy production, and energy price), and therefore upper-bounds the system performances.

5.5.1 ENERGY MANAGEMENT STRATEGY

The energy flows obtained with the Kalman and the FQL optimization methods are first presented in the unconstrained case in Fig. 5.8a and Fig. 5.8c, respectively. In these figures, we represent the average energy bought from and sold to the grid, the energy stored in the battery, the energy consumed by the SBS,

and the energy produced by the solar panel. In general, the ESS buys electricity when the price is low and the PV system cannot produce any energy (at night) to feed the SBS and charge the battery. When the PV production starts to rise during the day, and the price increases, the ESS prioritizes the use of the energy produced by the PV panels and the energy stored in the battery to feed the SBS, and sells a quantity of the surplus to the SG.

Fig. 5.8e shows the SoC variation corresponding to the power schedule of the Kalman and FQL strategies. It shows that the differences between the two strategies occur at the beginning of the day around the energy price valley of 04:00, around midday, and during the energy price peak of 21:00. While the FQL strategy charges gradually the battery from the grid early in the morning, the battery reaches its maximum capacity in only two hours with the Kalman scheme. A similar behavior is observed around 12:00 when the amount of energy sold back to the grid in the Kalman scheme is by far greater compared to the FQL strategy. This results in sub-optimal transactions with the SG in the Kalman strategy such that buying and selling energy does not take full advantage of the price variations.

The energy management in the SoH constrained case represented in Fig. (5.8b) and (5.8d) shows some similarities compared to the unconstrained case in the sense that the energy transactions respect the price trends and the production availability. However, unlike the previous case, it is clear from Fig. (5.8f) that the constraints on the SoC range and SoC variation are respected.

In the light of these results, we can conclude that the Kalman strategy chooses actions that results in considerable energy flows towards the SG and the battery. Clearly, in the present configuration, the Kalman method fully trusts its estimations and engages extreme decisions accordingly. However, these estimations are not always correct and therefore sub-optimal actions are taken. In contrast, the FQL algorithm improves more efficiently the long-term performance (see Section 5.5.3). In fact, the FQL approach enables a more progressive strategy to avoid sudden changes in the environment (such as clouds affecting energy production).

Concerning the algorithm complexity, both the Kalman and the FQL schemes have polynomial complexities. Kalman complexity is principally due to the use of Karmarkar's algorithm, whose complexity is $O(n_{\text{var}}^3 \cdot L_{\text{in}} \cdot \log(L_{\text{in}}) \cdot \log(\log(L_{\text{in}})))$, where n_{var} is the number of variables and L_{in} is the number of the bits in the input [Karmarkar 1984]. On the other hand, FQL complexity is due to the learning process: $O(|\mathcal{S}|^2 \cdot |\mathcal{A}|)$, where $|\mathcal{S}|$ (resp. $|\mathcal{A}|$) is the cardinality of the state (resp. action) space [Koenig 1992]. However, there is a major difference between the two solutions. The FQL scheme requires a learning phase in which the agent explores the state-action couples to converge towards the optimal policy. Fig. 5.9 shows the convergence of the sum (over the different states) of the momentary Q-values. Then, the optimal policy is stored in a look-up table that will be used during the exploitation process, which makes the complexity negligible during this phase. Conversely, the Kalman scheme does not require a learning phase but needs to solve the energy optimization problem at each time step.

5.5.2 BATTERY AGING

In this section, we evaluate the aging of the battery when operated according to each energy management policy. Fig. 5.10a shows the average time evolution of the SoH due to cycle aging for the Kalman and the FQL strategies in both the SoC constrained and unconstrained cases. We observe that the SoH decreases each time the battery is charged or discharged, whereas no degradation occurs during rest. Compared to the constrained case (0.02% SoH loss per day), the battery degradation in the unconstrained case (0.08% SoH loss per day) is approximately multiplied by four. The accelerated aging is caused by deep (dis)charges cycle, especially when the battery operates in extreme SoC areas (below 20% and above 90%). Also, note that the aging rates in the Kalman and the FQL schemes are very close, especially in the constrained case.

Similarly, Fig. 5.10b illustrates the calendar aging for the two strategies in the SoH constrained and unconstrained cases. The calendar aging corresponds to the capacity loss when the battery is in rest and depends on the rest duration, momentary voltage, and temperature. Because of the Joule effect, deep battery (dis)charges in the unconstrained case cause the internal battery temperature to attain very high values (34

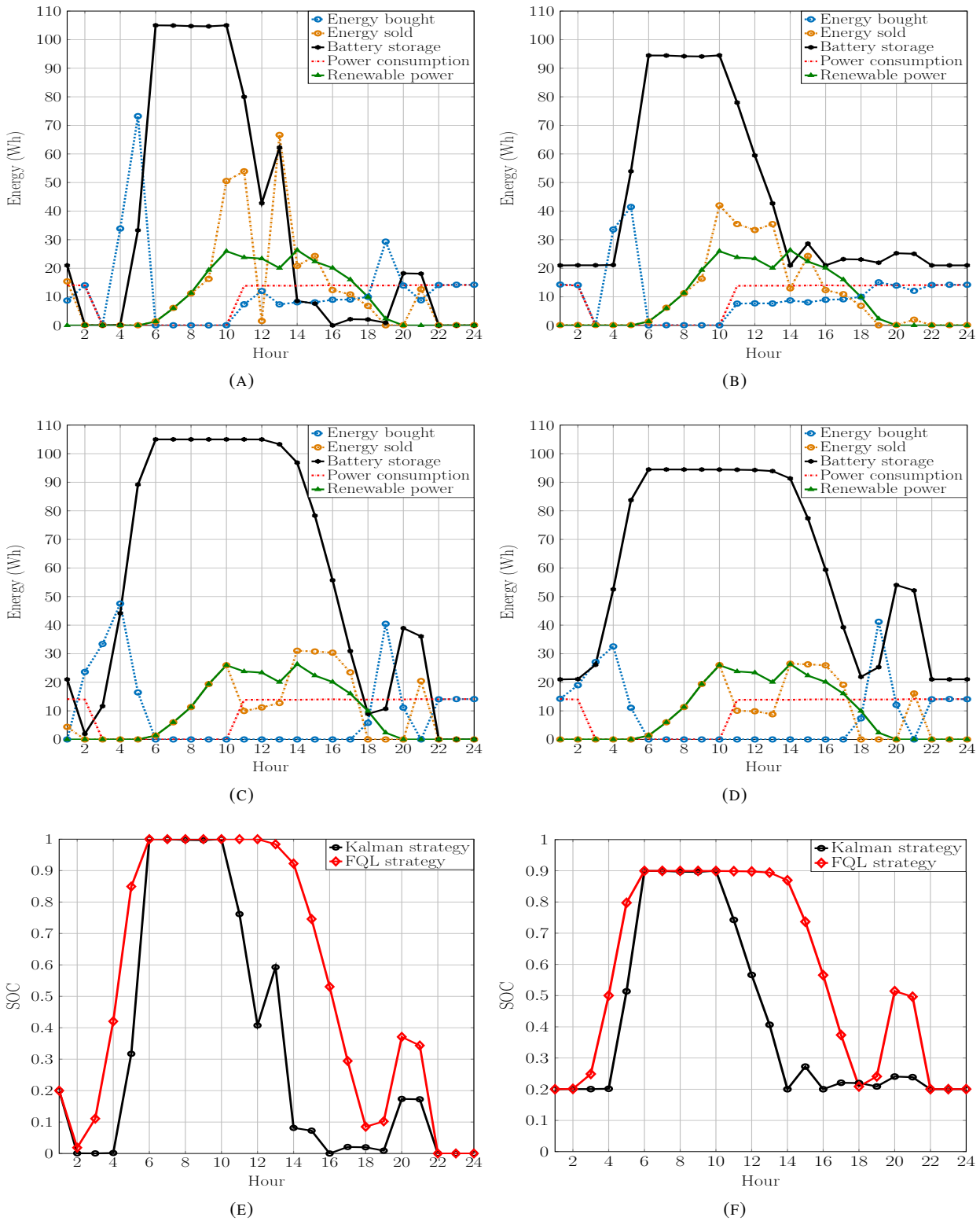


FIGURE 5.8: Average power flows with (a) unconstrained Kalman strategy (b) constrained Kalman strategy (c) unconstrained FQL strategy (d) constrained FQL strategy (e) SoC comparison between unconstrained Kalman and FQL strategies (f) SoC comparison between the SoC constrained Kalman and FQL strategies.

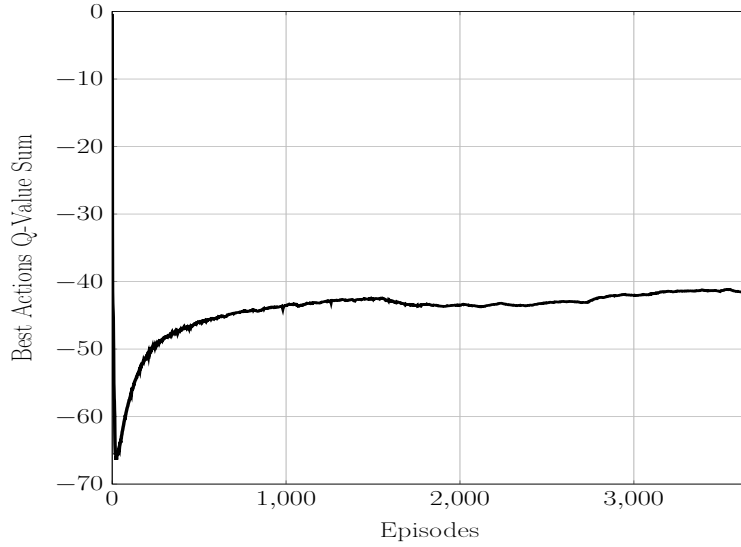


FIGURE 5.9: Convergence of the FQL algorithm.

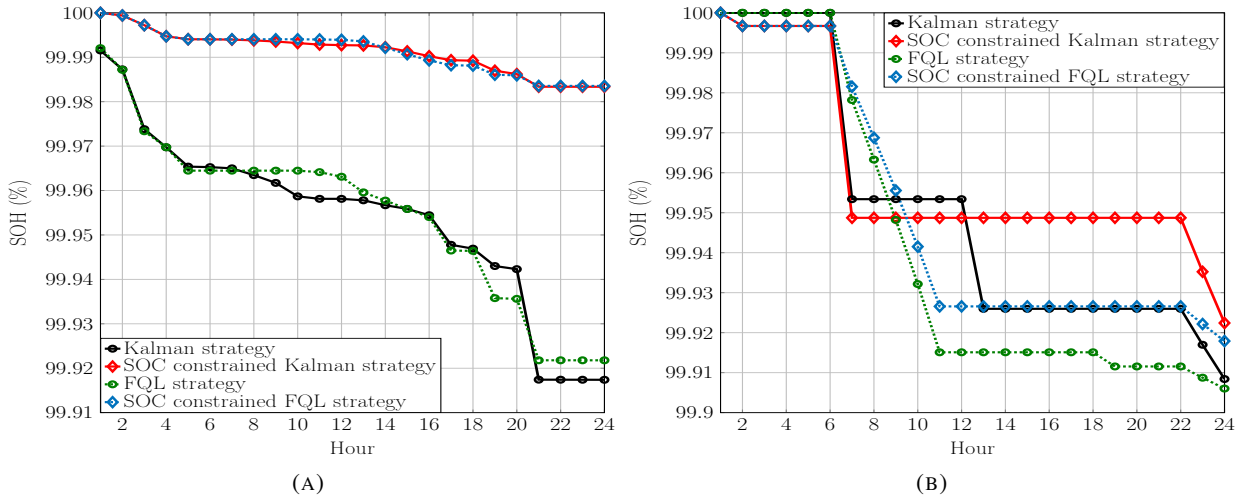


FIGURE 5.10: (a) Average cycle aging for Kalman and FQL strategies (b) Average calendar aging for Kalman and FQL strategies (with and without SoC constraints).

°C) as illustrated in Fig. 5.11. In this situation, in addition to long rest times and high operating voltages (due to high SoCs), the accumulated calendar aging can be considerable (0.1% SoH loss in one day). However, when the SoC constraints are respected, the overall calendar aging process is reduced (less than 0.08% per day).

Notice that in the Kalman scheme, the calendar aging is mainly caused by high operating temperature due to high charge and discharge rates. Whereas with FQL strategy, the principal reason of aging are the long rests (approximately 9 hours, which can be avoided by artificially cycling the battery, see Appendix A.1). By summing the cycle and calendar aging effects, we conclude that the respect of the SoC constraints enables considerable reduction of the battery degradation rate, which can reach 30% of the battery life preservation per year.

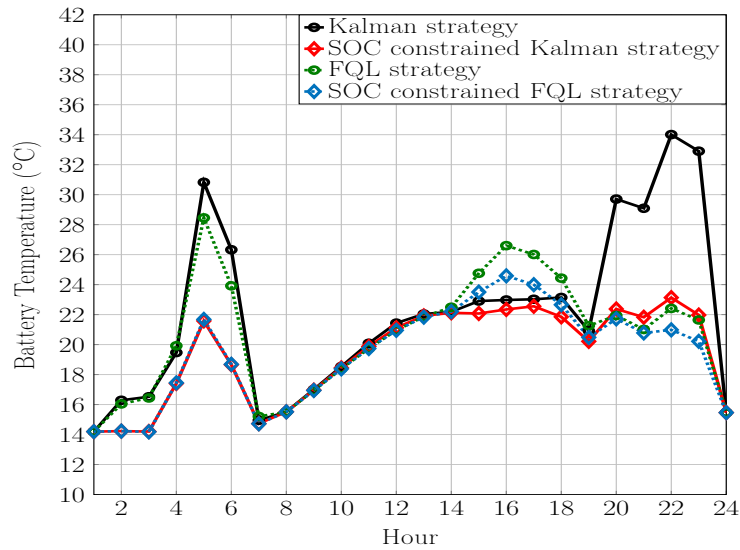


FIGURE 5.11: Average battery internal temperature for Kalman and FQL strategies (with and without SoC constraints).

5.5.3 ECONOMIC PERFORMANCE

In this section we present the economic performances of the FQL, the Kalman, and the three baseline strategies defined at the beginning of this section. These strategies are considered in both the SoH constrained and unconstrained cases except for the *naive* and *reference* policies where no battery is used. Table 5.2 shows the different strategy costs averaged over five years and normalized with respect to the *reference* policy. Negative costs mean that not only cost saving are achieved, but that the MNO is making profits. The largest cost saving is naturally achieved in the *ideal* case. As a matter of fact, the perfect knowledge of the stochastic variables enables an optimal use of the battery to adapt the energy purchase and create opportunities to increase the RE value by selling when the prices are high. The second performing strategy is the FQL, then the Kalman, the *naive*, and finally the *reference* policies. The advantages of each configuration can be enumerated as follows

1. for the *naive* scheme, the addition of a PV panel achieves cost savings as the local energy production substitutes a part of the energy purchased from the grid to feed the SBS;
2. the Kalman solution integrates a battery for energy flexibility and adopts an adaptive approach to predict the stochastic variables and reduce the energy cost of the SBS;
3. the FQL uses a model free energy management scheme. The ESS exhibits a remarkable capacity of adaptation such that the decision making takes into consideration the potential sudden variations of the environment and achieves a large long-term cost saving. In comparison, without having prior information about its environment, the FQL scheme performs only two points less than the *ideal* strategy in terms of energy cost.

When a given strategy respects the SoC constraints, the average cost saving is reduced by about ten points, which corresponds to a loss of \$1.6 in one year. However, the battery life span is extended for about 30%, equivalent to \$13 cost saving each year [Pillot 2013], which is by far more profitable given the current battery costs.

TABLE 5.2: Normalized average OPEX for different strategies.

Strategy	FQL	FQL (cons)	Kalman	Kalman (cons)	<i>Ideal</i>	<i>Ideal</i> (cons)	<i>Naive</i>	<i>Reference</i>
Cost	-0.43	-0.3	-0.35	-0.22	-0.45	-0.32	-0.11	1

5.6 CONCLUSION

In this chapter, we have proposed a FQL based energy controller to reduce the energy expenditure of MNO and the Carbon footprint of their networks. This controller can be used without prior knowledge of the weather, energy pricing, and mobile traffic demand profiles. Our simulation results showed that, using the designed SoC battery constraints at the energy controller allows to considerably reduce the battery calendar and cycle aging (30% per year). The respect of these constraints, however, causes a reduction in the OPEX cost saving of ten point, but remains negligible compared to the saving on the battery replacement costs. Besides, the proposed FQL based strategy enables considerable cost reduction compared to the method based on Kalman-filter proposed in the literature [Leithon 2013], and very close to the *ideal* strategy based on perfect prediction of the stochastic variables. To conclude with, the main strength of the FQL-based ESS lies in the rational use of the battery capacity to realize long term cost savings by performing actions that do not compromise the strategy in case of sudden environment changes.

In the next chapter, we will give perspectives on how to extend the actual optimization framework to the network level through energy-aware collaboration between the GSBS.

TOWARDS A COLLABORATIVE LARGE SCALE ENERGY MANAGEMENT

Contents

6.1	Introduction	82
6.1.1	Motivation	82
6.1.2	Related Works	83
6.1.3	Contribution	83
6.2	System Model	84
6.2.1	Traffic Model	85
6.2.2	Channel Model	86
6.2.3	Load and Power Models	87
6.3	Energy-Aware Management of Green HetNets	88
6.3.1	Problem Formulation	88
6.3.2	Two-stage heuristic	89
6.4	Simulation results	89
6.5	Conclusion	93

6.1 INTRODUCTION

6.1.1 MOTIVATION

In the previous chapter, we have proposed a local solution to increase the cost-efficiency of GSBS. It consisted on an optimized use of the battery for a better adaptation to the variation of the energy price, consumption, and production. An attractive aspect of this solution is the learning capability that enables its generalization with respect to the weather conditions, the energy market and the UEs' traffic.

This solution can be further enhanced if integrated in a holistic management of green HetNets. Especially, if we can reduce the energy cost of a single GSBS, we cannot decrease the amount of energy consumed by the SBS (regardless of the energy source) without affecting negatively the user's QoS. However, this is possible when operating at the level of a network of GSBS. In this scope, the service provided by a GSBS to a UE can be delegated to neighbor cells, which make energy consumption transferable to other GSBSs. This flexibility is interesting because it enables to redistribute the radio traffic on the GSBSs depending on the local availability of their energy resources. For example, a highly loaded GSBS with low energy stock

can share its traffic with the under-layer macro-cell or another GSBS with abundant energy production and storage. A smart holistic energy management for the HetNet that combines the local GSBS energy management and the energy-aware load-transfer strategy can not only reduce the energy cost of MNOs but also increase the energy efficiency of the mobile network.

6.1.2 RELATED WORKS

Several technologies such as cognitive radios have been proposed for wireless networks in the spirit of cooperation to mitigate the limitation of the two precious resources, power and spectrum, and the performance loss caused by wireless fading channels [Ku 2015]. The idea behind power (resp. spectrum) allocation is to smartly adjust the BS transmission power (resp. bandwidth allocated to the UE) to the conditions of the channel (such as interference and attenuation) and the configuration of the UE (such as location and service demand) to reduce the overall energy consumption and/or energy cost from the grid while maintaining an acceptable QoS. However, wireless networks with energy harvesting differ from their traditional counterparts in that the efficiency of power and spectrum allocation is further influenced by the availability of energy resource. Therefore, the design of energy-harvesting networks has been revisited to include the energy opportunities and trade-offs [Chia 2014].

Power and spectrum allocation can be divided into two families: short time scale scheduling (frame and subframe level) and long time scale scheduling (network-level). In the first category, Derrick Wing Kwan *et al.* [Ng 2013] have designed algorithms for power and sub-carrier allocation for an *Orthogonal Frequency-Division Multiple Access* (OFDMA) downlink network with energy harvesting base station. By taking into account circuit energy consumption, a finite energy storage capacity, and a minimum required data rate, an offline problem has been formulated to maximize the weighted energy efficiency of the network and solved by using Dinkelbach method. In another study, Gong *et al.* [Gong 2014] have formulated the problem of grid power minimization for a downlink cellular network with RE as a two-stage dynamic programming which determines the on-off state of the BSs and assigns the resource block. The dynamic resource allocation and BS activation is constrained by the blocking probability, which serve as the QoS metric. Concerning longer time scales, traffic offloading among BSs is considered as a network-level solution, wherein the cell-level traffic load is dynamically adjusted to balance the energy supply and demand of BSs. Zhang *et al.* [Zhang 2016] have proposed energy-aware traffic offloading for HetNets with multiple SBSs powered by diverse energy sources. The aim is to minimize the on-grid network power consumption through user associations and on-off states of SBSs, while satisfying the QoS requirement in terms of rate outage probability. Also, Wei *et al.* [Wei 2016] have proposed an offloading model to reduce the energy consumption of a network of SBS with RE. The model enables to obtain the maximum number of users that each SBS can offload theoretically by predicting the value of green energy collected and the level of the energy storage. None of these works has proposed an efficient local energy management that includes time-varying energy pricing and the battery aging mechanisms. Also, all the proposed approaches are off-line and need therefore to be adapted to more realistic conditions of RE generation, data traffic, and electricity price.

6.1.3 CONTRIBUTION

This Chapter aims to expose the perspectives of extending the local energy management solution presented in 5 to a network-level collaboration of the GSBS. We adopt a specific approach based on load-balancing to transfer the energy demand between several GSBSs by redistributing the mobile users with respect to the availability of the local energy resources and the QoS requirements. The proposed analysis is applied on a simplified network composed of two GSBSs and a macro-cell BS.

- *Contribution 1:* We formulate the energy-aware load-balancing problem to jointly reduce the total energy cost of the network and the system aging by combining hierarchical controllers at the GSBS-level (ESS) and the at the network-level (LBC).

- *Contribution 2:* We propose a two-stage algorithm to solve the formulated problem. The first stage occurs at the GSBS level and consists of learning the optimal management of the energy resources. The second stage happens at the network level and implements a load balancing strategy with respect to the average profiles of the users' traffic, RE production, and the electricity price. The two stages are alternated to continuously plan and adapt the energy management to the radio collaboration in the HetNet. Simulation results show that the obtained solution is able to increase the energy efficiency of the HetNet, reduce the energy cost, and decrease the battery aging.

The rest of the chapter is organized as follow. First, we detail the system model in Section 6.2. Then we formulate the energy-aware load-balancing problem in Section 6.3 and outline the proposed two-stage algorithm to solve it. In Section 6.4 we present and discussed the obtained simulation results. Finally, we conclude this Chapter in Section 6.5.

6.2 SYSTEM MODEL

Let's consider a two-tier network composed of a macro-cell BS and several GSBSs within its coverage area. Each GSBS is managed locally by an ESS to achieve cost saving in terms of OPEX (electricity bill) and CAPEX (battery replacement due to aging). The energy strategies implemented by the ESSs, described in Chapter 5, are local and independent.

To make the GSBSs cooperate, we adopt an energy-aware load balancing scheme. The redistribution of the UEs' traffic on the GSBSs allows to use more efficiently the energy resources, which ultimately leads to achieve additional cost saving on the on-grid electricity fees and the battery replacement cost. For example, during peak-price periods, a highly loaded GSBS with low energy availability can share its traffic with the under-layer macro-cell or another GSBS with abundant energy production and storage. Furthermore, putting some GSBS in the sleep mode can enhance the energy efficiency of the HetNet.

Let's suppose that all the ESSs are connected to a central LBC, which is in charge of redistributing the traffic among the GSBSs (co-tier load transfer) or between the GSBS and the macro-cell BS (cross-tier load transfer). The architecture is illustrated in Fig. 6.1.

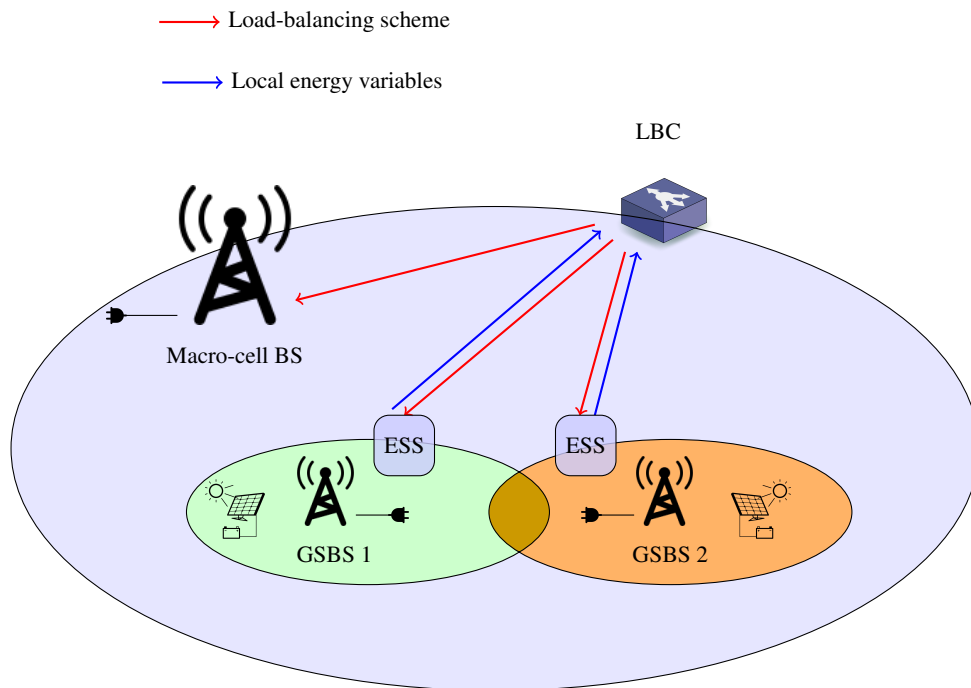


FIGURE 6.1: Two-tier green HetNet architecture.

In this work, the energy-aware load balancing solution relies on two stages. In the following, we present the system model. We use a general notation to make the actual framework more easily generalizable.

6.2.1 TRAFFIC MODEL

Let's consider two GSBSs covering an area \mathcal{A}_U . As represented in Fig. 6.2, we partition \mathcal{A}_U into K disjoint and equal sub-areas $\mathcal{A}_{k \in \{1, \dots, K\}}$, delimited by x_k and $x_{k+1} = x_k + \Delta x$, such that:

$$\mathcal{A}_U = \cup_{k=1}^K \mathcal{A}_k. \quad (6.1)$$

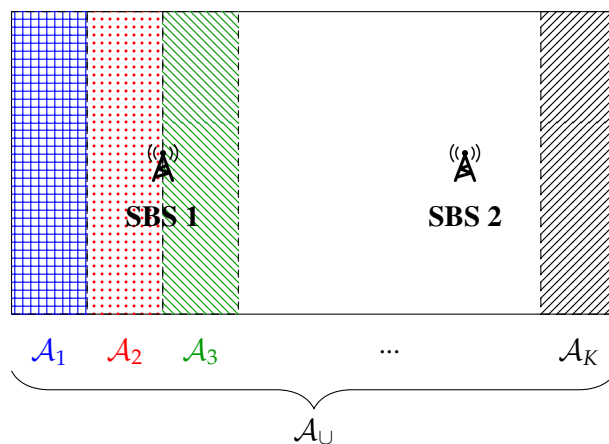


FIGURE 6.2: Area \mathcal{A}_U partition.

The arrival of the UEs in each area \mathcal{A}_k at time t is a Poisson process of intensity $\lambda'(t)/K$. The position of each UE is chosen at random according to the uniform probability density $f_{\mathcal{A}_k}$:

$$f_{\mathcal{A}_k}(x, y) = \frac{1}{(x_{k+1} - x_k) \cdot (y_t - y_b)}. \quad (6.2)$$

where y_t (resp. y_b) is the y coordinate of the top (resp. bottom) edge of the area \mathcal{A}_U .

We suppose that each UE ask for the same bit-rate r_0 and that the duration of each transmission is constant, equal to a time step. Note by setting r_0 at a small value, we can model users who ask for any rate r as an aggregation of several users asking for r_0 . In other words:

$$\exists c \in \mathbb{N}^*, \quad r = c \cdot r_0. \quad (6.3)$$

We assume that all the traffic in a sub-area is entirely served by one SBS (no macro-diversity). The serving SBS for each sub-area is decided by the LBC and allocates bandwidth to its users to meet their rate requirement r_0 . Each SBS allocates disjoint sub-carriers to its users. Thus, any given UE receives other-SBSs interference on the sub-carriers allocated to him by his SBS. The bandwidths available to the macro-cell BS and the other GSBSs are orthogonal, so there is no cross-tier interference with the under-layer macro-cell. Furthermore, the following simplifying assumptions are considered:

- **Assumption 1:** The number of sub-carrier allocated by a BS to a UE u is $\frac{w_{u(x,y) \rightarrow \text{BS}}}{W}$, where $w_{u(x,y) \rightarrow \text{BS}}$ is the bandwidth requirement of user u and W is the system bandwidth. According to LTE standard [Ozel 2011], the transmit power per-sub-carrier is constant. As a result, the power transmit by SBS i to u is:

$$P_{\text{BS} \rightarrow \text{UE}} = \frac{w_{u(x,y) \rightarrow \text{BS}}}{W} \cdot P_{\text{max}}, \quad (6.4)$$

where P_{max} is the maximum downlink RF power.

- **Assumption 2:** The load ρ_i of a BS is defined as the ratio of the bandwidth used by all the associated UEs to the available bandwidth W . Based on **assumption 1**, the total RF power of a BS is:

$$P_{\text{BS} \rightarrow \Sigma \text{UE}} = \rho \cdot P_{\text{max}}. \quad (6.5)$$

- **Assumption 3:** The power spectral density of co-tier interference is averaged over the whole spectrum. A further justification of this assumption based on fast sub-carrier permutation is given by M. Karray [Karray 2010].

6.2.2 CHANNEL MODEL

Since we aim to design a long time-scale policy (minutes or hours), small scale fast fading and shadowing are ignored. Hence, we focus only on the propagation and slow-fading loss in the channel model.

According to **assumption 3**, the co-tier interference caused by a BS j and perceived by a user u associated to BS i and located at (x, y) is:

$$I = \frac{w_{u(x,y) \rightarrow \text{BS}_i}}{W} \cdot P_{\text{BS}_j \rightarrow \Sigma \text{UE}} \cdot \text{PL}(d_{u \rightarrow \text{BS}_{j \neq i}})^{-1}, \quad (6.6)$$

where PL is the pathloss function, $d_{u \rightarrow \text{SBS}_j}$ is the distance between the BS j and the user u .

The *Signal-to-Interference-plus-Noise Ratio* (SINR) of user u associated to BS i is:

$$\text{SINR}_{u(x,y) \rightarrow \text{BS}_i} = \frac{P_{\text{BS}_i \rightarrow u} \cdot \text{PL}(d_{u \rightarrow \text{BS}_i})^{-1}}{w_{u(x,y) \rightarrow \text{BS}_i} \cdot N_0 + \sum_{j \neq i} \frac{w_{u(x,y) \rightarrow \text{BS}_j}}{W_j} \cdot P_{\text{BS}_j} \cdot \text{PL}(d_{u \rightarrow \text{BS}_j})^{-1}}, \quad (6.7)$$

where PL is the pathloss function, $d_{u \rightarrow \text{BS}_i}$ is the distance between the BS i and the user u , and N_0 denotes the power spectral density of external noise at the user side.

The expression (6.7) is further simplified using **assumption 1** and **assumption 2** as follows:

$$\text{SINR}_{u(x,y) \rightarrow \text{BS}_i} = \frac{P_{\text{max}} \cdot \text{PL}(d_{u \rightarrow \text{BS}_i})^{-1}}{W \cdot N_0 + \sum_{j \neq i} \rho_j \cdot P_{\text{max}} \cdot \text{PL}(d_{u \rightarrow \text{BS}_j})^{-1}}, \quad (6.8)$$

Shannon's formula gives the bandwidth requirement of a user u located at (x, y) :

$$w_{u(x,y) \rightarrow \text{BS}_i} = \frac{r_0}{\log_2(1 + \text{SINR}_{u(x,y) \rightarrow \text{BS}_i})}. \quad (6.9)$$

The normalized average bandwidth requirement $\bar{w}_{\text{BS}_i, \mathcal{A}_k}(t)$ at time t of the UEs in an area \mathcal{A}_k associated to BS i is:

$$\bar{w}_{\text{BS}_i, \mathcal{A}_k} = \int_{x_k}^{x_{k+1}} \int_{y_b}^{y_t} w_{u(x,y) \rightarrow \text{BS}_i} \cdot f_{\mathcal{A}_k}(x, y) dx dy. \quad (6.10)$$

All the sub-areas \mathcal{A}_k contain the same number of UEs in average (same distribution density function). Consequently, the normalized average bandwidth requirement of the UEs located in area \mathcal{A}_1 to area \mathcal{A}_j and associated to BS i is the sum of the normalized average bandwidth requirement in each of these areas:

$$\bar{w}_{\text{BS}_i, \mathcal{A}_1 \rightarrow \mathcal{A}_j} = \sum_{k=1}^j \bar{w}_{\text{BS}_i, \mathcal{A}_k}. \quad (6.11)$$

In the following, we replace the index BS by SBS (resp. MBS) when referring to a SBS (macro-cell BS).

6.2.3 LOAD AND POWER MODELS

We denote γ_i as the proportion of the total traffic in \mathcal{A}_U served by SBS i , which can be seen as the ratio of the partitions of \mathcal{A}_k served by the SBS i :

$$\gamma_i(t) = \frac{\text{number of areas served by SBS } i}{K}. \quad (6.12)$$

For a two-tier network composed of two pico-cells and a macro-cell, each area is associated to one and only one BS. Therefore, at all times, the following condition is required:

$$\forall t, \quad \sum_{i=1}^2 \gamma_i(t) \leq 1. \quad (6.13)$$

The sub-areas not associated to a SBS is attached to the macro-cell BS. Therefore the proportion of the traffic served by the macro-cell BS is $1 - \sum_{i=1}^2 \gamma_i(t)$.

For a given load balancing scheme (γ_1, γ_2) , we suppose that LBC associate first to SBS i the furthest sub-areas from SBS $i' \neq i$. The SBS 1 starts associating the UEs from \mathcal{A}_1 to \mathcal{A}_K and stops at the area \mathcal{A}_j , where $j(t) = K \cdot \gamma_1(t)$. Contrarily, SBS 2 associates UEs from \mathcal{A}_K to \mathcal{A}_1 and stops at the area index $j'(t) = K \cdot \gamma_2(t)$. Finally, the macro-cell BS serves the sub-areas \mathcal{A}_{j+1} to $\mathcal{A}_{j'-1}$. Accordingly, the average normalized bandwidth requirements for UEs associated to SBS 1, and SBS 2, and MBS are:

$$\bar{w}_{\text{SBS}_1}(\gamma_1) = \sum_{k=1}^{K \cdot \gamma_1} \bar{w}_{\text{SBS}_2, \mathcal{A}_k}, \quad (6.14)$$

$$\bar{w}_{\text{SBS}_2}(\gamma_2) = \sum_{k=1}^{K \cdot \gamma_2} \bar{w}_{\text{SBS}_2, \mathcal{A}_{K-k+1}}. \quad (6.15)$$

$$\bar{w}_{\text{MBS}}(\gamma_1, \gamma_2) = \sum_{k=K \cdot \gamma_1 + 1}^{K \cdot \gamma_2 - 1} \bar{w}_{\text{MBS}, \mathcal{A}_k}. \quad (6.16)$$

Notice that when $\Delta x \rightarrow 0$, the discrete sums \sum in eq. (6.14) and eq. (6.15) are replaced by continuous sums \int .

Finally, the load of the SBS i , noted ρ_i , is calculated as the ratio of the used bandwidth to the available bandwidth W (**assumption 2**). Therefore, the average loads of SBS 1 and SBS 2 are:

$$\hat{\rho}_{\text{SBS}_1}(t) = \frac{\lambda'(t)}{K} \cdot \frac{\bar{w}_{\text{SBS}_1}(\gamma_1(t))}{W}, \quad (6.17)$$

$$\hat{\rho}_{\text{SBS}_2}(t) = \frac{\lambda'(t)}{K} \cdot \frac{\bar{w}_{\text{SBS}_2}(\gamma_2(t))}{W}, \quad (6.18)$$

$$\hat{\rho}_{\text{MBS}}(t) = \frac{\lambda'(t)}{K} \cdot \frac{\bar{w}_{\text{MBS}}(\gamma_1(t), \gamma_2(t))}{W}. \quad (6.19)$$

The power consumption of SBS i is given by (3.4) in Chapter 3. Besides, the traffic served in the area \mathcal{A}_U constitutes just a part of the global traffic load of the macro-cell BS. Therefore, we suppose that the macro-cell BS is always on and consider only the load variation due to the area \mathcal{A}_U (eq. (6.20)). This assumption is valid because of the linear behavior of the macro-cell power consumption with respect to the traffic load [[Auer 2011](#)].

$$\Delta P_{\text{MBS}}(t) = \Delta_p \cdot \hat{\rho}_{\text{MBS}}(t) \cdot P_{\text{max}}. \quad (6.20)$$

6.3 ENERGY-AWARE MANAGEMENT OF GREEN HETNETS

Recall that our objective is to reduce the carbon emissions in the HetNet, the on-grid power consumption and the battery aging phenomenon. To do so, there are two levels of action: 1) the GSBS level at which the ESS optimizes individually the cost savings of a GSBS (refer to Chapter 5) and 2) the HetNet level at which the LBC implements the energy-aware load-balancing strategy. These two level of actions are not independent, and therefore need to be jointly addressed.

In this section, we present first the mathematical formulation of the joint load balancing and local energy management problem for a two-tier network composed of two GSBSs (pico-cells) overlaid by a macro-cell BS. Then, we detail a two-stage heuristic to solve the problem.

6.3.1 PROBLEM FORMULATION

The energy-aware load balancing problem is based on the average profiles of the UE' traffic, energy production, and electricity price. It consists in jointly distributing the sub-areas \mathcal{A}_k on the SBSs and the macro-cell BS (γ_1, γ_2) and tuning the SoC strategy at the ESS level for each GSBS (\mathbf{z}_1 and \mathbf{z}_2) for the optimization horizon N . The objective is to minimize the on-grid energy consumption under the battery and load balancing constraints:

$$\mathbf{P}_4 : \min_{\mathbf{z}_1, \mathbf{z}_2, \gamma_1, \gamma_2} \sum_{i=1}^N p_i(t) \cdot \left[\sum_{i=1}^2 (E_{b,i}(t) + \kappa \cdot E_{s,i}(t)) + \Delta P_{\text{MBS}}(t) \right], \quad (6.21)$$

such that for $i \in \{1, 2\}$

$$E_{b,i}(t) = \max(0, P_{\text{BS},i}(t) + P_{\text{Batt},i}(\mathbf{z}_i(t), \mathbf{z}_i(t+1)) - P_{\text{PV},i}(t)), \quad 1 \leq t \leq N, \quad (6.22)$$

$$E_{s,i}(t) = \min(0, P_{\text{BS},i}(t) + P_{\text{Batt},i}(\mathbf{z}_i(t), \mathbf{z}_i(t+1)) - P_{\text{PV},i}(t)), \quad 1 \leq t \leq N, \quad (6.23)$$

$$\mathbf{z}_i(t) \in \Delta_{\text{SOC}}, \quad 1 \leq t \leq N+1, \quad (6.24)$$

$$\Delta \text{SOC}_{\min} \leq \mathbf{z}_i(t+1) - \mathbf{z}_i(t) \leq \Delta \text{SOC}_{\max}, \quad 1 \leq t \leq N, \quad (6.25)$$

$$\sum_{i=1}^2 \gamma_i(t) \leq 1, \quad 1 \leq t \leq N, \quad (6.26)$$

$$0 \leq \hat{p}_i(t) \leq 1, \quad 1 \leq t \leq N, \quad (6.27)$$

The index i is added to notation of the energy bought from the grid E_b , energy sold to the grid E_s , power consumed by the SBS P_{BS} , power produced by the PV P_{PV} , and battery power P_{Batt} to specify the involved GSBS. The electricity price is supposed the same for the three BSs. At all time steps, the balance between the power supply and demand is expressed by the constraints 6.22 and 6.23. For a GSBS i , when the energy consumed is greater than the energy provided by the PV system and the battery (*i.e.*, $P_{\text{BS},i}(t) + P_{\text{Batt},i}(\mathbf{z}_i(t), \mathbf{z}_i(t+1)) - P_{\text{PV},i}(t) \geq 0$), the ESS perceives a cost $p_i(t) \cdot E_{b,i}(t) \geq 0$ corresponding to the energy bought from the SG. In contrast, when the energy available is superior to the energy consumption (*i.e.*, $P_{\text{BS},i}(t) + P_{\text{Batt},i}(\mathbf{z}_i(t), \mathbf{z}_i(t+1)) - P_{\text{PV},i}(t) \leq 0$), the ESS receives a negative cost $\kappa p_i(t) \cdot E_{s,i}(t) \leq 0$ (that can be seen as a reward) associated to the energy sold to the SG. The constraints (6.24) and (6.25) represent the constraints on the SoC that have to be respected to improve the battery life span. The condition (6.26) means that each sub-area is associated to one and only one SBS. Finally, the constraint (6.27) represents the limitation on the SBSs' load to serve the UEs with a guaranteed QoS.

The problem is a non-linear optimization problem, because the objective function and the constraint (6.27) are non-linear. We use *fmincon* solver to approximate a solution.

6.3.2 TWO-STAGE HEURISTIC

The basic idea of the two-stage optimization algorithm is to divide the action process into two steps. The networks then alternates periodically between the two stages as showed in Algorithm 5.

Algorithm 5: Two-stage heuristic

Initialization :
Initialization of the sub-areas \mathcal{A}_k association: **for** $i \in \{1,2\}$ **do**
 $\gamma_i(t) \leftarrow 50\%$;
Initialization of the Q-functions at each GSBS i : **for** $i \in \{1,2\}$ **do**
 $q_{\text{ESS}_i} \leftarrow 0_{|\mathcal{S}_i|, |\mathcal{A}_i|}$;
for each period do
 Stage 1 :
 for $i \in \{1,2\}$ **do**
 while no convergence do
 $q_{\text{ESS}_i}^* \leftarrow$ learning phase (Algorithm 4);
 Stage 2 :
 $(\hat{\gamma}_1^*, \hat{\gamma}_2^*) \leftarrow$ solve \mathbf{P}_4 ;
 for $i \in \{1,2\}$ **do**
 $\gamma_i(t) \leftarrow \hat{\gamma}_i^*$;
 $q_{\text{ESS}_i} \leftarrow q_{\text{ESS}_i}^*$;

Initialization: The UEs are associated to the SBS with the highest signal power.

Stage 1: The FQL-based ESSs at the level of each GSBS learn the local energy strategy as presented in Chapter 5 in order to optimizes the cost saving and reduce the battery aging. Simultaneously, the ESSs collect local data related the energy production, users traffic, and electricity price. This information are sent periodically to the LBC.

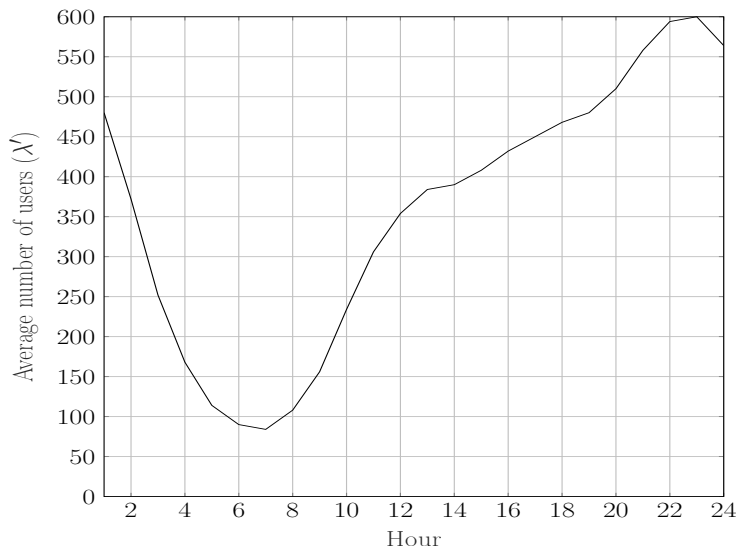
Stage 2: The LBC establishes a predictive load balance strategy, by solving the optimization problem \mathbf{P}_4 , considering that all the energy variables are described by their average profiles. The implementation of the load balancing scheme results in a new association of the UEs with the SBSs, which in turn changes their energy consumption.

At this point, the energy strategies learned by the ESS are out-dated and another learning phase is triggered in which, based on their previous learning phase, the energy strategy is adjusted to the load balancing scheme.

6.4 SIMULATION RESULTS

We adopt the energy consumption model of Chapter 3 for the SBSs, the macro BS power model from the EARTH project [Auer 2010], and the channel model from 3GPP LTE [3GPP 2011] for numerical simulations. For the macro-cell, $\Delta_p = 4.7$, the maximum transmit power $P_{\text{max}} = 120$ W. The system bandwidth is set to $W = 10$ MHz. The path-loss for the macro-cell BS is $\text{PL}^{dB} = 128.1 + 37.6 \cdot \log_{10}(d_{u \rightarrow \text{BS}_i})$ (distance in km), and $\text{PL}^{dB} = 38 + 30 \cdot \log_{10}(d_{u \rightarrow \text{BS}_i})$ for the SBSs (distance in m). The noise power density is -174 dBmHz. The intensity of UEs arrival λ' in the area \mathcal{A}_U is described in Fig. 6.3. Auer *et al.* [Auer 2010] have considered two categories of UEs: heavy users that consume 900 Mbph, and normal users that consume 125.5 Mbph. According to the same source, the most relevant European scenario that reflects the share of mobile broadband subscribers consists of 20% of heavy users and 80% of normal users. Based on this, we consider the average bit-rate demand $r_0 = 75$ kbps.

The area \mathcal{A}_U is a square of 160×80 m² and the partition step is $\Delta x = 1$ m. The location of the two GSBSs is illustrated in Fig. 6.4. The macro-cell BS is equally distant from the two GSBSs by 500 m. In

FIGURE 6.3: Average number of users in area \mathcal{A}_U .

the following, we refer to the energy-aware load-balancing scheme as the collaborative scheme, and we compare the obtained solution to the non-collaborative scheme, where the macro-cell BS is not solicited and proportion of the area \mathcal{A}_U served by each SBS is 50%.

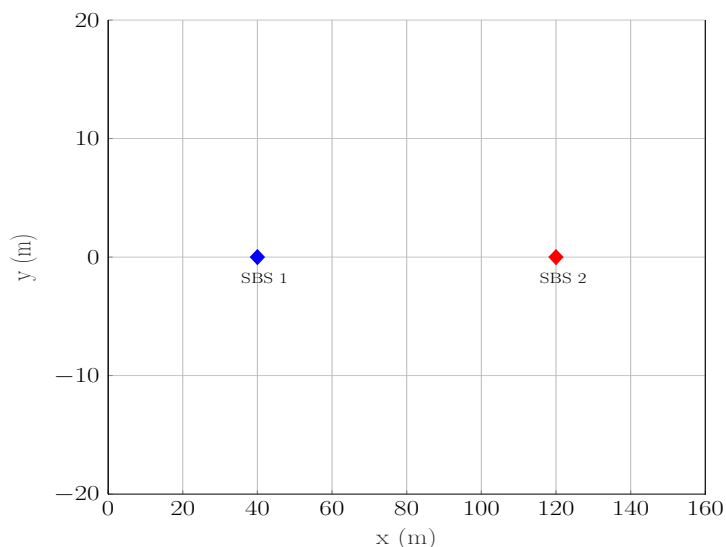


FIGURE 6.4: Location of the network's components.

Recall that there is no cross-tier interference between the macro-cell and the small-cells. However, we account for the co-tier interference between the two GSBSs. Fig. 6.5 illustrates the amount of bandwidth that has to be allocated by the SBS 1 with respect to the load of SBS 2 and the location of UEs. It shows that the higher the load, the larger bandwidth is required by SBS 1 to serve the traffic demand. Also, the bandwidth requirements increase when the distance of the UEs from SBS 1 increases and the distance to SBS 2 decreases. The bandwidth requirement per sub-area is further detailed for the two SBSs for three specific loads : 0%, 50%, and 100%. Additionally, the bandwidth requirement of SBS 2 is symmetric with respect to axis at mid-distance between the two SBSs, due to the uniform distribution of the UEs. Therefore, by considering SBS 1, the following analysis apply symmetrically to SBS 2.

When the neighboring SBS has no traffic load, the RF power is zero (Recall that the RF power is proportional to the traffic load). In this case, there is no interference for SBS 1 and the variation of bandwidth requirement is only due to the attenuation caused by the path-loss, slow fading, and background noise.

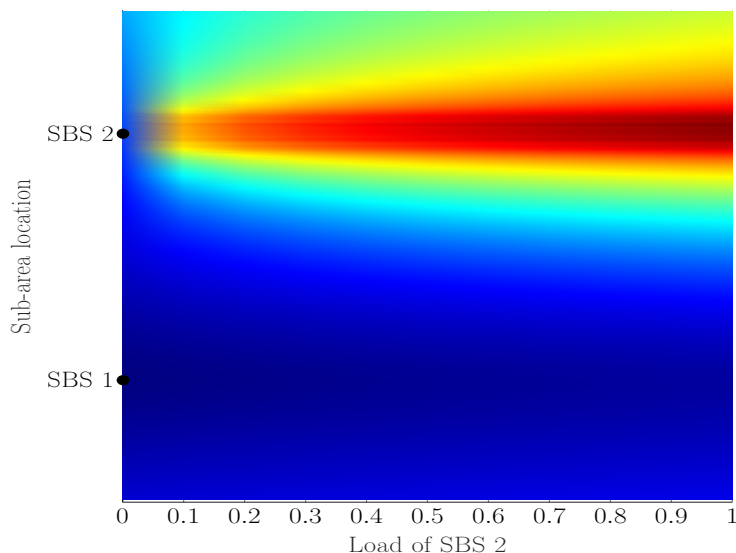
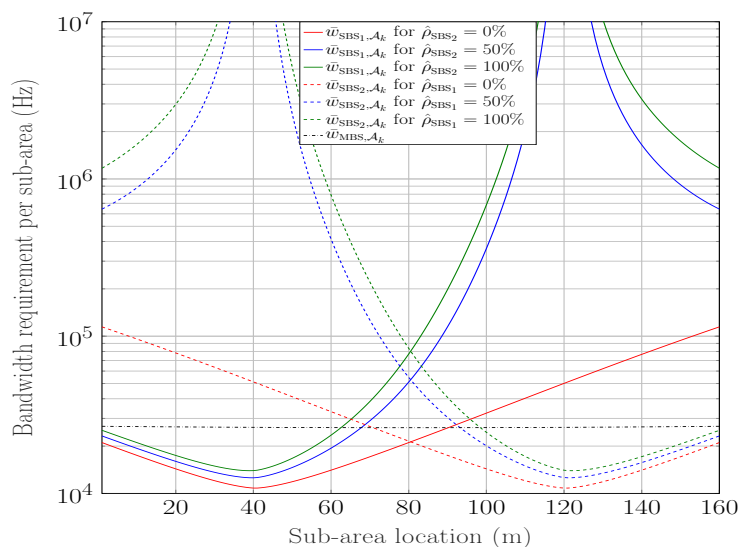
FIGURE 6.5: SBS 1 Bandwidth requirement per sub-area ($\bar{w}_{\text{BS}_1, \mathcal{A}_k}$).

FIGURE 6.6: Bandwidth requirement per sub-area.

When the load of SBS 2 increases, its RF power increases as well. The interference power adds up to the previous attenuation phenomena, which leads to an exponential growth of the bandwidth requirement as the UE's location approaches SBS 2. Also, we represent in the 6.6 the bandwidth requirement of the macro-cell BS in each sub-area. Given the size of \mathcal{A}_U and the absence of interference, the variation of bandwidth requirement per sub-area is relatively constant compared to the SBSs.

The obtained load balancing at the end of stage 1 is illustrated in 6.7. We can observe that: 1. The macro-cell BS is not solicited. 2. The UEs in the area \mathcal{A}_U are all associated to SBS 1 between 03:00 and 10:00. Thus, SBS 2 is turned off. 3. For the rest of the day, the LBC associates equally 50% of the area \mathcal{A}_U to the two SBSs.

The cumulative power consumption of the network is represented in Fig. 6.8 in the collaborative and non-collaborative schemes. In average, 16% (108 Wh) of the energy consumption is saved each 24 hours thanks to the load-balancing strategy.

Fig. 6.9 represents the variation of energy consumption of a macro-cell BS and energy consumption in

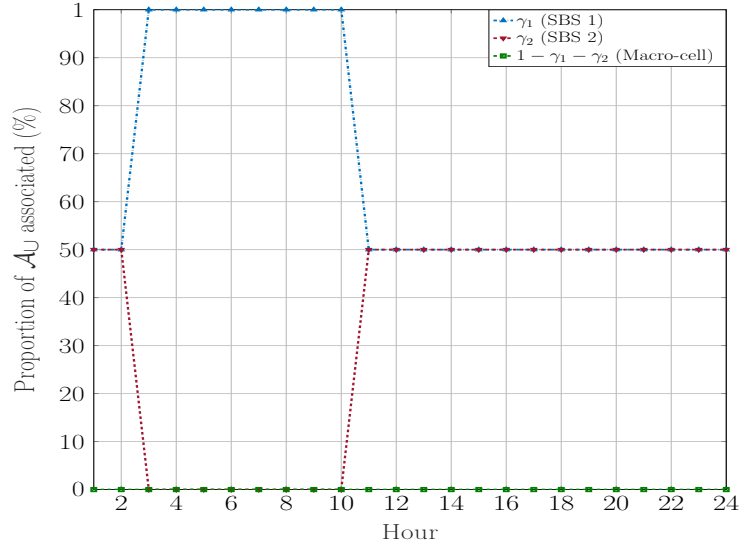


FIGURE 6.7: Load balancing.

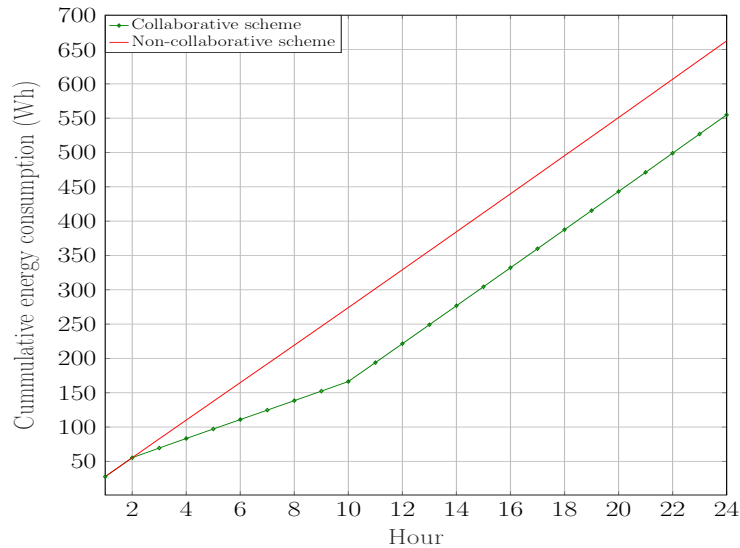


FIGURE 6.8: Cumulative energy consumption of the network in the collaborative and non-collaborative schemes.

a pico-cell BS with respect to the number of users in the area \mathcal{A}_U . We see that the energy consumption of the macro-cell is highly dependent of the number of users, which is relatively not the case for the pico-cell BS. Up to 10 UEs, offloading all the traffic to the macro-cell BS is the most energy efficient. In area \mathcal{A}_U , the number of users is greater than 10; the energy saved by turning off the SBS is smaller than the energy consumed by the macro-cell BS to serve this traffic. Therefore, in this scenario, the LBC does not offload the traffic of the SBSs to the macro-cell BS.

Compared to macro-cells, the power consumption of pico-cell BSs is less affected by the traffic load. The most efficient way to save energy is to turn off the SBS. For this reason, the load-balancing strategy turns off SBS 2 as long as the QoS constraints are not violated. When it is not possible, both SBSs are on and the LBC associates equally half of the area \mathcal{A}_k to each of them. Qualitatively, we can see from Fig. 6.6 that extending the coverage of SBS 1 beyond 80 m (more that half) leads to a higher growth of bandwidth requirements for SBS 1 than the decrease of it for SBS 2. Because the power consumption of a SBS is proportional to the load (which in turn, is proportional to the sum of bandwidth requirement in the associated sub-area), the global energy demand of the network increases. Given the symmetry between the two SBSs, the same analysis is valid for SBS 2. For this reason, the mid-distance axis is an equilibrium for

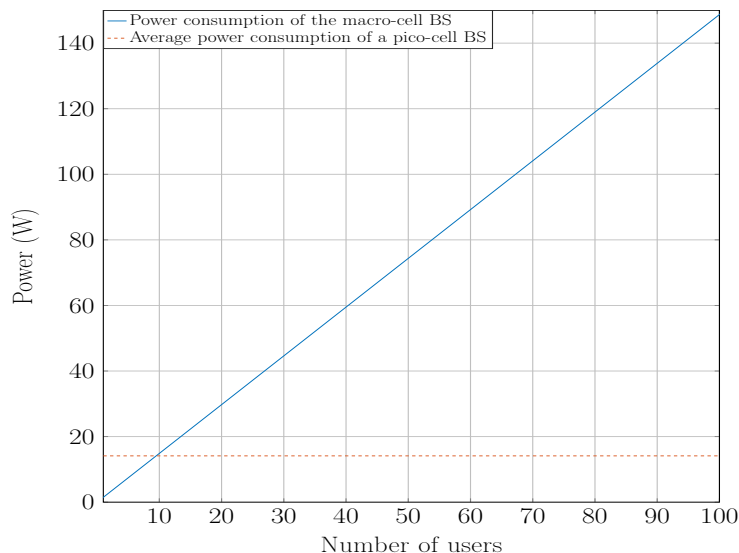


FIGURE 6.9: *Power consumption vs number of users*

load-balancing.

Besides, we investigate the impact of the traffic transfer on the energy policy. The energy strategies of the ESS at the level of each SBS in the non-collaborative and collaborative schemes are illustrated in Fig. 6.10. First, the energy saved by turning off the SBS enables to buy less electricity from the grid. Compared to the non-collaborative case, the ESS in the collaborative scheme acquires 44% less energy from the grid between 03:00 and 10:00. Also, the lower energy demand allows to dedicate more energy produced to be sold to the SG. During sunlight (from 06:00 to 19:00), an additional 30% of the energy produced is sold to the SG in the collaborative scheme. In average, the load-sharing reduces the incurred energy cost by 27%.

In this scenario, the battery aging is similar in both collaborative and non-collaborative. The battery-aging related results are therefore described in Chapter 5. However, the battery aging can be additionally decreased in the collaborative scheme by slightly deviating from the equilibrium (50%-50%) to cycle the battery and avoid long rests that increase the calendar aging (see Appendix A.1).

6.5 CONCLUSION

In this Chapter, we have outlined a possible approach to extended the local energy management to a network-level collaboration of the GSBS. The energy-aware load-balancing problem has been formulation for a network composed of two GSBSs and a macro-cell BS. Then we derived a solution using a two-stage algorithm. The first stage occurs at the GSBS level and consists of learning the optimal management of the energy resources. The second stage happens at the network level and implement a load balancing strategy with respect to the average profiles of the users' traffic, RE production, and the electricity price. The two stages are alternated to continuously plan and adapt the energy management to the radio collaboration in the HetNet. Simulation results show that the obtained solution is able to increase the energy efficiency of the HetNet, reduce the energy cost, and decrease the battery aging.

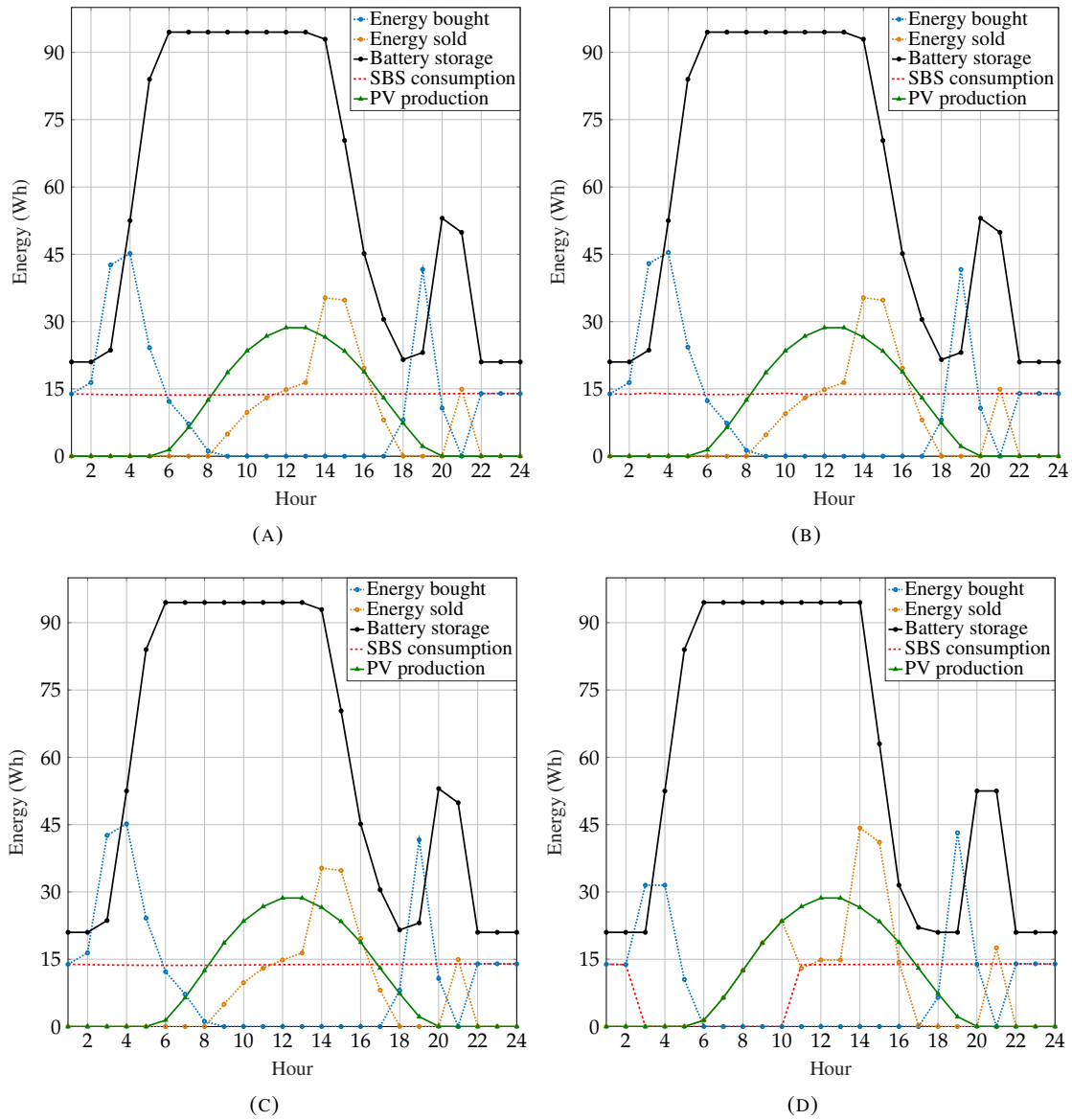


FIGURE 6.10: Average power flows for (A) SBS 1 (non-collaborative) (B) SBS 1 (collaborative) (C) SBS 2 (non-collaborative) (D) SBS 2 (collaborative).

CONCLUSIONS AND FUTURE WORK

CONCLUSIONS

With the rapid increase of mobile data demand, *Mobile Network Operators* (MNOs) are densifying their networks through the deployment of *Small-cell Base Stations* (SBSs), low-range radio-access transceivers that offer enhanced capacity and improved coverage. Because more equipment are deployed, this new architecture –called *Heterogeneous cellular Network* (HetNet)– leads to an increase in the global energy consumption of mobile networks.

In the actual context of climate change, energy-harvesting technologies have gained particular interest to support the growing power demand of the HetNets. In Chapter 2, we have presented the merits of integrating a *Photo-Voltaic* (PV) system in mobile networks to support a cost-efficient deployment of HetNets. We have also presented the *Smart Grid* (SG) as an enabler for using *Renewable Energy* (RE), as it allows *Distributed Generation* (DG) and energy storage to be efficiently integrated in the distribution network as well as in a liberalized energy market that creates economic value through *Demand Response* (DR). However, there are research issues related to the complexity of introducing and controlling PV panels and batteries in HetNets. In particular, we have noted that the complexity of sizing the energy harvesting SBSs and controlling their energy-flux is even more increased because of the interdependence between these two processes.

In Chapter 3, we have presented the proposed *Green Small-cell Base Station* (GSBS) architecture that relies on a PV panel as RE source, a battery as energy storage, and the SG, all of which supply the SBS to serve the momentary traffic load. We have observed that the multitude of power sources, the battery aging phenomena, and the varying price signal of the SG are factors that require a management to efficiently control the energy consumption. Accordingly, we have elaborated an energy management framework for the GSBS centered around the battery, allowing the MNOs to jointly reduce their electricity expenses and the equipment degradation. We have chosen to simulate the randomness of the system environment (traffic of *User Equipments* (UEs), solar irradiance, ambient temperature, and electricity price) with realistic stochastic models. Also, the power model of each component of the GSBS has been selected to find the good trade-off between the time scale of control and the involved physical dynamics. In particular, we detailed the battery model to capture its non-linear behaviors and aging mechanisms, in contrast with existing works in the literature that have simplified the battery as an energy buffer.

In Chapter 4, we have investigated the sizing problem of a GSBS, which depends on the estimation of the energy management strategy. The optimization problem has been formulated to include three parameters: 1) the *Fixed Cost* (FC) of the investment that is related to the equipment purchase and installation 2) the *Running Cost* (RC) due to system aging, and 3) the cost saving achieved by the investment, which is obtained by solving the underlying energy management problem. Our study has been conducted in both grid-connected and off-grid cases. We have solved the respective sizing problems using an iterative approach, based on the average profiles of the state variables, *i.e.*, energy consumption, production, and cost in different economic configurations. Simulation results have showed that there is a unique battery size that optimizes the investment, which depends on the deployed PV panel, the SBS power consumption, and the energy market conditions. Specifically, the dependency between the benefit and the battery storage capacity is a bell-shaped function. This is due to the fact that very large and very small batteries (compared to the optimal size) are more affected by the aging mechanisms. Especially, the calendar aging has a no-

table impact on large batteries while cycle aging particularly degrades small batteries. We also proposed a practical sizing approach based on the fact that the system benefits increase linearly with the PV panel size. As a consequence, the optimal PV size should be set equal to the whole physical space allocated to the GSBS. Then, the battery capacity is optimally defined according to the system conditions. Besides, the hypothesis of average knowledge of the system parameters, used to estimate the energy management strategy, is not constraining when dimensioning the system: the obtained optimal sizing is the same as in the ideal knowledge case, in which the future states of the system variables are known. Finally, We evaluated the profitability of connecting an off-grid GSBS to the SG. The results have allowed to define the maximum acceptable connection cost and the critical distance from the grid after which the connection is not economically valuable.

Once the GSBS sized and deployed, the energy management strategy needs to be adapted to real conditions, which differ from the average profiles considered in the sizing study. For that purpose, we have proposed in Chapter 5 an energy controller provided with learning capabilities to reduce the energy expenditure of MNO and the Carbon footprint of their networks. This controller is based on the *Fuzzy Q-Learning* (FQL) algorithm that requires no prior knowledge of the weather, energy pricing, or mobile traffic demand profiles. The obtained simulation results have shown that, using the designed *State of Charge* (SoC) battery constraints, the energy controller is able to considerably reduce the battery calendar and cycle agings (30% per year). Fulfilling these requirements, however, causes a reduction in the *Operating Expenditures* (OPEX) cost saving of ten point, but remains negligible compared to the saving on the battery replacement costs. Besides, the proposed FQL based strategy enables considerable cost reduction compared to the other methods such as the Kalman-filter proposed in the literature [Leithon 2013]. The performances are also very close to the *ideal* strategy based on perfect prediction of the stochastic variables.

In Chapter 6, we have outlined a possible approach to extend the local energy management to a network-level collaboration of the GSBS. The simplified energy-aware load-balancing problem has been formulated for a network composed of two GSBSs and a macro-cell *Base Station* (BS). Then we have derived a solution using a two-stage algorithm, in which the first stage occurs at the GSBS level and consists of learning the optimal management of the energy resources, and the second stage happens at the network level and implements a load balancing strategy with respect to the average profiles of the users' traffic, RE production, and the electricity price. The two stages are alternated to continuously plan and adapt the energy management to the radio collaboration in the HetNet. The preliminary simulation results have shown the potential of such solution to increase the energy efficiency of the HetNet, to reduce the energy cost, and to decrease the battery aging.

CONTRIBUTIONS

The novelty of this PhD work is summarized by the following contributions:

- *Contribution 1*: We design a GSBS architecture composed of a SBS connected to the SG, integrating RE (PV panel) and energy storage (battery). The purpose of such architecture is to jointly improve the economical –OPEX and *CAPital Expenditures* (CAPEX)– and environmental impact of HetNets. The proposed energy management framework relies on the efficient use of RE and the battery, in a context of time-varying electricity price and two-way energy flow between the GSBS and the SG. Unlike existing works, the actual energy management considers realistic battery models that capture the non-linear behaviors and aging mechanisms. The proposed design considers a time-scale where the physical dynamics of the system components are consistent with the decision making.

The novelty of this contribution is based on one patent [P1], one journal article [J2], and a conference paper [C2].

- *Contribution 2:* We propose an approach to find the optimal capacity sizing of the PV panel and the battery in a GSBS. The related problem is formulated to include 1) the FC of the investment related to the equipment purchase/installation, 2) the RC due to system aging, and 3) the cost saving achieved by the investment, obtained by solving the associated energy management problem. We solve the sizing problem by using an iterative method, which relies on the average profiles of the state variables, *i.e.*, energy consumption, production, and cost. Extensive simulations show the existence of a unique optimal solution that depends on the system conditions. Following a similar approach, we formulate and solve the sizing problem for a stand-alone (*i.e.*, off-grid)GSBS. An analysis of the obtained results enables to assess the critical connection distance between the GSBS and the SG as well as the economical value of this connection.

The novelty of this contribution is based on one journal article [J1].

- *Contribution 3:* We propose a model-free *Energy Supervision System* (ESS) for the GSBS based on FQL. The FQL combines the advantages of Q-Learning and *Fuzzy Inference System* (FIS) and enables to design a controller that does not need any prior knowledge on the energy consumption, energy production, and energy price. In other words, the actual proposal enable a plug-and-play deployment of GSBSs, with the ability to improve the operating energy cost of the system and preserves the battery lifetime.
- *Contribution 4:* We compare the FQL-based method with other approaches, namely: 1) the online Kalman filter technique from the literature [Leithon 2013] and 2) what we refer to as the *ideal* strategy, which is aware of the future states of the system variables. System simulations show that the FQL controller achieves considerable cost reduction compared to the method based on Kalman filter and other baseline strategies. Furthermore, the obtained energy management policy performs very closely to the *ideal* strategy. Simulation results also show that by taking into account the battery aging processes, the proposed energy management strategy enhances the battery life span by 30% per year. The battery aging awareness also leads to an increase in the OPEX, however negligible compared to the cost saving on the battery replacement.

The novelty of contribution 3 and contribution 4 is based one journal article [J2], and a conference paper [C1].

- *Contribution 5:* We formulate an energy-aware load-balancing problem for a network of GSBSs. The aim is to jointly reduce the total energy cost of the network and the system aging by combining hierarchical controllers at the GSBS-level (ESS) and at the network-level (*Load Balancing Controller* (LBC)). We propose a two-stage algorithm to solve the formulated problem. The first stage occurs at the GSBS level and consists of learning the optimal strategy for managing the local energy resources. The second stage happens at the network level and implements a load balancing strategy with respect to the average profiles of the users' traffic, RE production, and the electricity price. The two stages are alternated to continuously plan and adapt the energy management to the radio collaboration in the HetNet. Simulation results show that the obtained solution is able to increase the energy efficiency of the HetNet, reduce the energy cost, and decrease the battery aging.

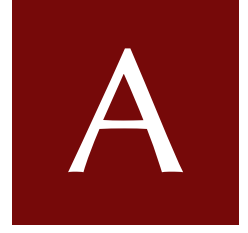
FUTURE WORK

In the following, we draw the main directions for future works:

- Firstly, several studies have highlighted that the backhaul has a non-negligible impact on the overall power budget of HetNets [Tombaz 2014]. In some cases, the power consumption of backhauling operations at one SBS might be comparable to the amount of power necessary to operate the SBS it-

self [Tombaz 2011]. Therefore, The energy consumption of the backhaul turns out to be an important criterion in the energy management of the GSBSs. We envision to include the backhaul share in the SBS power model.

- Secondly, even if the sizing problem has been formulated analytically, the resolution approaches that have been used in this work do not always guarantee the convergence towards the global optimum. This is a general concern for solving non-linear optimization problem with numerical methods. As future work, we aim to derive analytically a solution for the proposed problem by relaxing it or exploiting specific mathematical properties of the result to guarantee the global convergence. This will not alter the obtained trends nor the conclusions of our studies, but will enable to grasp the system performances in a more rigorous way.
- We want also to draw the reader's attention on the extrapolation made during the sensitivity study in Chapter 4. It is clear that the obtained results are dependent on the chosen hypotheses. At this regard, we want to validate these extrapolations by actually evaluating the performances in the other configurations, for different types of SBSs and PV technologies, and specific energy-related markets in some countries.
- Another envisaged perspective is to improve the configuration of the FQL presented in Chapter 5. Specifically, the membership function to the fuzzy sets are dependent on how they are defined, both in terms of shape (such as triangular, trapezoidal, and S-function) and partitioning of the attributes domains (number of fuzzy sets and their distribution in the domains). In our case, they have been defined a priori through human expertise (or intuition), regarding the general profiles of the system state variables. Even if the subjectivity of choosing the membership functions is partially absorbed by the FQL, this raises the question of automation and generalization to other contexts completely different from the one we suppose. In the future, we aim to derive a comprehensive methodology for defining the membership functions used by ESSs in the GSBS.
- Finally, the natural follow-up of this work is to investigate the holistic radio and energy management of green HetNets. In Chapter 6, the proposed energy-aware radio collaboration in a HetNet has been simplified as the goal was to show the potential of such mechanism of achieving energy savings. We plan to study the presented Load balancing framework in a realistic network of GSBSs that considers all relevant cross-tier/co-tier interference and considers asymmetric behavior of the data traffic, energy production, and potentially electricity price at the different GSBSs.



APPENDICES

A.1 HOW TO FURTHER REDUCE THE CALENDAR AGING OF THE BATTERY: ARTIFICIAL CYCLING

The calendar aging model presented in Section 3.5.4.2 suggests that Li-ion batteries must be used within a safe operating region restricted by the temperature, current, and SoC windows. Not respecting these restrictions leads to a rapid attenuation of the battery performance (see Section 5.5.2). In this work, we have already analyzed how the two following aging constraints can preserve the battery from rapid degradation:

- \mathcal{C}_1 : restricted range of the SoC $\Delta_{\text{SOC}} = [20\%, 90\%]$. As discussed earlier, operating the battery outside this range accelerates the cycle aging by factor χ . In addition, the calendar aging is amplified when the battery voltage is high, which corresponds to a high SoC.

$$\mathcal{C}_1 : \quad \forall t, z(t) \in \Delta_{\text{SOC}}.$$

- \mathcal{C}_2 : restricted (dis)charge currents that cause accelerated cycle aging (due to deep cycling) and calendar aging (due to heat generation). The current constraint can be reformulated as a limitation of the SoC variation in each decision period:

$$\mathcal{C}_2 : \quad \forall t, \Delta \text{SOC}_{\min} \leq z(t + \Delta t) - z(t) \leq \Delta \text{SOC}_{\max},$$

where $\Delta \text{SOC}_{\max} \geq 0$ (resp. $\Delta \text{SOC}_{\min} \leq 0$) is the maximum variation of the SoC during charge (resp. discharge).

Also, the calendar aging depends on how long the battery stays inactive (eq. 3.15). Therefore, we suggest reducing further the calendar aging by shortening the inactivity periods. It is possible to completely avoid rest periods and force the battery into permanent cycling. However, according to Eddahech *et al.* [Eddahech 2013] and Rashid *et al.* [Rashid 2015], providing batteries with a rest period after (dis)charging might be essential for relaxation of gradients generated due to the passage of current and could enable capacity recovery. Such phenomenon is not represented in the proposed aging model but we can consider it in practice by allowing at most one time step rest between charges and discharges. eq. A.1 expresses this constraint \mathcal{C}_3 by imposing a minimum variation of the SOC (be it positive or negative) over any two consecutive time steps:

$$\mathcal{C}_3 : \quad \forall t, [z(t + 2\Delta t) - z(t + \Delta t)]^2 + [(z(t + \Delta t) - z(t))]^2 \geq \epsilon, \quad (\text{A.1})$$

where ϵ is strictly positive.

To evaluate the effect of these constraints on the battery aging, we simulate the *ideal* strategy (which has a perfect knowledge of the stochastic variables) under three configurations:

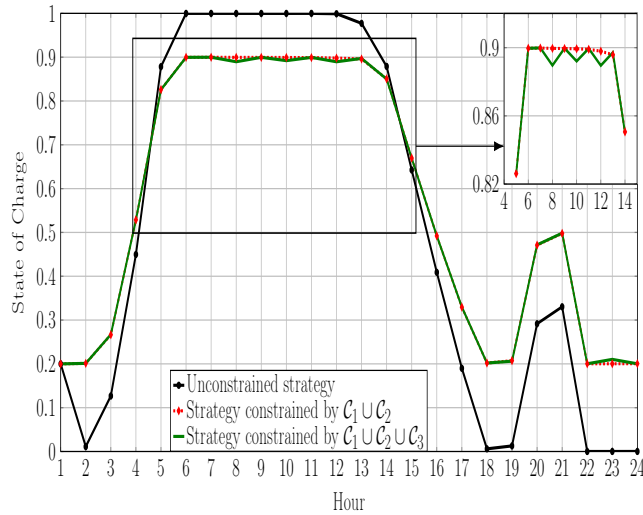


FIGURE A.1: Average SoC strategy under different sets of battery constraints.

- Unconstrained *ideal* strategy.
- *Ideal* strategy constrained by C_1 and C_2 .
- *Ideal* strategy constrained by C_1 , C_2 , and C_3 .

The parameters settings are the same as in Chapter 5 Section 5.5, *i.e.*, the optimization horizon is 24 hours and the simulation is performed 1825 times (equivalent of five years) for each configuration. The obtained results are averaged over all the realizations.

Fig. A.1 shows the average SoC strategies under the different battery constraints. In the absence of constraints, the battery power flow is characterized by high battery currents (high SoC differential) and extreme SoCs. Including the constraints C_1 and C_2 enables progressive battery (dis)charge such that the aging constraints are respected. The two constrained strategies are very similar, the only differences being the battery usage between 7:00-13:00 and 22:00-0:00. This difference is due to C_3 , which restricts the battery rest during two consecutive time steps and generates a sawtooth pattern with respect to the SoC.

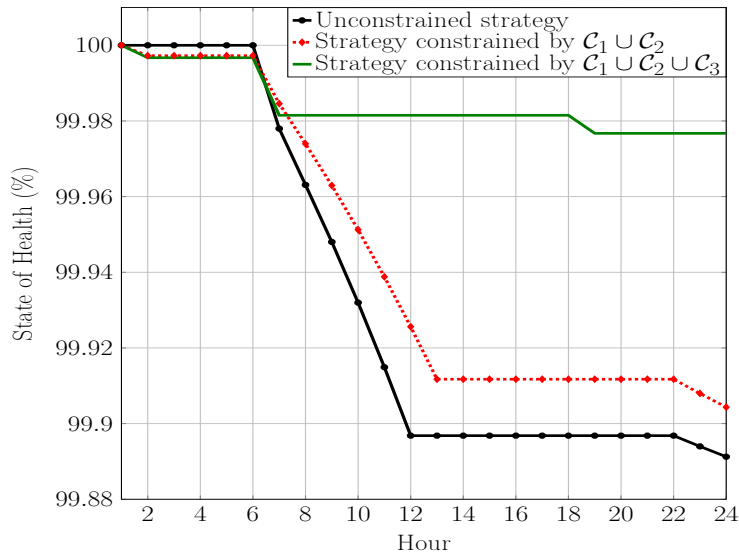


FIGURE A.2: Average evolution of the SoH due to calendar aging under different sets of battery constraints.

The evolution of the battery SoH due to calendar aging in the three configurations is represented in Fig. A.2. The aging is the highest in the absence of any battery constraint, where 0.11% of the SoH in

average is lost every day. The conditions on the SoC introduced by \mathcal{C}_1 and \mathcal{C}_2 contribute to reduce the impact of the calendar aging process thanks to current and voltage limitations (0.09% of SoH average loss per day). Furthermore, when the constraint \mathcal{C}_3 is respected, the battery spends less time in the inactive state. This completely avoids the calendar aging especially in some periods marked by disadvantageous storage conditions (high voltage and temperature). The resulting battery degradations are therefore limited in average to 0.02% of SoH loss per day.

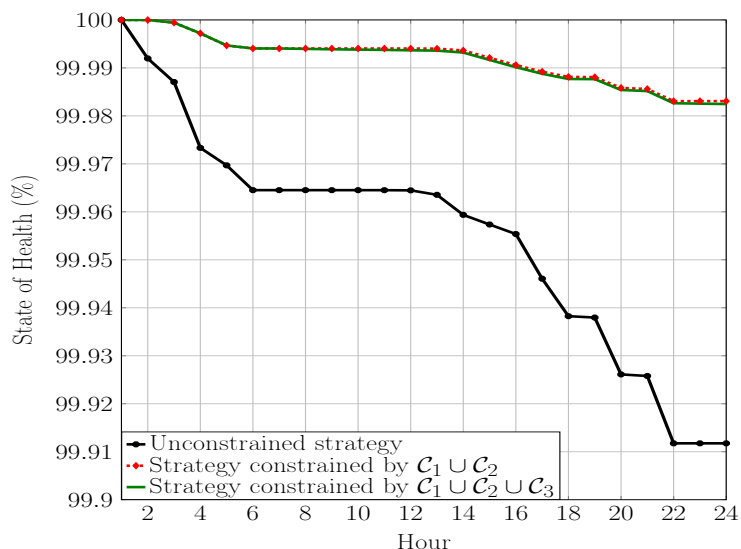


FIGURE A.3: Average evolution of the SoH due to cycle aging under different sets of battery constraints.

Note from Fig. A.3 that adding the constraint \mathcal{C}_3 causes a slight (nearly negligible) increase of the cycle aging because of the additional cycling that prevents long battery rests (Fig. A.3).

Finally, by summing the cycle and calendar agings effects, we conclude that the artificial cycling can further enhance the sustainability of Li-ion batteries. This allows in average 51% (resp. 30%) of the battery SoH preservation per year when operating under \mathcal{C}_1 , \mathcal{C}_2 , and \mathcal{C}_3 (resp. under \mathcal{C}_1 and \mathcal{C}_2) compared to the unconstrained case.

A.2 NON-LINEAR PROGRAMMING

An optimization problem can be represented in the following way:

$$\min_{\mathbf{x}} f(\mathbf{x}) \quad (\text{A.2})$$

subject to $g_i(\mathbf{x}) \leq 0, \quad i = 1, \dots, m$ and $h_j(\mathbf{x}) = 0, \quad j = 1, \dots, p$

where $f(x)$ is the objective function, $g_i(\mathbf{x})$ are the inequality constraints, and $h_j(\mathbf{x})$ are the equality constraints.

Non-linear programming involves minimizing or maximizing an objective function subject to equality and/or inequality constraints, where some of the constraints and/or the objective function are non-linear.

When the optimization problem is convex, there exist algorithms that guarantee the global convergence to the optimum [Boyd 2004]. More generally, non-linear optimization problems are difficult to solve because the nonlinear constraints form feasible regions that are difficult to find and the nonlinear objectives contain local minima that trap the search methods [Shang 1997]. In order to find good solution, there are two key issues to handle: nonlinear constraints and how to avoid local minima.

To overcome local minima, we consider solving unconstrained optimization problems using iterative methods that generate a sequence of points with gradually smaller values on the function f_{unconstr} which is to be minimized. There are two main types of algorithms in this category:

- Line search methods: the algorithm chooses a search direction \mathbf{d}_k and tries to solve the following one-dimensional minimization problem:

$$\min_{\alpha \geq 0} f_{\text{unconstr}}(\mathbf{x} + \alpha \mathbf{d}_k), \quad (\text{A.3})$$

where α is a scalar called the step length.

- Trust region methods: in these methods, the objective function is approximated in some neighborhood of the current point \mathbf{x}_k . The approximate function $\hat{f}_{\text{unconstr}}$ is simpler than f_{unconstr} and is minimized in the mentioned neighborhood. The obtained minimizer is then the starting point of in next iteration \mathbf{x}_{k+1} .

The line search and trust-region methods are typically both based on quadratic approximation of f_{unconstr} . Also, when combined with efficient initialization schemes, they are called globalization strategies, since they modify a *core* method (such as Newton's method to find local minima) to become globally convergent [Börlin 2007].

Concerning the non-linear constraints issue, they are generally handled by converting the constrained problem into an unconstrained one, and then using the unconstrained resolution methods. The unconstrained problems are formed by adding a term to the objective function that consists of a penalty parameter multiplied by a measure of violation of the constraints. The most known approach uses lagrangian multipliers algorithms such as augmented Lagrangian and interior point methods [Bertsekas 1999].

The solver used in this work to solve some non-linear optimization problems is *fmincon*, provided by Matlab. It relies, amongst others, on a combination of the trust region methods and the interior point methods.

BIBLIOGRAPHY

- [3GPP 2010] 3GPP. *Telecommunication management; Self-Organizing Networks (SON); Concepts and requirements*. Technical Specification (TS) 32.500, 3rd Generation Partnership Project (3GPP), 2010.
- [3GPP 2011] 3GPP. *Evolved Universal Terrestrial Radio Access (E-UTRA); Radio Frequency (RF) requirements for LTE Pico Node B*. Technical Report (TR) 36.931, 3rd Generation Partnership Project (3GPP), 2011. version 9.0.0 Release 9.
- [Alsharif et al. 2016] Mohammed H. Alsharif et al. *Green wireless network optimisation strategies within smart grid environments for Long Term Evolution cellular networks in Malaysia*. *Renewable Energy*, vol. 85, pages 157–170, 2016.
- [Ameren] Ameren. *Ameren Price Database*.
- [Andrews 2012] Jeffrey G Andrews, Holger Claussen, Mischa Dohler, Sundeep Rangan and Mark C Reed. *Femtocells: Past, present, and future*. *IEEE Journal on Selected Areas in Communications*, vol. 30, no. 3, pages 497–508, 2012.
- [Andrews 2014] Jeffrey G Andrews, Stefano Buzzi, Wan Choi, Stephen V Hanly, Angel Lozano, Anthony CK Soong and Jianzhong Charlie Zhang. *What will 5G be?* *IEEE Journal on selected areas in communications*, vol. 32, no. 6, pages 1065–1082, 2014.
- [Auer 2010] Gunther Auer, Oliver Blume, Vito Giannini, Istvan Godor ETH, Muhammad Ali Imran, Ylva Jading EAB, Efsthios Katranaras, Magnus Olsson EAB, Dario Sabella TI and Per Skillermark EAB. *INFSO-ICT-247733 EARTH D2.3, Energy Efficiency Analysis of the Reference Systems, Areas of Improvements and Target Breakdown*. 2010.
- [Auer 2011] Gunther Auer, Vito Giannini, Claude Desset, Istvan Godor, Per Skillermark, Magnus Olsson, Muhammad Ali Imran, Dario Sabella, Manuel J. Gonzalez, Oliver Blume and others. *How Much Energy is Needed to Run a Wireless Network?* *IEEE Wireless Communications*, 2011.
- [Badia 2017] Leonardo Badia, Elisa Feltre and Elvina Gindullina. *A Markov Model Accounting for Charge Recovery in Energy Harvesting Devices*. In *Wireless Communications and Networking Conference Workshops (WCNCW)*, 2017 IEEE, pages 1–6. IEEE, 2017.
- [Barre 2014] Anthony Barre, Frédéric Suard, Mathias Gérard, Maxime Montaru and Delphine Riu. *Statistical Analysis for Understanding and Predicting Battery Degradations in Real-Life Electric Vehicle Use*. *Journal of Power Sources*, vol. 245, pages 846–856, Janvier 2014.
- [Barré 2013] Anthony Barré, Benjamin Deguilhem, Sébastien Grolleau, Mathias Gérard, Frédéric Suard and Delphine Riu. *A review on lithium-ion battery ageing mechanisms and estimations for automotive applications*. *Journal of Power Sources*, vol. 241, pages 680–689, Novembre 2013.
- [Bertsekas 1999] Dimitri P Bertsekas. *Nonlinear programming*. Athena scientific Belmont, 1999.

- [Biason 2016] Alessandro Biason and Michele Zorzi. *On the effects of battery imperfections in an energy harvesting device*. In Computing, Networking and Communications (ICNC), 2016 International Conference on, pages 1–7. IEEE, 2016.
- [Blasco 2013] Pol Blasco, Deniz Gunduz and Mischa Dohler. *A learning theoretic approach to energy harvesting communication system optimization*. IEEE Transactions on Wireless Communications, vol. 12, no. 4, pages 1872–1882, 2013.
- [Borenstein 2002] Severin Borenstein, Michael Jaske and Arthur Rosenfeld. *Dynamic pricing, advanced metering, and demand response in electricity markets*. 2002.
- [Börlin 2007] Niclas Börlin. *Nonlinear Optimization: Overview of methods; the Newton method with line search*. Umea University, 2007.
- [Boyd 2004] Stephen Boyd and Lieven Vandenberghe. *Convex optimization*. Cambridge university press, 2004.
- [Broussely 2005] M. Broussely, Ph. Biensan, F. Bonhomme, Ph. Blanchard, S. Herreyre, K. Nechev and R.J. Staniewicz. *Main aging mechanisms in Li ion batteries*. Journal of Power Sources, vol. 146, no. 1-2, pages 90–96, Aot 2005.
- [Busoniu 2007] Lucian Busoniu, Damien Ernst, Bart De Schutter and Robert Babuska. *Fuzzy approximation for convergent model-based reinforcement learning*. In Fuzzy Systems Conference, 2007. FUZZ-IEEE 2007. IEEE International, pages 1–6. IEEE, 2007.
- [Byrd 2000] Richard H Byrd, Jean Charles Gilbert and Jorge Nocedal. *A trust region method based on interior point techniques for nonlinear programming*. Mathematical Programming, vol. 89, no. 1, pages 149–185, 2000.
- [C2P] C2P. *Cognitive radio and Cooperative strategies for power saving in multi-standard wireless devices - Home page*. <https://www.it.pt/Projects/Index/1343>. Accessed: 2018-01-22.
- [Cavallaro 2015] Fausto Cavallaro. *A Takagi-Sugeno Fuzzy Inference System for Developing a Sustainability Index of Biomass*. Sustainability, vol. 7, no. 9, pages 12359–12371, 2015.
- [Chang 2013] Wen-Yeau Chang. *The State of Charge Estimating Methods for Battery: A Review*. ISRN Applied Mathematics, vol. 2013, pages 1–7, 2013.
- [Chia 2014] Yeow-Khiang Chia, Sumei Sun and Rui Zhang. *Energy cooperation in cellular networks with renewable powered base stations*. IEEE Transactions on Wireless Communications, vol. 13, no. 12, pages 6996–7010, 2014.
- [Communities 2008] Commission Of The European Communities. *Addressing the challenge of energy efficiency through information and communication technologies*. 2008.
- [Cordoba-Arenas et al. 2015] Andrea Cordoba-Arenas et al. *A control-oriented lithium-ion battery pack model for plug-in hybrid electric vehicle cycle-life studies and system design with consideration of health management*. Journal of Power Sources, vol. 279, pages 791–808, Avril 2015.
- [Couture 2010] Toby Couture and Yves Gagnon. *An analysis of feed-in tariff remuneration models: Implications for renewable energy investment*. Energy policy, vol. 38, no. 2, pages 955–965, 2010.
- [De Domenico 2014a] Antonio De Domenico, Emilio Calvanese Strinati and Antonio Capone. *Enabling Green cellular networks: A survey and outlook*. Computer Communications, vol. 37, pages 5–24, Janvier 2014.

- [De Domenico 2014b] Antonio De Domenico, Emilio Calvanese Strinati and Antonio Capone. *Enabling green cellular networks: A survey and outlook*. Computer Communications, vol. 37, pages 5–24, 2014.
- [Divya 2009] KC Divya and Jacob Østergaard. *Battery energy storage technology for power systems—An overview*. Electric Power Systems Research, vol. 79, no. 4, pages 511–520, 2009.
- [Dolara 2015] Alberto Dolara, Sonia Leva and Giampaolo Manzolini. *Comparison of different physical models for PV power output prediction*. Solar Energy, vol. 119, pages 83–99, 2015.
- [Dusonchet 2015] L Dusonchet and E Telaretti. *Comparative economic analysis of support policies for solar PV in the most representative EU countries*. Renewable and Sustainable Energy Reviews, vol. 42, pages 986–998, 2015.
- [EARTH] EARTH. *Energy aware radio and network technologies - Home page*. <https://www.ict-earth.eu/>. Accessed: 2018-01-22.
- [Ecker 2012] Madeleine Ecker, Jochen B. Gerschler, Jan Vogel, Stefan Käbitz, Friedrich Hust, Philipp Dechent and Dirk Uwe Sauer. *Development of a lifetime prediction model for lithium-ion batteries based on extended accelerated aging test data*. Journal of Power Sources, vol. 215, pages 248–257, Octobre 2012.
- [Eddahech 2013] Akram Eddahech, Olivier Briat and Jean-Michel Vinassa. *Lithium-ion Battery Performance Improvement Based on Capacity Recovery Exploitation*. Electrochimica Acta, vol. 114, pages 750–757, dec 2013.
- [EPEC] EPEC. *Energy Density Comparison of Size and Weight*. <http://www.epectec.com/batteries/cell-comparison.html>. Accessed: 2018-01-22.
- [Fang 2012] Xi Fang, Satyajayant Misra, Guoliang Xue and Dejun Yang. *Smart grid—The new and improved power grid: A survey*. IEEE communications surveys & tutorials, vol. 14, no. 4, pages 944–980, 2012.
- [Farhangi 2010] Hassan Farhangi. *The path of the smart grid*. IEEE power and energy magazine, vol. 8, no. 1, 2010.
- [FP7] FP7. *Seventh framework programme - Home page*. https://ec.europa.eu/research/fp7/index_en.cfm. Accessed: 2018-01-22.
- [Gong 2014] Jie Gong, John S Thompson, Sheng Zhou and Zhisheng Niu. *Base station sleeping and resource allocation in renewable energy powered cellular networks*. IEEE Transactions on Communications, vol. 62, no. 11, pages 3801–3813, 2014.
- [Grewal 2011] Mohinder S Grewal. *Kalman filtering*. In International Encyclopedia of Statistical Science, pages 705–708. Springer, 2011.
- [Hasan 2011a] Ziaul Hasan, Hamidreza Boostanimehr and Vijay K Bhargava. *Green cellular networks: A survey, some research issues and challenges*. IEEE Communications surveys & tutorials, vol. 13, no. 4, pages 524–540, 2011.
- [Hasan 2011b] Ziaul Hasan, Hamidreza Boostanimehr and Vijay K. Bhargava. *Green Cellular Networks: A Survey, Some Research Issues and Challenges*. IEEE Communications Surveys & Tutorials, vol. 13, no. 4, pages 524–540, 2011.
- [Ho 2010] Chin Keong Ho, Pham Dang Khoa and Pang Chin Ming. *Markovian models for harvested energy in wireless communications*. In Communication Systems (ICCS), 2010 IEEE International Conference on, pages 311–315. IEEE, 2010.

- [IAE 2015] IAE. *Survey Report of Selected IEA Countries between 1992 and 2014*. Technical report, IEA Photovoltaic Power Systems Program, IEA PVPS T1-27, 2015.
- [IEA-PVPS 2015] IEA-PVPS. *Trends 2015 in Photovoltaic Applications*, 2015.
- [Kaewpuang 2012] Rakpong Kaewpuang, Dusit Niyato and Ping Wang. *Decomposition of Stochastic Power Management for Wireless Base Station in Smart Grid*. IEEE Wireless Communications Letters, vol. 1, no. 2, pages 97–100, 2012.
- [Karmarkar 1984] N. Karmarkar. *A New Polynomial-time Algorithm for Linear Programming*. In Proceedings of the Sixteenth Annual ACM Symposium on Theory of Computing, STOC '84, pages 302–311, New York, NY, USA, 1984. ACM.
- [Karray 2010] Mohamed Kadhem Karray. *Analytical evaluation of QoS in the downlink of OFDMA wireless cellular networks serving streaming and elastic traffic*. IEEE Transactions on Wireless Communications, vol. 9, no. 5, 2010.
- [Khalilpour 2016] Rajab Khalilpour and Anthony Vassallo. *Planning and operation scheduling of PV-battery systems: A novel methodology*. Renewable and Sustainable Energy Reviews, vol. 53, pages 194–208, 2016.
- [Koenig 1992] Sven Koenig and Reid G. Simmons. *Complexity analysis of real-time reinforcement learning applied to finding shortest paths in deterministic domains*. Technical report, DTIC Document, 1992.
- [Komor 2015] Paul Komor and Timothy Molnar. *BACKGROUND PAPER ON DISTRIBUTED RENEWABLE ENERGY GENERATION AND INTEGRATION*. 2015.
- [Koutitas et al. 2010] George Koutitas et al. *A review of Energy Efficiency in Telecommunication Networks*. Telfor journal, vol. 2, no. 1, pages 2–7, 2010.
- [Ku 2015] Meng-Lin Ku, Wei Li, Yan Chen and K. J. Ray Liu. *Advances in Energy Harvesting Communications: Past, Present, and Future Challenges*. IEEE Communications Surveys & Tutorials, pages 1–1, 2015.
- [Kwasinski 2013] Andres Kwasinski and Alexis Kwasinski. *Architecture for green mobile network powered from renewable energy in microgrid configuration*. In Wireless Communications and Networking Conference (WCNC), 2013 IEEE, pages 1273–1278. IEEE, 2013.
- [Leithon et al. 2016] Johann Leithon et al. *Renewable energy management in cellular networks: An online strategy based on ARIMA forecasting and a Markov chain model*. In Wireless Communications and Networking Conference, pages 1–6. IEEE, 2016.
- [Leithon 2013] Johann Leithon, Teng Joon Lim and Sumei Sun. *Online Energy Management Strategies for Base Stations Powered by the Smart Grid*. In IEEE SmartGridComm, pages 199–204, 2013.
- [Leithon 2014] J. Leithon, S. Sun and T. J. Lim. *Energy management strategies for base stations in a smart grid environment*. Transactions on Emerging Telecommunications Technologies, Aot 2014.
- [Lemaire-Potteau 2008] Elisabeth Lemaire-Potteau, Florence Mattera, Arnaud Delaille and Philippe Malbranche. *Assessment of storage ageing in different types of PV systems: technical and economical aspects*. In 23rd European Photovoltaic Solar Energy Conference (Valencia, Spain, 2008), pages 2765–2769, 2008.
- [Little 1999] Arthur D Little. *Distributed Generation: System Interfaces*, an Arthur D. Little White Paper, Cambridge, 1999.

- [Liu 2015a] Chang Liu and Balasubramaniam Natarajan. *Power Management in Heterogeneous Networks with Energy Harvesting Base Stations*. Phys. Commun., vol. 16, no. C, pages 14–24, sep 2015.
- [Liu 2015b] Chang Liu and Balasubramaniam Natarajan. *Power management in heterogeneous networks with energy harvesting base stations*. Physical Communication, vol. 16, pages 14–24, 2015.
- [Luo 2015] Xing Luo, Jihong Wang, Mark Dooner and Jonathan Clarke. *Overview of current development in electrical energy storage technologies and the application potential in power system operation*. Applied Energy, vol. 137, pages 511–536, 2015.
- [Mao 2016] Yuyi Mao, Jun Zhang and Khaled Ben Letaief. *Grid Energy Consumption and QoS Tradeoff in Hybrid Energy Supply Wireless Networks*. IEEE Transactions on Wireless Communications., vol. 15, no. 5, may 2016.
- [Michelusi 2013] Nicolò Michelusi, Leonardo Badia, Ruggero Carli, Luca Corradini and Michele Zorzi. *Energy management policies for harvesting-based wireless sensor devices with battery degradation*. IEEE Transactions on Communications, vol. 61, no. 12, pages 4934–4947, 2013.
- [Ministériel 2017] Arrêté Ministériel. *Arrêté tarifaire du 9 mai 2017*. <https://www.legifrance.gouv.fr/affichTexte.do?cidTexte=JORFTEXT000034631446>, 2017. Accessed: 2018-01-22.
- [Morris 2016] Craig Morris and Arne Jungjohann. *Will the Energiewende Succeed?* In Energy Democracy, pages 379–412. Springer, 2016.
- [MpowerUK] MpowerUK. *Lithium Battery Failures*.
- [Muratori 2010] Matteo Muratori. *Thermal characterization of Lithium-ion battery cell*. 2010.
- [Nerini 2015] Francesco Fuso Nerini, Roger Dargaville, Mark Howells and Morgan Bazilian. *Estimating the cost of energy access: The case of the village of Suro Craic in Timor Leste*. Energy, vol. 79, pages 385–397, 2015.
- [Ng 2013] Derrick Wing Kwan Ng, Ernest S Lo and Robert Schober. *Energy-efficient resource allocation in OFDMA systems with hybrid energy harvesting base station*. IEEE Transactions on Wireless Communications, vol. 12, no. 7, pages 3412–3427, 2013.
- [Niyato 2012] Dusit Niyato, Xiao Lu and Ping Wang. *Adaptive Power Management for Wireless Base Stations in a Smart Grid Environment*. IEEE Wireless Communications, vol. 19, no. 6, pages 44–51, 2012.
- [Ozel 2011] Omur Ozel, Kaya Tutuncuoglu, Jing Yang, Sennur Ulukus and Aylin Yener. *Transmission with energy harvesting nodes in fading wireless channels: Optimal policies*. IEEE Journal on Selected Areas in Communications, vol. 29, no. 8, pages 1732–1743, 2011.
- [Ozel 2014] Omur Ozel, Khurram Shahzad and Sennur Ulukus. *Optimal energy allocation for energy harvesting transmitters with hybrid energy storage and processing cost*. IEEE Transactions on Signal Processing, vol. 62, no. 12, pages 3232–3245, 2014.
- [Parida 2011] Bhubaneswari Parida, S. Iniyam and Ranko Goic. *A review of solar photovoltaic technologies*. Renewable and Sustainable Energy Reviews, vol. 15, no. 3, pages 1625–1636, 2011.
- [Pillot 2013] Christophe Pillot. *Li-ion battery material market review and forecast 2012-2025*. In Avicenne Energy, Presentation at 3rd Israeli Power Sources Conference, Hertzlia (Israel), 2013.
- [Platform 2010] Smart Grids European Technology Platform. *Strategic Deployment Document for Europe's Electricity Networks of the Future*. 2010.

- [Plett 2004] G.L. Plett. *High-Performance Battery-Pack Power Estimation Using a Dynamic Cell Model*. IEEE Transactions on Vehicular Technology, vol. 53, no. 5, pages 1586–1593, Septembre 2004.
- [Poudineh 2014] Rahmatallah Poudineh and Tooraj Jamasb. *Distributed generation, storage, demand response and energy efficiency as alternatives to grid capacity enhancement*. Energy Policy, vol. 67, pages 222–231, 2014.
- [Qualcomm 2011] Qualcomm. *Advanced: Heterogeneous networks, White Paper, Jan. 2011*, 2011.
- [Rahimi 2010] Farrokh Rahimi and Ali Ipakchi. *Demand response as a market resource under the smart grid paradigm*. IEEE Transactions on Smart Grid, vol. 1, no. 1, pages 82–88, 2010.
- [Rami 2004] G. Rami, T. Tran-Quoc, N. Hadjsaid and J. L. Mertz. *Energy Supply for Remote Base Transceiver Stations of Telecommunication*. In IEEE PESGM, pages 1916–1921, 2004.
- [Rashid 2015] Muhammad Rashid and Amit Gupta. *Effect of Relaxation Periods Over Cycling Performance of a Li-ion Battery*. Journal of The Electrochemical Society, vol. 162, no. 2, pages A3145–A3153, 2015.
- [REN21 2017] REN21. *Advancing the Global Renewable Energy Transition*. Technical report, Renewable energy policy network for the 21st century, 2017. Accessed: 2018-01-22.
- [Riffonneau 2011] Y Riffonneau, S Bacha, F Barruel and S Ploix. *Optimal Power Flow Management for Grid Connected PV Systems With Batteries*. IEEE Transactions on Sustainable Energy, vol. 2, no. 3, pages 309–320, Juillet 2011.
- [Ru 2013] Yu Ru, Jan Kleissl and Sonia Martinez. *Storage Size Determination for Grid-Connected Photovoltaic Systems*. IEEE Transactions on Sustainable Energy, vol. 4, pages 68–81, Janvier 2013.
- [Santhanagopalan 2006] Shriram Santhanagopalan, Qingzhi Guo, Premanand Ramadass and Ralph E White. *Review of models for predicting the cycling performance of lithium ion batteries*. Journal of Power Sources, vol. 156, no. 2, pages 620–628, 2006.
- [Shang 1997] Yi Shang. *Global search methods for solving nonlinear optimization problems*. Citeseer, 1997.
- [SOLAR] GeoModel SOLAR. *Solar Radiation Time Series*.
- [Sutton 1998] Richard S Sutton and Andrew G Barto. *Reinforcement Learning: An Introduction*, volume 1. MIT press Cambridge, 1998.
- [Sutton 2017] Richard S Sutton and Andrew G Barto. *Reinforcement Learning: An Introduction Second Edition*. MIT press Cambridge, 2017.
- [Swider 2008] Derk J Swider, Luuk Beurskens, Sarah Davidson, John Twidell, Jurek Pyrko, Wolfgang Prügler, Hans Auer, Katarina Vertin and Romualdas Skema. *Conditions and costs for renewables electricity grid connection: Examples in Europe*. Renewable Energy, vol. 33, no. 8, pages 1832–1842, 2008.
- [Sánchez Muñoz 2016] Ana Sánchez Muñoz, Maria Garcia and Matthias Gerlich. *Overview of storage technologies*. Technical report D2.1, Sensible, 2016. Accessed: 2018-01-22.
- [Tombaz 2011] Sibel Tombaz, Paolo Monti, Kun Wang, Anders Vastberg, Marco Forzati and Jens Zander. *Impact of backhauling power consumption on the deployment of heterogeneous mobile networks*. In Global Telecommunications Conference (GLOBECOM 2011), 2011 IEEE, pages 1–5. IEEE, 2011.

- [Tombaz 2014] Sibel Tombaz, Paolo Monti, Fabricio Farias, Matteo Fiorani, Lena Wosinska and Jens Zander. *Is backhaul becoming a bottleneck for green wireless access networks?* In Communications (ICC), 2014 IEEE International Conference on, pages 4029–4035. IEEE, 2014.
- [Torriti 2011] Jacopo Torriti, Matthew Leach and Patrick Devine-Wright. *Demand side participation: price constraints, technical limits and behavioural risks*. The Future of Electricity Demand: Customers, Citizens and Loads. Department of Applied Economics Occasional Papers (69). Cambridge University Press, Cambridge, pages 88–105, 2011.
- [TREND] TREND. *Towards real energy-efficient network design - Home page*. <http://www.fp7-trend.eu/>. Accessed: 2018-01-22.
- [Truong 2016] Cong Nam Truong, Maik Naumann, Ralph Ch Karl, Marcus Müller, Andreas Jossen and Holger C Hesse. *Economics of residential photovoltaic battery systems in Germany: The case of Tesla's Powerwall*. Batteries, vol. 2, no. 2, page 14, 2016.
- [Uddin 2014] Kotub Uddin, Alessandro Picarelli, Christopher Lyness, Nigel Taylor and James Marco. *An Acausal Li-Ion Battery Pack Model for Automotive Applications*. Energies, vol. 7, no. 9, pages 5675–5700, Aot 2014.
- [Ulukus 2015a] Sennur Ulukus, Aylin Yener, Elza Erkip, Osvaldo Simeone, Michele Zorzi, Pulkit Grover and Kaibin Huang. *Energy harvesting wireless communications: A review of recent advances*. Selected Areas in Communications, IEEE Journal on, vol. 33, no. 3, pages 360–381, 2015.
- [Ulukus 2015b] Sennur Ulukus, Aylin Yener, Elza Erkip, Osvaldo Simeone, Michele Zorzi, Pulkit Grover and Kaibin Huang. *Energy harvesting wireless communications: A review of recent advances*. IEEE Journal on Selected Areas in Communications, vol. 33, no. 3, pages 360–381, 2015.
- [Vereecken 2010] Willem Vereecken, Ward Van Heddeghem, Didier Colle, Mario Pickavet and Piet Demeester. *Overall ICT footprint and green communication technologies*. ISCCSP, vol. 10, pages 1–6, 2010.
- [Wang 2015] Heng Wang, Hongjia Li, Chaowei Tang, Lingbao Ye, Xin Chen, Hui Tang and Song Ci. *Modeling, Metrics, and Optimal Design for Solar Energy-powered Base Station System*. EURASIP Journal on Wireless Communications and Networking, vol. 2015, no. 1, Dcembre 2015.
- [Watkins 1992] Christopher JCH Watkins and Peter Dayan. *Q-learning*. Machine learning, vol. 8, no. 3-4, pages 279–292, 1992.
- [Webb 2008] Molly Webbet *al*. *Smart 2020: Enabling the low carbon economy in the information age*. The Climate Group. London, vol. 1, no. 1, pages 1–1, 2008.
- [Wei 2016] Yifei Wei, Chenying Ren, Mei Song and Richard Yu. *The offloading model for green base stations in hybrid energy networks with multiple objectives*. International Journal of Communication Systems, vol. 29, no. 11, pages 1805–1816, 2016.
- [zad 1965] *Fuzzy sets*. Information and Control, vol. 8, no. 3, pages 338 – 353, 1965.
- [Zadeh 1974] Lotfi A. Zadeh. *The Concept of a Linguistic Variable and its Application to Approximate Reasoning*. Springer, 1974.
- [Zhang 2016] Shan Zhang, Ning Zhang, Sheng Zhou, Jie Gong, Zhisheng Niu and Xuemin Shen. *Energy-aware traffic offloading for green heterogeneous networks*. IEEE Journal on Selected Areas in Communications, vol. 34, no. 5, pages 1116–1129, 2016.
- [Zheng 2015] Qipeng P Zheng, Jianhui Wang and Andrew L Liu. *Stochastic optimization for unit commitment—A review*. IEEE Transactions on Power Systems, vol. 30, no. 4, pages 1913–1924, 2015.

